Fate of Hydroxyapatite Nano particles during *In Vitro* Gastrointestinal Digestion

A thesis presented in partial fulfilment of the requirements for the degree of

Master in Food Technology

at Massey University, Riddet Institute and Massey Institute of Food Science and Technology, Palmerston North, New Zealand

MASSEY UNIVERSITY

Riddet Institute
FOOD | INNOVATION | HEALTH

Kinley Choki

2018

Abstract

There is an increasing change in population demographics towards an aging population in the world, which had led to the availability of various commercial nutritionally supplemented products. Hydroxyapatite (HA), with chemical formula $Ca_{10}(PO_4)_6(OH)_2$, is an insoluble calcium salt used for calcium supplementation because of its similarity to the minerals found in human bone and teeth. The insoluble calcium salts are preferred over the soluble ones because of their high heat stability during milk processing under high heat treatment. However, the drawback of insoluble calcium salts is the tendency to sediment during storage resulting in unfavourable gritty texture. Thus, reduction in particle sizes into micron to nano-size improves the dispersion of these insoluble salts. However, the application of nano-sized particles in food products have raised concerns from both the regulatory organizations and consumers on the implications related to both the environmental and health safety aspects. Thus, the objective of the study is to determine the digestion behaviour of nano-sized needle/rod shaped HA (nHA) when added into skim milk during *in vitro* gastrointestinal digestion. Determination of calcium such as soluble and ionic calcium was conducted to determine the dissolution of nHA. The structural changes and the crystallographic changes of nHA were determined using electron microscopy and x-ray diffraction techniques. The results of *in vitro* gastric digestion showed presence of undissolved nHA particles even after 240 min of gastric and 120 min of intestinal digestion when examined under TEM, while the XRD analysis detected the presence of crystalline nHA in the first 120 min of gastric digestion. Thus, the possible mechanisms leading to the incomplete dissolution of nHA under acidic conditions of the stomach are discussed subsequently.

Acknowledgement

First, I would to thank New Zealand Aid scholarship, MFAT (Ministry of Foreign Affairs and Trade) for providing me the opportunity to study in New Zealand. I would also like to thank the New Zealand Aid ISSO staffs for their support and making me feel at home.

I would like to sincerely thank my supervisor Aiqian Ye and my co-supervisor Harjinder Singh for their scientific comments, support and guidance in completion of this thesis. I am grateful to the Riddet Institute Centre of Excellence (CoRE) for the financial support in conducting this study and to the staff of the Riddet Laboratory for their support.

I would also like to express my gratitude to Siqi Li, for his valuable time during many long hours of discussions, for his guidance and encouragements.

Many thanks to Manawatu Microscopy and Imaging Centre (MMIC), Fundamental Science Institute, Massey University for the training and use of their equipment in this research especially, Taylor Jordan and Nikki Minards for their time and support. Geoffrey B. Jameson for his valuable time and comments especially on XRD analysis, and Anja Moebis for her time and support in preparation of the samples for EDS analysis.

Lastly, I am grateful to my parents and my sisters for their unconditional love and support especially in taking care of my son back at home. Heartiest thanks to my husband for being my companion, providing me strength and confidence that has allowed me to complete this thesis.

List of figures

List of tables

List of abbreviations

°C	Degree(s) Celsius
%	Percent
CCP	Colloidal calcium phosphate
CaP	Calcium phosphate
EDS	Energy dispersive spectroscopy
g	gram(s)
GI	Gastrointestinal
h	hour(s)
HA	Hydroxyapatite
HGS	Human gastric simulator
L	Litre(s)
nHA	Nano hydroxyapatite particles
nHA blank	nHA_{blank}
nHA in milk	nHA_{milk}
mg	Milligram(s)
min	Minute(s)
ml	Millilitre(s)
mM	Millimolar (mmol.L-1)
mmol	Millimole(s)
mol	Mole(s)
Milk blank	$Milk_{blank}$
nm	Nanometre(s)
NMs	Nano materials
NPs	Nano particles
RDA	Recommended dietary allowance

SBF	Simulated biological fluid
SGF	Simulated gastric fluid
SIF	Simulated intestinal fluid
SM	Skim milk
TEM	Transmission electron microscopy
WP	Whey protein
WPI	Whey protein isolate
XRD	X-ray diffraction

List of appendices

Table of contents

Chapter 1 Introduction

There is an increasing change of population demographics in the world towards an older ageing population according to the United Nations Department of Economic and Social Affairs and Population Division (2015). As per the report by the end of 2030, the population of world aged over 60 would increase by 56 %. Unlike other young adult population these vulnerable population requires specific needs to cater towards their health and wellbeing. A bone health issue known as osteoporosis is one of the biggest concerns related to aging population. Osteoporosis is related to calcium deficiency which is characterized by reduced bone mass causing bones to become fragile (Cashman, 2006). Thus, as a counter measure there is an increasing trend towards calcium fortification. Calcium is an essential mineral required for the bone development and other vascular functioning and metabolism in the human body (Ross, 2011). The recommcended dietary allowance (RDA) for different age groups is "800 to 900 mg for adults, 1000 mg for pregnant and lactating women, and 1200 mg for adolescents and elderly persons" (Gaucheron, 2011, p. 402S). Milk and dairy products are the major known sources of calcium in the human diet. The increasing acceptance of consumers on the nutritional benefit of milk as a source of calcium has encouraged the fortification of milk with calcium.

Calcium salts of both organic and inorganic calcium forms are used for calcium fortification (Munchbach & Gerstner, 2010; Rafferty, Walters, & Heaney, 2007). However, in the dairy industry heat treatment (pasteurization and ultra-high temperature) of milk is the most common technological process applied for extending the shelf life, as well as an intermediate step in the processing of other dairy products. Soluble calcium salts disrupts the mineral equilibrium in milk leading to reduced heat stability (Omoarukhe, On-Nom, Grandison, & Lewis, 2010). Hydroxyapatite ($Ca_{10}(PO_4)^6(OH)_2$) is thermodynamically stable and resembles the bone inorganic mineral phase, thus HA finds its application in biomedical bone implants and grafts. Furthermore HA is often used in calcium fortification in milk and soy milk products because HA is said to be inert and does not cause any changes in the milk mineral balance (Tercinier, Ye, Singh, Anema, & Singh, 2014b). However, the problem associated with the addition of insoluble calcium salt is sedimentation

of salts resulting in undesirable gritty texture (Munchbach & Gerstner, 2010). The sedimentaton problem is solved through additon of nano sized HA particles (< 100 nm) that increases the dispersibility of HA during calcium fortification (Gerhart & Schottenheimer, 2013).

Application of nanoparticles (NPs) in food has led to better and faster delivery of nutrients in the food system; in nutritional supplement and fortified food products. With the application of nano-sized ingredients in food systems, it has also raised curiosity and concerns pertaining to the health and environmental impacts through its application from both the regulatory organizations and the customers. The consumers are now increasingly interested in the food they ingest and the stated benefits and effects on the body by consumption of these so called nutritionally supplemented or fortified commercial food products. After the ingestion of such food systems one of the implications is related to the translocation of these nano particles (NPs) from the gastrointestinal (GI) tract to other surrounding organs in the body. Little work has been reported on the fate of HA during the digestion process. Schoepf et al. (2017) reported on the dissolution of HA using simulated gastric fluid under static digestion models. However, the study on dynamic *in vitro* model mimicking human digestive process has not yet been carried out.

Therefore the main objectives of the study are:

i. To determine the dissolution behaviour of nHA in milk under simulated dynamic gastrointestinal conditions.
ii. To determine the effect of milk matrix on the dissolution of nHA during *in vitro* gastro intestinal digestion.
iii. Determining the presence and absence of any undissolved nHA in the digesta.

Chapter 2 Literature review

2.1 Nanotechnology

The concerns of the food producers in meeting the demands of providing safe and healthy food products at par with the growing population worldwide has led to venture into novel technologies. Nanotechnology is one such technology that has captured the interest of many researchers and is growing at a rapid pace in the food industry since its introduction. According to FSANZ (Food standards of Australia and New Zealand), the term nanotechnology in food is described as the technologies which manipulate material into a nanoscale of less than 100 nm in size. There is no collective definition for nanotechnology where different organizations have their own definitions thus, the term nanotechnology can be generally used to describe a nanoscale dimension of less than 100 nm (Shatkin, 2017). In addition, the term nano itself also implies that the size is minute and the higher surface to volume enables the material to react readily as compared to its original micro or macrostructures (Bouwmeester et al., 2009; Rossi et al., 2014). This novel property of nanomaterials has contributed to the rapid adoption and growth of nanotechnology in various industrial fields of material and environmental science, medicine and biomedical science, food and agricultural science and electronics. The Woodrow Wilson International Centre project on emerging nanotechnologies stated in their report in 2014; there are a total of "1814 consumer products from 622 companies in 32 countries". Among the lists, the health and fitness category listed the highest in products category at "42 % of the total", which included personal care, clothing, sporting goods, and dietary supplements in the form of calcium and magnesium (Vance et al., 2015, p. 1769).

Nanomaterials (NMs) can be classified into natural and engineered nanomaterials (ENMs). Some of the naturally occurring nanostructures in food systems are proteins, fats, starches and casein micelles in milk (Pathakoti, Manubolu, & Hwang, 2017) and ENMs are those which are created or produced deliberately, mainly man-made. These natural nanostructures are known to undergo structural changes during processing at both nano and microstructural levels. For example, β-lacto globulin (3.6 nm) under high heat and pressure undergoes denaturation forming

aggregates of protein fibrils; in the case of fat globules in milk the process of homogenization breaks milk fat globules into nano level of 100nm in size (Sekhon, 2010). ENMs are further sub classified into three types; first the inorganic nanomaterial of metal oxides like zinc oxide, silver NPs, titanium oxide and alkaline earth metals such as calcium, magnesium, second the organic nanomaterial from food and plant sources like chitosan and, third, from carbon-based materials such as carbon nanotubes (CNT) (De Matteis, 2017; Sekhon, 2010)

2.1.1 Nanotechnology in food

Nano-food refers to the application of nanotechnology and nanoparticles in the food industry during processing, packaging, and preservation (Bai & Liu, 2016). The introduction of nanotechnology in the food industry has revolutionize the conventional food sector to the next level finding its application in a wide ranges of areas like food processing, packaging, preservation, additives, nutrition and functional foods (He & Hwang, 2016; Pathakoti et al., 2017) particularly in food packaging and additives (Sekhon, 2010). The added advantage of nanotechnology in food processing is the production of food products without affecting the desired sensory attributes and the textural properties (Pradhan et al., 2015). Figure 2.1 lists the applicability of nanotechnology in diverse food areas.

The application of nanotechnology involves mainly the “top-down or bottom-up” method. The top-down process is the breakdown of larger particles into a smaller nanoscale through physical and chemical processes. The bottom-up approach involves complex build-up processes of adding onto the substrate to create a nanostructure such as crystallization, deposition of films (Henchion et al.). Food processing mostly involves the change or reduction of raw material used during manufacture into nanoscale or addition of nano additives for faster and better uptake of bioactive compounds after ingestion of food (Bai & Liu, 2016). Nano-encapsulation in food has attributed to controlled release, improved delivery and bioavailability of the so-called functional and nutritive ingredients for their intended purpose through protection of the components under adverse conditions (Pradhan et al., 2015). Nano-emulsions are thermally stable during processing thus retaining the characteristics sensory properties of the product moreover, the small

size readily allows interaction with the enzymes in the gastrointestinal tract readily (Hamad, Jong-Hun, Kim, & Rather, 2017). One of the biggest concern in the food industry is preservation to prevent food spoilage. Nanotechnology in food packaging prevents spoilage and prolongs the shelf life of food until acquired and ingested by the consumers (Kour et al., 2015). Nanocomposites polymers and polymer-metal oxides are often used in food application (Honarvar, Hadian, & Mashayekh, 2016), where these nanocomposites serve as fillers in the packaging material. The inherent properties of high surface ratio of NPs provide improved contact surface area for the release of preservatives, improved barrier and strength properties as compared to the conventional polymer materials. For example, a copolymer made of nano-clay in ethylene-vinyl alcohol and poly (lactic acid) have demonstrated increased oxygen barrier properties (Kour et al., 2015). NPs of silver, zinc oxide, titanium oxide, and chitosan in packaging materials have shown to inhibit microbial contamination (Chellaram et al., 2014). In addition, the application of nano-sensors in smart packaging enables the detection and sensing of a change in the temperature, gases, chemicals and microbiological contamination providing an accurate date of expiration, thus eliminating cost and waste of food through false expiration (Honarvar et al., 2016). Liao, Chen, and Subramanian (2005) demonstrated the application of thin-film-transistors (TFTs) in the electronic nose for sensing any changes in gases inside the package. Smart labelling in the form of nano-barcodes in the packages ensures safety, and traceability along the food supply chain (Chellaram et al., 2014). With the growing environmental issues related with the use of polymer materials, natural biodegradable polymers of polysaccharide and proteins are available but have comparatively less gas and vapour barrier properties and the incorporation of biodegradable nano-clay composites has improved barrier and mechanical properties (Honarvar et al., 2016).

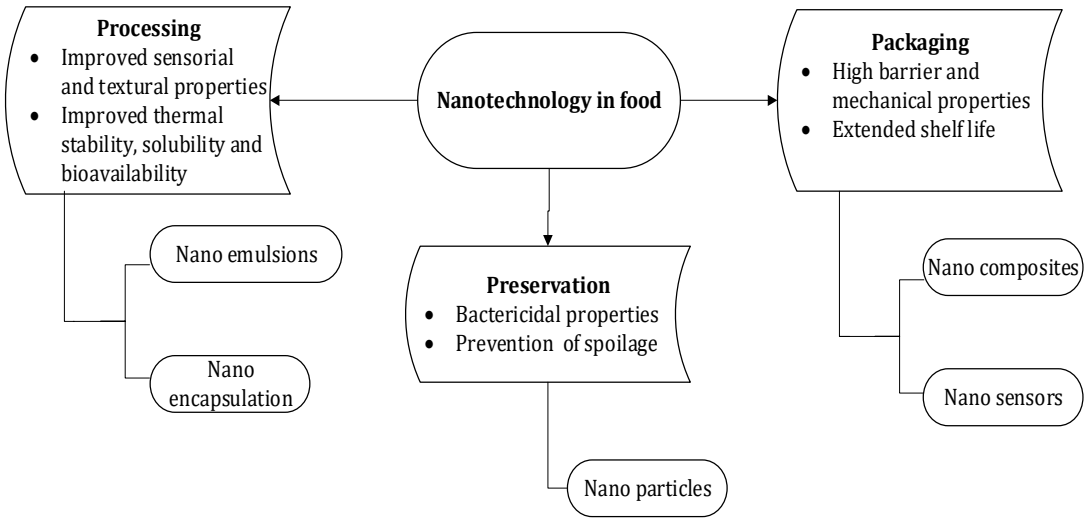

Figure 2.1 Application of nanotechnology in food.

2.1.2 Challenges and implications of nanotechnology

There is always a negative outcome from the application of any technologies and nanotechnology is no exception. The applications of nanotechnology is a well-explored area however, the understanding of implications and toxicological effects in terms of both human health and environment are limited. One of the challenges of nanotechnology faced by both the producers and the consumers is the worldwide lack of well-established, standardized and uniform monitoring and regulations pertaining to the application and disposal of nanomaterials (Bai & Liu, 2016) as well as the lack of systematic validation procedures in nanotechnology assessment (Pico, 2016). In addition, the unavailability of accurate data on the worldwide production of nanomaterial and no such requirements by the companies for the declaration of its use in products makes it even more challenging to determine the exposure quantities of engineered nanomaterials ENMs (Piccinno, Gottschalk, Seeger, & Nowack, 2012; Sodano, 2018). Adding up to the challenges is the complexity of food matrixes themselves which makes it harder for the detection of such minute materials in the food products (Rossi et al., 2014). Therefore, it is crucial to differentiate and separate ENMs from the naturally occurring nanoscale food components as these nanoscale components are known to hinder in the detection of NPs in food matrix (Pico, 2016). Likewise, Jain, Ranjan, Dasgupta, and Ramalingam

(2018) also advise the importance of distinguishing the naturally occurring NMs of food components or those formed during manufacturing processes like grinding and spray drying are often mistaken for intentionally added NMs. Furthermore, the concentration of these NPs are relatively small in food (Pico, 2016; Singh, Stephan, Westerhoff, Carlander, & Duncan, 2014) making it difficult for the researchers to obtain appropriate quantification data of NPs. Thus, the difficulty in NPs detection and measurement in a complex matrix and biological system adds up to the trouble in determining and predicting the potential of these uniquely different NMs to cause risks to both human health and environment as compared to the original bulk material. Thus, emphasizing the requirement of more research on toxicity and concrete safety monitoring and a regulation system put in place.

2.1.2.1 Characterization and detection of nanomaterial

Characterization of NPs is imperative to obtain a better understanding of the interactions of NPs in the biological environment as well as a foremost step in nano toxicity assessment (Caballero-Diaz & Valcarcel Cases, 2016; Elsaesser & Howard, 2012). The characterization of NPs includes chemical composition, size, shape, surface area, surface charge and agglomeration/aggregation state. The different analytical techniques available for characterization of NPs is illustrated in Table2.1.

Table 2.1 Analytical techniques available for the characterization of NMs and its relevance to nano toxicity.

Physiochemical characteristics	**Analytical techniques**	**Nanotoxicity relevance**	**Reference**
Chemical composition	Inductively coupled plasma (ICP) analyses, X-ray photoelectron spectroscopy (XPS), Fourier transform infrared spectroscopy (FTIR), Raman spectroscopy, X-ray fluorescence spectroscopy (XRF), energy dispersive X-ray analysis (EDX) and nuclear magnetic resonance (NMR)	Chemical interactions in a biological conditions	(Rossi et al., 2014)
Size, shape and crystallinity	Transmission electron microscopy (TEM), scanning electron microscopy (SEM), Atomic force microscopy (AFM), Nuclear magnetic resonance (NMR) and X-ray diffraction (XRD)	Transport and absorption mechanisms	
Surface area and charge	Dynamic light scattering (DLS), Zeta potential,	Induced cytotoxicity mechanisms	
Agglomeration status	NP-tracking analysis (NTA), Dynamic light scattering (DLS), Transmission electron microscopy (TEM),Atmospheric scanning electron microscopy (ASEM), atomic force microscopy (AFM)	Toxicity related to aggregated NPs as a function of concentration	

Detection of NPs in a complex food matrix and biological system is challenging due to some of the aforementioned issues and NPs inherent potency to undergo various physiochemical changes. Direct analysis of NPs in a complex matrix in most of the analytical equipment is not feasible, thus requiring sample preparation techniques. The principle of sample preparation techniques as mentioned in the literature is to separate the NPs from the complex matrices in their native form without causing any alterations. The sample preparation techniques also differ from NPs types, for example, wet digestion using mostly nitric acid, microwave and hot plate assisted digestion methods are used to separate inorganic NPs. Digestion techniques are used mainly in elemental analysis of NMs. Some metals such as Ag and Zn were found to dissolve in certain acids. Therefore, for the NMs which are not compatible with digestion in acids, (Pico, 2016) recommends an alternative techniques like centrifugation, filtration, separation using field flow fractionation (FFF), hydrodynamic chromatography (HDC) and other extraction techniques using water and organic solvents (Singh et al., 2014). Jain et al. (2018) also states that while the detection techniques for inorganic NMs such as gold, silver, and silica are well established, it is not easy to detect organic NMs as compared to inorganic ones because organic NMs such as proteins, lipids, polymers, and polysaccharides resemble the components that constitute the food and biological matrixes. Szakal et al. (2014) states that the choice of detection techniques also dependent on the individual research questions. For instance, can elemental techniques such as atomic absorption spectroscopy, inductively coupled plasma (ICP) with mass spectrometry (MS) or optical emission spectrometry (OES) be applied to determine the presence and absence of NPs? Electron microscopy techniques are used to answer the questions related to shape and size. Moreover, due to the complexity of NMs, a single method is not sufficient to address the research question leading to the application of a combination of analytical techniques (Laborda et al., 2016). The application of combined techniques used are, for example, electron microscopy coupled with x-ray spectroscopy and secondary ion mass spectroscopy for analysis of mixed NMs of organic outer and inorganic core (Jain et al., 2018; Singh et al., 2014).

2.1.2.2 Exposure routes of nanomaterial

A better understanding of the intended end utilization and disposal of nanomaterial is necessary for finding the possible routes of release and exposure of nanomaterial in terms of both human health safety and environmental implications. The NPs emission from the manufacturing industries gains entry into the environment. The effluents from the manufacturers and discharge from the consumer products entering the environment ultimately gain entry into the food chain (Jain et al., 2018). There are various methods applied by the researchers to understand and evaluate the safety and risks of ENMs emission into the environment, the life cycle model being the most applicable and reliable (Rossi et al., 2014). In a study by Keller, McFerran, Lazareva, and Suh (2013), from the total global production around, 63-91 % of ENMs are entering into the soil, 0.4-7 % into the water and 1.5 % into the air. Thus, with the increasing production and application of nanomaterial, it is of utmost importance to understand the safety implications. The basis of NMs exposure assessment is similar to that of chemicals assessment in foods. For example detection and analysis of NMs in food, consumption data from various scientific database, surveys, food additives labelling, combinational analysis of consumption data and quantities present in food using statistical tools and finally through various toxic kinetics models for determination of dissolution and absorption of NMs through the GI (gastrointestinal) tract (Bouwmeester et al., 2009).

The three main entry routes of NPS into the human body as described by many scientists are entry through, the respiratory tract, skin and GI tract. The entry of NPs through the skin is mainly associated with the application of cosmetics like TiO_2 found in sunscreens (Elsaesser & Howard, 2012; Jain et al., 2018). The NPS released into the air can gain entry through the respiratory tracts as in the case of asbestos particles. NPs after gaining entry into the respiratory tract can translocate through the olfactory bulb to other organs including the central nervous system reaching the brain (Elsaesser & Howard, 2012). ENMs can come in direct contact through production processes like the direct addition of nutrient additives, in form of nano delivery systems in the food or through in direct contact form the packaging

materials. For instance, there is likelihood of nanoparticles with antimicrobial properties coming into direct contact with the food surfaces to migrate from the packaging material into food (Bouwmeester et al., 2009). Consumption of food and beverages is the main exposure route of nanomaterial in the human gut (Handford et al., 2014). However, the exposure of the human body to ENMs is not only limited to ingestion of food, others sources also includes pharmaceutical drugs and cosmetics.

The process of digestion takes place firstly in the mouth, where the food is broken down into a uniform bolus by the chewing action of the teeth and the salivary enzymes in the mouth. This is followed by the mechanical grinding action of the stomach and digestion by the gastric enzymes and finally further digestion by the intestinal enzymes and absorption of nutrients from the digested food in the intestine. The design of the gastrointestinal wall is such that it ensures the digestion of food and absorption of nutrients and simultaneously prevents the entry of foreign and large materials through the gastrointestinal wall. However, research studies have demonstrated that the nanoparticles can translocate through the mucus and epithelium of the GI tract with a higher probability of entering into the other organs and tissues of the human body due to its smaller size and increased surface reactivity. Powell, Faria, Thomas-McKay, and Pele (2010) and Yada et al. (2014) states four possible mechanisms of translocation of nanoparticles in the GI tract as depicted in Figure 2.2. Transcellular through the epithelial cells, paracellular across the tight junctions of the epithelial cells, preposition “Volkhemir’s passage” through the gap of the villous tip and lastly cytosis and accumulation through the M-cell on the surface intestinal lymphoid. The passage of nanoparticles from the GI tract into the circulatory system and cellular level have been found to be related to cytotoxicity, genotoxicity, oxidative stress, and inflammation (Rossi et al., 2014).

Figure 2.2 Mechanisms of NMs uptake in the GI tract adapted from (Yada et al., 2014).

2.1.2.3 Toxicity of nano particles

The toxicity of nanoparticles is dependent on the physiochemical properties of the nanoparticles, structural changes occurring in the biological environment and vulnerability of the host (Powell et al., 2010). For example, gold nanoparticles of 15 nm size have been demonstrated to distribute widely in the blood, liver, spleen, lungs, gold nanoparticles size range of 15 - 50 nm can cross the blood brain barrier reaching the brain and better uptake of spherical shaped gold NPs as compared to rod shaped by the HeLa cells (Arora, Rajwade, & Paknikar, 2012). The toxicological effect of NPs differs depending on their physiochemical properties thus, requiring a separate risk assessment for each different NPs (Rossi et al., 2014). Elsaesser and Howard (2012) states that the main concerns arising from NPs are the ones, which are not bound, and moreover those incorporated into a liquid or gas matrix because of the NPs ability to move freely within the body as well as the environment. After gaining entry into the NPs body are ultimately cleared from the circulatory system by the action of liver and spleen in the form of faeces and urine, although some also accumulate in certain organs (Arora et al., 2012). Therefore, bio-distribution studies

of NPs are also important, where most studies revealed widespread distribution and traces of NPs in some organs. On the other hand, a better understanding of the connection between NPs physiochemical properties and ADME (absorption, distribution, metabolism, and elimination) is essential for toxicokinetics studies. Despite the growing concern of the toxicological effect of NPs, the information gap in understanding the properties, changes in the biological system, and quantification in food and exposures level obstruct the work of the safety and risk assessors (Handford et al., 2014).

2.1.2.3.1 Gastric models

The fate of the nanoparticles in the gastrointestinal tract in terms of structural changes and reaction with the digestive enzymes and acids is crucial in nanoparticles risk and safety assessment. Most of the toxicological studies are based on several *in vivo* and *in vitro* study models stimulating human GI physiology for determining the digestion, dissolution, and permeability of NMs in the GI tract. These study models have their own share of applicability and drawbacks.

In vivo models mostly includes oral administration in the form of food or water and analysis of the test animal's excreta, blood, lymph and GI tract for detection and permeability of NMs after exposure. Oral administration has the advantage of being more realistic and the gavage method has higher accuracy. The *In situ* perfusion model involves the determination of the permeability coefficient through live anesthetized animals usually rodents for having a similar coefficient of permeability with that of the human GI tract (Lefebvre et al., 2015). However, *in vivo* animal studies are usually subjected to higher dosages in simulated experimental conditions (Bouwmeester et al., 2009), thus questioning the validity and sensitivity of the test procedures for risk assessment. Owing to considerations about the animal welfare, ethical issues, and approval requirements, an alternative to *in vivo* toxicological studies are the *in vitro* models.

The *Ex vivo* study model utilizes the tissues taken out from the GI tract from an animal, kept under conditions similar to its normal functioning with higher output

compared to *in vivo*. However, the limiting factors are the absence of digestive fluids, difficulty in maintaining the cells viable for a long time (Lefebvre et al., 2015) and also lacking the ability to determine the physiochemical changes that can occur to the NMs when in contact with the digestive fluids along the GI tract.

In vitro models includes cell culture models and non-cellular fluid models. It is also crucial to consider the concentration of NPs in terms of initial quantity and uptake by cells during *in vitro* toxicological studies to come to a definitive decision (Elsaesser & Howard, 2012). The cell culture model uses cultured cells line form an organism or human GI tract mimicking the epithelium of the GI tract. Studies on cell cultures model have an added advantage of higher throughput, less cost and reliable permeability determination and prediction method (Lefebvre et al., 2015). The non-cellular fluid model is based on the application of simulated digestive fluids of the saliva, gastric and intestinal under static and dynamic process imitating the human digestion process. The *in vitro* fluid with lipid infused artificial membrane is able to determine passive transport of the NMs across the membranes. The *In silico* model is a computational system based on extrapolation of the existing data on digestion, permeability from various *in vivo* and *in vitro* studies. These models are cost efficient and useful for screening of solubility and absorption of NMs. However, the system requires more data and expertise to predict, validate and interpret the files (Lefebvre et al., 2015).

Regardless of many models available to determine the fate of NPs during gastrointestinal assimilation, the unavailability of standardized and valid methodology, the difficulty in imitating the exact human digestive physiology and the constant physiochemical changes of NPs in a biological environment. There is a further requirement of addressing the issues in developing a well-established risk assessment, regulatory and monitoring norms, detection and characterization of NPs, enhancement in the toxicological assessments models applicable to different NPs and validation of their results.

2.1.2.3.2 Toxicity

The studies conducted mostly include exposure to acute, subacute and sub chronic dosage, however, adequate information on the long-term exposure of NPs at acute low dosage is still lacking (Bouwmeester et al., 2009), because of NPs novel properties as compared to its original bulk chemical component. According to Elsaesser and Howard (2012), the interaction of NPs in the biological environment can be described as chemical mechanisms mainly due to the production of reactive oxygen species (ROS) which ultimately leads to secondary reactions causing damage to cells and also physical mechanisms due to textural and surface properties of NPs. In addition, NPs toxicity in the cellular system is considered to be mostly related to the generation of ROS (Powell et al., 2010) affecting the host's immune system (Bouwmeester et al., 2009). Apart from the generation of ROS, nano toxicity at the cellular level also includes neurotoxicity, genotoxicity and inflammation. NPs are known to cross the blood brain barrier reaching the brain, and there is a possible chance of crossing the blood milk barrier. The exposure of brain cells to NPs may be linked to neurodegenerative diseases like Alzheimer's disease, Parkinson's disease and Huntington disease (Win-Shwe & Fujimaki, 2011) due to the high susceptibility of the brain to oxidative stresses (Zhou, Peng, Seven, & Leblanc, 2018). A study under taken by Linse et al. (2007) showed NPs induces nucleation of protein fibrils in human β2-microglobulin which increases the formation of toxic amyloid related to amyloidosis disease. Arora et al. (2012) describe genotoxicity types as a primary, which is due to direct exposure of the NPs and a secondary by the interaction of the NPs with cells leading to the generation of secondary effects like oxidative stress and inflammation. Again, ROS has been identified to cause DNA damage and oxidative stress because of its high reactivity (Arora et al., 2012; Elsaesser & Howard, 2012). In addition, there is a potential for the development of allergies due to the exposure of the GI tract to high surface activity NPs capable of absorbing biomolecules (Bouwmeester et al., 2009). Chuang et al. (2013) revealed the silver NPs (AgNPs) association in causing increased allergenicity and inflammation in both healthy and allergic mice. On contrary, the principle of nanotechnology application in medicine includes NPs mediated drug delivery for treatment of neurodegenerative disease (Kolter, Ott, Hauer, Reimold, & Fricker, 2015), diagnosis and treatment of cancer,

and allergen specific immunotherapy (Di Felice & Colombo, 2017; Pohlit, Bellinghausen, Frey, & Saloga, 2017). However, studies on the toxic effects due to presence and accumulation of NPs still requires further research, validation and also the threshold levels of NPs toxicity potential when applied for their therapeutic purposes.

2.2 Hydroxyapatite (HA)

The word apatite comes from a Greek word "apiti" which means to deceive, as it has been mistaken by earlier mineralogist for precious gems like aquamarines, and amethysts (Sakae, Nakada, & LeGeros, 2015). This term "Apatite" describes a group of compounds with a generic formula $M_{10}(XO_4)_6Z_2$, where M^{2+} is a metal cation and XO_4^{3-} and Z^- are anions, having a hexagonal crystal system with space group P6/3mc (Legeros, Ito, Ishikawa, Sakae, & Legeros, 2010). Biological apatite is calcium phosphate salts, which is the main inorganic mineral constituent of bone and teeth. Biological apatite, consist mostly of carbonated hydroxyapatite, lacking hydroxyl groups and small amounts of Mg^{2+}, K^+, Na^+, Mn^{2+}, HPO_4^{2-}, and SiO_4^{4-} (Kolmas, Groszyk, & Kwiatkowska-Rozycka, 2014).

Hydroxyapatite (HA) is a crystalline hexagonal system with the chemical formula $Ca_{10}(PO_4)_6(OH)_2$ having a lattice parameter of $a = b = 9.432$ Å, $c = 6.881$ Å, and $\gamma = 120$ Å and stoichiometric with Ca/P ratio of 1.67 (Rivera-Munoz, 2011). X-ray diffraction studies are important techniques for determination of HA crystallographic since the early 1950s. At the molecular level HA, the crystal structure consists of ten calcium (Ca), six phosphates (PO_4) and two hydroxyls (OH) occupying well-defined positions in each unit cell. The (PO_4) group provides the skeletal framework of the unit cell (Shepherd & Best, 2011) in a tetrahedral arrangement of two layers in a set of three at a height ¼ and ¾ (Legeros et al., 2010). In the unit cell, there are two sites of calcium ions namely, Ca I and Ca II. Among the ten Ca atoms, four are Ca I in a set of two, while the other six Ca atoms are in a set of three as Ca II (Legeros et al., 2010). Ca I, the columnar Ca is positioned at a level of z =0 and z =0.5. Ca II the skew Ca is positioned at z = ¼ (0.25) and z = ¾ (0.75) creating

a triangle and then the calcium tunnel surrounding the OH ions located at the corners (Liu, Huang, Matinlinna, Chen, & Pan, 2013; Rivera-Munoz, 2011; Sakae et al., 2015).

Figure 2.3 Crystalline structure of Hydroxyapatite adapted from (Rivera-Munoz, 2011).

Figure 2.4 The structure of HA showing the columnar Ca and screw Ca forming a triangular tunnel adapted from (Sakae et al., 2015).

One of the primary features of the apatite structure is the ability to allow substitution of different ions in its three sub lattices of Ca^{2+}, PO_4^{3-}, or OH^- groups (Kolmas et al., 2014). For example, the substitution of Ca^{2+} ion sites by bivalent or monovalent cations such as Mg^{2+}, Sr^{2+}, Ba^{2+}, K^+ and Na^+, substitution of P by atoms such as C, As, V, S, and hydroxyl (OH^-) can be either left vacant or substituted by CO_3^{2-}, F^-, Cl^- (Liu et al., 2013). The substitution of ions causes variations to its crystallographic, physical and chemical properties and degree of change is proportional to the amount and size of the substituting ions. The substitution of F^- in OH^- causes a contraction in the *a*-axis with not much change in the *c*-axis while Cl^- substitution causes expansion in both *a* and *c*-axis (Legeros et al., 2010). The substitution capability of HA has been exploited and found useful in the production of HA with different chemical and mechanical properties as per their proposed application.

2.2.1 Production and physiochemical properties of hydroxyapatite nanoparticles (nHA)

Among the various methods of HA synthesis included in the literature, the production methods can be largely classified into different methods and sub-methods (Sadat-Shojai, Khorasani, Dinpanah-Khoshdargi, & Jamshidi, 2013).

1. Dry method

   Use of dry ingredients without requiring dispersing liquid and are suitable for mass production (Sadat-Shojai et al., 2013).

   i. Solid state

      This method involves the addition of dry solid ingredients containing calcium, phosphate, hydroxyl ions (Shepherd & Best, 2011) and previously prepared calcium phosphate (CaP) salt which is milled and calcified at a high temperature (1000^{o}C) (Sadat-Shojai et al., 2013). Even though this technique is relatively cheaper compared to wet preparation, it is not frequently sought technique (Chetty, Wepener, Marei, Kamary, & Moussa, 2012).

   ii. Mechanochemical

This method is similar to the solid-state process and the difference is with the type of ingredients used and operating parameters applied during the milling process like ball size, milling steps, milling duration and so forth. The advantage of mechanochemical is said to produce powders with a well-defined structure in nano-size range as compared to the heterogeneous structure in the solid state method (Sadat-Shojai et al., 2013).

2. Wet preparation

   This is the most sought after technique among the different production methods (Nayak, 2010) because it is simple and cost effective (Cox, 2012). HA crystal is produced through precipitation by the reactions of calcium and phosphate sources in an aqueous solution under wide temperature ranges, from 23^{o}C to < 100^{o}C (room temperature to close to the boiling point of water) at pH values > 4.2 (Sadat-Shojai et al., 2013).

   i. Chemical precipitation

      Dropwise addition of chemicals under continuous stirring and the resultant aqueous suspension is aged under atmospheric conditions, washed, filtered, dried and crushed into powder. The formation of the crystal is determined by the degree of solution saturation. Once the solution is supersaturated nucleation and crystal growth takes place (Cox, 2012). The final powder characteristics are dependent on the aging time and synthesis method. The crystallinity is determined by the reaction temperature. The temperature at 60 ^{o}C is referred to as transitional temperature where, temperature less than 60 ^{o}C gives the monocrystalline structure and higher than 60 ^{o}C gives a polycrystalline structure (Ferraz, Monteiro, & Manuel, 2004).

   ii. Hydrolysis method

      Involves hydrolysis of CaP phase into HA through dissolution and precipitation process. The phase transformation process is determined by parameters such as pH, temperature, and presence of other ionic impurities (Sadat-Shojai et al., 2013).

iii. Sol–gel method

This process involves the addition of calcium and phosphorous sources into a liquid dispersion to form "sol". The addition of a gelling agent leads to hydrolysis and polycondensation reactions aiding in the formation of a gel. This gel is subjected to a drying/calcification process of low heat treatment (less than 400^{o}C). During the production of fine powder, the incorporation of the aging step before drying prevents cracking of the crystal structure (Cox, 2012).

iv. Hydrothermal method

The reaction of chemicals at an elevated temperature and pressure during ripening step. The morphological structure is dependent on the pH during synthesis, like the production of a spherical or very short rod at higher pH values, nano-rod shaped crystals of one dimension or nano-rod plate of two dimensions at lower pH values (Sadat-Shojai et al., 2013). In comparison to other techniques like wet chemicals and sol-gel, the formation of HA crystals involves a one-step process (Cox, 2012). The crystals formed are homogenous in their composition having high density due to the compact and less porous structure (Shepherd & Best, 2011).

v. Emulsion method

The addition of two thermodynamically stable micro emulsions causing fusion-fission between the reverse micelles leads to the formation of HA crystals (Sadat-Shojai et al., 2013).

vi. Sono-chemical method.

The application of ultrasound produces acoustic cavitation generating bubbles. The collapse of the bubbles in the aqueous solution results in the formation of HA crystals (Sadat-Shojai et al., 2013).

3. High temperature

As the name suggests this method involves synthesis at a very high temperature causing full or partial burning of CaP sources.

i. Combustion

The basis behind the combustion method is similar to that used in explosives and propellants (Sadat-Shojai et al., 2013). Also known as self-propagating combustion synthesis (SPCS), it is a recent technique requiring less processing time (Cox, 2012). Initiation of reaction takes place at a low temperature, the increase in temperature causes sudden combustion reaching the maximum temperature promoting crystal growth and cooled rapidly for nucleation and inhibition of crystal growth. The combustion takes place with the aid of fuel like urea, glycine, and sucrose etcetera. (Sadat-Shojai et al., 2013).

ii. Pyrolysis

Spraying of a solution of CaP precursors into a flame inside a hot furnace by an ultrasonic generator results in complete vaporization of the droplets. Simultaneously, nucleation and growth of crystals occur in the vapour phase of the furnace (Sadat-Shojai et al., 2013).

4. Biogenic sources

Production of HA is similar to that of human bone apatite for better compatibility with the use of various biogenic sources like bio-waste, bovine and pig bones, fish scales, eggshell, seashells. The production of HA involves different synthesis process such as calcification, enzymatic or hydrothermal hydrolysis, extraction process, chemical treatment are applied (Sadat-Shojai et al., 2013). Simulated biological fluid (SBF) can also be applied in the production of HA. The calcium and phosphate ingredient is added into SBF with a salt composition similar to that of the human plasma producing bone mimic HA (Ferraz et al., 2004). The nucleation and growth of nano-sized crystals occur under physiological conditions at 37^{o}C temperature and at pH 7.4 (Nayak, 2010).

5. Combination process

Combination of two or more different methods provides a synergistic effect to with each other. For example, the combination of hydrothermal and mechanochemical, hydrothermal and emulsion, and hydrothermal and

hydrolysis methods are shown to accelerate the rate of chemical reactions, reduction in energy consumption required as compared to a hydrothermal method alone and also improves the properties of final resultant crystals (Sadat-Shojai et al., 2013).

The overall summary of the different HA production techniques in terms of crystal characteristics, advantages and disadvantages is depicted below in Table 2. 2.

Table 2.2 Summary of different HA production techniques.

Production Methods	Crystal Characteristics	Advantages	Disadvantage	References
Dry methods	Diverse morphology with high crystallinity and stoichiometric	Inexpensive	Larger particle size, low phase purity	(Montero, Saenz, & Castano, 2009; Sadat-Shojai et al., 2013)
Wet methods	Diverse morphology usually needle shaped in nano and micro size range with low crystallinity and both non-stoichiometric and stoichiometric	Relatively inexpensive and accurate control over the size and morphology	Low phase purity, time consuming.	(Sadat-Shojai et al., 2013)
High temperature	Diverse irregular in morphology of nano size with high crystallinity and stoichiometric	Chemical homogeneity	Secondary aggregates and poor process control	
Biogenic sources	Diverse morphology with high crystallinity and stoichiometric	Better chemical properties	Large particle size in blocks	
Combination process	Diverse morphology in nano size range with variable crystallinity and stoichiometric			

Even with all the different methods of HA powder production there are still issues related to phase purity and difficulty in regulating the properties such as morphology, size and size distribution, crystallinity, Ca/P ratio and degree of particle agglomeration (Sadat-Shojai et al., 2013). Thus, the choice of different

production methods plays a critical role in the production of crystals with specific properties. The nano sized material properties are different from the micro-sized bulk material. Hence, nano-sized HA crystals have high surface area and defects on the surface influences the adsorption of proteins, high diffusion forces at an elevated temperature, causing self-agglomeration and increased solubility (Demirchan & Gshalaev, 2012).

2.2.2 Applications of HA

Among the CaP salts the major mineral phase in calcified human tissues mainly the bone and teeth is carbonated hydroxyapatite (Sadat-Shojai et al., 2013). The application of HA is dominant in the biomedical engineering fields of bone grafts and dental implants due to its high resemblance to bone mineral. During bone grafting under biological conditions, the HA demonstrates excellent biocompatibility, bioavailability and, osteoconductivity without having any negative effect of toxicity (Chetty et al., 2012). HA can also be applied in therapeutic drug delivery system for the prevention of infection after bone surgery (Stigter, Bezemer, de Groot, & Layrolle, 2004). The other areas of applications include soil and water treatment, fertilizer, aquatic and waste treatment.

There are various forms of commercially available food grade HA serving as a source for calcium supplementation in the diet. Among the calcium salts sources for calcium supplementation, insoluble calcium salts are preferred over soluble calcium salts because of their higher heat stability (Tercinier, Ye, Anema, Singh, & Singh, 2014a). Thus, HA as one of the insoluble calcium sources is applied in the fortification of dairy and soy-based products demonstrating good bioavailability (López-Huertas et al., 2006).

2.2.3 Crystal growth and dissolution/solubility of HA

Generally, crystallization of calcium phosphate involves the formation of a metastable precursor phase such as amorphous calcium phosphate, brushite (dicalcium phosphate dihydrtae), octa calcium phosphate, and tricalcium phosphate

that transforms into the final product, the least soluble hydroxyapatite phase (Wang & Nancollas, 2008). The different phase can be determined by the Ca/P molar ratio; low Ca/P ratio indicates an acidic phase with a more soluble Ca/P phase. For instance, in acidic conditions, brushite (DCPD), octacalcium phosphate is formed, whereas in neutral or basic conditions, the least soluble HA is formed (Wang & Nancollas, 2008).

The growth of crystal is dependent on different solution parameters such as super saturation, pH, temperature and ionic strength. These parameters govern both the thermodynamic and kinetics of crystallization (Orme & Giocondi, 2007; Wang, Lu, Xu, & Zhang, 2011). The super saturation ratio (S) value determines whether the crystal will dissolve or grow for instance, the value $S > 1$, the solution is supersaturated leading to dissolution while $S < 1$, the solution is under saturated causing crystal growth and $S = 1$, the solution is in equilibrium. The lowering of pH results in the reduction in the degree of saturation shifting the surface charge (positively charged acidic and negatively charged basic solution) by altering the distribution of proton and hydroxyl groups hydrating the interface. Ionic strength influences the ion-ion electrostatic interaction and electrostatic interactions between the solution and the surface crystallization (Orme & Giocondi, 2007; Wang et al., 2011). Temperature affects the kinetics of adsorption, desorption, diffusion, the solubility product and association constant ultimately affecting the solution speciation. However, the temperature inside the body remains inside the body hence, is a parameter during *in vitro* for measurement of activation energy. The Ca/P activity ratio affects the growth of crystals, which depends on the concentration of rate limiting ions rather than only on saturation and free energy. In a multispecies, system the growth rate depends on the rate of adsorption and desorption of ions making the unit cell (Orme & Giocondi, 2007).

In classical nucleation theory (CNT), crystallization occurs by the nucleation of the unit cell ions in a saturated solution with phase transformation in later stages (Wang et al., 2011). Most of the crystallization studies are undertaken in colloidal systems of organic proteins because the suspended solids are visible under microscope and

similarity of its crystallization phase to that of the atomic and molecular system (Wang & Nancollas, 2008). In 1897, Ostwald stated the two-step nucleation theory (TSN); the formation of the first phase is usually unstable and followed by transformation into a state of increasing stability that can be accomplished by overcoming free energy closest to the mother phase. Wolde and Frenkel (1997) demonstrated the Ostwald's rule in their study showing the occurrence of intermediate dense fluids leading to systematic growth and crystallization of proteins. Chung, Kim, Kim, and Kim (2008) studied the crystallization in the inorganic system of metal phosphate. They also demonstrated the Ostwald's rule of phase transition, the conversion of amorphous phase into a stable crystalline phase through transitional crystalline phases. Zhang and Liu (2007) demonstrated the multistage nucleation theory (MNT); firstly, nucleation of amorphous dense droplets from the mother phase occurs. This is followed by the creation of a few unstable sub crystalline nuclei produced through fluctuation from the tiny dense droplets, which is in contrast to earlier theoretical calculations.

The number of available *in situ* measurement techniques to measure the dynamics of crystallization are limited because of the difficulty in maintaining the feasibility in a liquid environment. These include spectroscopic techniques such as x-ray diffraction measurement, Raman spectroscopy, Fourier infrared spectroscopy, scanning probe microscopy/atomic force microscopy. Solution probes such as pH meter, ion-selective electrodes are available for the measurement of solution chemistry (Orme & Giocondi, 2007). The constant composition experiment is prominently used in the determination of solution kinetics that the variation in the solution composition is due to nucleation and crystal growth, however, it has limited ability to quantify at the molecular state (Orme & Giocondi, 2007). Atomic force microscopy is considered as an important tool in investigating the crystallization process at a molecular level. As per AFM, the crystal surface consists of flat regions known as terraces and raised layers called steps. The binding of the neighbouring molecules during growth is stronger as it takes place at the edge from the step layers as compared to the flat region. The most reactive part of the step edges are the kink sites, both attachment and detachment occur from the step edges. The formation of

new steps are dependent on critical size. In the case where there are no pre-existing steps, nucleation occurs via dislocation hillock (Wang & Nancollas, 2008). The growth and stability of calcium phosphate crystals are influenced by the presence of several other impurities present in the matrix solution such as ions of Mg, F, Cl, Na, and presence of proteins, other phosphates and carboxyl molecules. The attachment of these impurities on the steps edge and active site kinks behaves as blockers in preventing crystal growth known as inhibition through step pinning. Similarly, the addition of citrate also showed inhibition of crystal growth reduction through step density. Here, the inhibition of crystal growth is due to alteration in the rate at which the steps are generated rather than changing the step speed (Orme & Giocondi, 2007).

Solubility properties are important in determining various chemical reactions such as hydrolysis, dissolution, precipitation and phase transformation of chemicals (Pan, Chen, & Darvell, 2010). Most dissolution studies are based on assumption that the dissolution process is a spontaneous process continuing until equilibrium is reached or all the solid phases are dissolved. The rate law is usually applied to express the dissolution process (Tang, Wang, & Nancollas, 2004a).

HA is thermodynamically stable in the pH (4.2-12.4) having a solubility product Ksp of 58.65 at 37^{o}C (Uskokovic & Uskokovic, 2011). The determination of solubility is based on a large addition of an excess of solids under continuous stirring. The solubility product is generally accepted as Ksp = -log ($[Ca^{2+}]^5$ $[PO_4^{3}-]^3[OH^-]$) or Ksp $[Ca^{2+}]^5[PO_4^{3}-]^3[OH^-]$. However, according to Pan et al. (2010), calcium phosphate dissolution is a complex process because of incongruent dissolution (co-existence of many bulk and surface phases), occurrence of non-stoichiometric phases, lattice substitutions by the impurities, and the existence of other ions species in solutions which are not usually taken into account during calculation of solubility product. They worked on the development of a new technique of solid titration for determining the true equilibrium in complex solids and solutions, which demonstrated excellent reliability and reproducibility.

Factors such as preparation methodology, crystalline structure, and substitution of lattice structure affect the solubility of hydroxyapatite. For example, highly crystalline structure and substitution on the crystal lattice reduces the solubility (Fulmer, Ison, Hankermayer, Constantz, & Ross, 2002). Ehrlich, Koutsoukos, Demadis, and Pokrovsky (2009) notes that the pH of the solution strongly influences calcium phosphate dissolution as depicted from the solubility isotherm calculation in Figure 2.5 below.

Figure 2.5 Solubility isotherm calculation of Calcium phosphate at 37^{o}C, 0.15 M NaCl adapted from (Ehrlich et al., 2009)

In addition, the effect of pH on the formation of calcium phosphate is related to the properties of phosphate in the solution. This is explained by the presence of triprotic equilibrium in the system; changes in pH gives four forms of protonated phosphoric acid (Lynn & Bonfield, 2005) as depicted in Figure 2.6.

Figure 2.6 Schematic representation of tripotic equlibrium in a sytem adapted form (Lynn & Bonfield, 2005).

Dorozhkin (2002) has presented a detailed review on the dissolution models for calcium apatite which consisted of eight dissolution models, taking into account all the possible conditions in a solution such as pH, the extent of saturation, composition, solubility, particle size, phase transformation, ions substitution and surface defects. However, the dissolution behaviour of HA is greatly relevant to the study, thus a brief description of these eight dissolution models are presented as follows:

i. Diffusion or kinetic controlled

   Also known as the two-site model, the diffusion controlled model is determined by the transport of chemicals from the bulk solution (saturated) to surface of crystals while kinetically controlled the solution is under saturated and is determined by chemical transformation on the surface (Fox, Higuchi, Fawzi, & Wu, 1978). The diffusion model is based on the concentration gradient within the Nernst diffusion layer while the kinetic model is the ionic gradient of ionic chemical potentials between the apatite crystal surface and bulk solution. However, the model is sensitive to experimental conditions, only specific to those particular experimental conditions and hence cannot be extrapolated (Dorozhkin, 2012).

ii. Mono and Poly nuclear model

The model is based on the study under constant composition conditions. Depending on the experiment, calcium apatite samples are placed in a solution (under saturated for dissolution and saturated for growth), pH (acidic for dissolution and base for growth) and an amount of chemicals added as a function of time (Dorozhkin, 2012). In a poly nuclear dissolution model, the lateral growth rate of the nuclei is relative to the difference in the total concentration of Ca^{2+} in a saturated solution and in the solution, and the rate constant is related to the frequency for a Ca^{2+} to overcome the diffusion layer and simultaneously, moderately dehydrate (Christoffersen, Dohrup, & Christoffersen, 1998). Figure 2.7 demonstrates the schematic illustration on the different models.

(A) (B) (C) (D)

Figure 2.7 Different models adapted from (Ehrlich et al., 2009).

According to Ehrlich et al. (2009) the detachment of ions takes place; from (the center leading to step disintegration (Figure 2.7 A), from multiple centers (Figure 2.7 B), from multiple centres in multiple steps (Figure 2.7 C), and from the active sites in a spiral at a constant velocity (Figure 2.7 D).

iii. Self-inhibition

According to this model, the development of a layer rich in calcium as depicted in Figure 2.8, on the surface inhibits the dissolution process of apatite. The dissolution of apatite takes place from loss of ions from the calcium and phosphate from the surface. After the initial dissolution of the

apatite, some of the ionic calcium is adsorbed back on the surface of the apatite forming a layer rich in calcium (Mafe, Manzanares, Reiss, Thomann, & Gramain, 1992). However, the positively charged apatite in acidic solution may not be due to the attachment of calcium ions but due to absorption of protons and other impurities present in the solution (Dorozhkin, 2012).

Figure 2.8 Adsorbed layer of calcium ions of the HA surface. The calcium ions are assumed as a hard disk of radius $2L_D$ from (Mafe et al., 1992).

iv. Stoichiometric/nonstoichiometric dissolution

In stoichiometric (congruent) dissolution, the ionic concentration is proportional to molar concentration whereas in nonstoichiometric (incongruent) dissolution the release of ions is different resulting in the formation of a layer on the surface with a different composition from the bulk solid. The experimental conditions determine the dissolution mechanisms, which could be either congruent or incongruent or combination of congruent and incongruent (Dorozhkin, 2012).

v. Chemical model

The chemical model is based on the order of release of ions from the surface; first from fluro or hydroxylapatite, next from calcium followed by phosphate as shown below (Dorozhkin, 1997):

$Ca_5(PO_4)_3(F, OH) + H_2O + H+ = Ca_5(PO_4)_3(H_2O)+ + HF, H_2O$ (1)

$2Ca_5(PO_4)_3(H_2O)+ = 3Ca_3(PO_4)_2 + Ca^{2+} + 2H_2O$ (2)

$Ca_3(PO_4)_2 + 2H+ = Ca^{2+} + 2CaHPO_4$ (3)

$CaHPO_4 + H+ = Ca^{2+} + H_2PO_4$ (4)

vi. Etch pit formation

The structural defects, like dislocation on the surface of apatite lead to the formation of pits that initiates the dissolution process. The occurrence of pits is proportional to dissolution kinetics and dissolution time that grows with the progression of dissolution, moreover the crystals should be large enough to allow the formation of large pits. However, the addition of NaCl can suppress the formation of pits. The pits formed are usually hexagonal in shape owing to their crystal symmetry and nonhomogeneous dissolution whereby, some pits dissolve faster than the others (Dorozhkin, 2012). Recently the phenomenon of size effect is considered a limiting factor in pit formation. The dissolution process is spontaneous when the etch pit size is independent of critical size. A higher the critical value is able to overcome the free energy barrier leading to the formation of pits. However, the reduction of crystal size due to dissolution leads to a lower critical size value ultimately suppressing/inhibiting the dissolution process (Tang et al., 2004a). This size effect is particularly important in dealing with nanostructured bio minerals, where the dissolution is inhibited even when the biological matrix is under saturated (Tang et al., 2004b).

vii. Ion exchange

In this model, there is an exchange between the anions of the solution on the surface of the apatite and simultaneous release of calcium and phosphate into the solution. (Lopez-Macipe, Gomez-Morales, & Rodriguez-Clemente,

1998) found the adsorption to be time dependent and followed the *Langmuir* isotherm. They used a sodium citrate concentration of (0.05-1 mmol/L) under continuous stirring maintained at pH 6-8 for 14 h. The results demonstrated that the absorption of citrate ions occurs in two ways; cit^{3-} interacted weakly (one citrate per two Ca sites) while the $Hcit^{2-}$ interacted strongly (one citrate per one Ca site). Yoshida et al. (2001) proposed the "adhesion/decalcification concept", and, according to this concept the interaction with HA occurs in two phases. First, the interaction of carboxyl group of the acid on the Ca surface through formation of the ionic bond. Simultaneously, the PO_4^{3-} and OH^- are released into the solution. In the second phase, the acid remained attached on the surface with a smaller amount of decalcification or the acid is detached from the surface leading to extensive decalcification. The diffusion rate of calcium ions in the acidic solution determines the adhesion and decalcification of acid.

viii. Hydrogen catalytic

The protonation of the negatively charged oxygen ions of the phosphate group resulting in changes on the surface catalyses the dissolution process by the breaking of Ca-O bonds. Protonation results in the reduction of the surface anions charge lowering the Coulomb attraction. This is similar to where the decrease in pH leads to higher dissolution. However, due to the lack of experimental techniques, this catalytic effect has not yet been elucidated (Dorozhkin, 2012).

As per Ehrlich et al. (2009) dissolution mechanisms generally follows two methods; "diffusion reaction" and "surface layer". In diffusion reaction, there is a formation of the Nernst diffusion layer at the solid-liquid interface. This thickness of the layer decreases with increasing agitation and reducing crystal size. In surface reaction, the defects present on the crystal surface like kinks, steps, terraces, ledges and holes or vacancies leads to dissolution via detachment of crystal units. However, none of the models provides a generalized dissolution mechanism. This does not indicate

the models are wrong but are accurate in terms of their own experimental conditions (Dorozhkin, 2012).

HA is predominately applied to biomedical science hence, many of the studies related to HA dissolution, precipitation, and any negative side effects from its use are carried out in human body fluid physiological conditions. Similarly, Dorozhkin (2012) states that the dissolution models stated above have mostly been carried out in less acidic conditions of pH >4.5 to 8 with no studies under acidic pH <2. Dissolution studies of HA in stimulating human digestive conditions are lacking and only one relevant study was found. Schoepf et al. (2017) studied the dissolution of HA using simulated body fluids in static digestion models. However, the study on dynamic *in vitro* model mimicking human digestive process has not yet been investigated. Thus, the main objective of this thesis is to determine the behaviour of nHA under simulated gastric conditions.

2.3 Milk calcium and its significance

2.3.1 Calcium in milk

Water, milk fat (lipids), proteins and lactose (milk sugar) constitutes the major components in milk along with several minor components also known as trace elements, which includes minerals (salts), vitamins, enzymes, hormones and miscellaneous compounds (Fox, 2008). The mineral component of milk represents a minor fraction of only about 8-9 g/L, however the minerals component plays a significant role in the structure and stability of milk caseins, source of nutrition for the growth of new born, bone formation and processing of dairy products (Gaucheron, 2005; Lucey & Horne, 2009). The different mineral components of milk is presented in Table 2.3.

Factors such as different breed, lactation time, seasonal change and diet as well as other factors like faulty procedures, error during analysis and contamination from collection and processing equipment cause minor variations in the mineral compositions. For instance, colostrum milk contains higher calcium content than

usual milk, whereas mastitis milk contains an increased amount of sodium and chloride content (Cashman, 2011; Lucey & Horne, 2009).

Table 2.3 Mineral composition of milk adapted from (Lucey & Horne, 2009).

Mineral	Concentration (mg/kg)	Concentration (mmol/kg)
Calcium	1043-1283	26-32
Magnesium	97-146	4-6
Inorganic phosphate	1805-2185	19-23
Total phosphate	930-992	30-32
Citrate	1323-2079	7-11
Sodium	391-644	17-28
Potassium	1212-1681	31-43
Chloride	772-1207	22-34

Milk salts based on their solubility are partitioned between the serum (diffusible) and (colloidal) micellar phases (Table 2.4). While most of the salts are soluble in the serum phase, the calcium and inorganic phosphate salts are supersaturated in the serum phase. Only about one-third of calcium, half of the inorganic phosphate, two-third of magnesium and 90 % of citrates are found in the serum phase and very few calcium bound to α-lactalbumin (Fox, 2008; Gaucheron, 2005). While the non-diffusible salts are found mostly in the colloidal phase bound to casein micelles known as the colloidal calcium phosphate (CCP) or micellar calcium phosphate (Holt, 2004). Different methods such as dialysis and ultrafiltration membranes with a molecular weight limit of 10000–15000 Da, ultracentrifugation at 80000 g for 2 h and 100000 g for 1h and preparation of whey after rennet coagulation can be applied for partitioning of serum and colloidal phases (Gaucheron, 2005). de la Fuente, Fontecha, and Juarez (1996) describes the applicability of the various salt partition methods and suggested the use of correction factor to take into account the excluded volume in calculating the serum concentration.

Table 2.4: Salt partition in cow's milk from (Gaucheron, 2005).

Constituents	Concentration
Casein	26.1 g/L
Total Ca	29.4 mM
Soluble Ca	9.2 mM
% of soluble Ca	31
Micellar Ca	20.2 mM
Micellar Ca/g casein	0.77 mM
Total Pi	20.9 mM
Soluble Pi	11.2 mM
Micellar Pi	9.7 mM
% of soluble Pi	54
Total Mg	5.1 mM
Soluble Mg	3.3 mM
% soluble Mg	65
Micellar Mg	1.8 mM
Ester phosphate	3.5 mM
Total Citrate	9.2 mM
Soluble Citrate	8.2 mM
% soluble Citrate	89
Soluble Na	24.2 mM
Soluble K	34.7 mM
Soluble Cl	30.2 mM

2.3.1.1 Milk mineral equilibrium

The ions in the diffusible phase are found as free ions and in association with different ions (ion pairs), this association is dependent on the solubility of the salts and the affinity (association constant) of the different ions together (Gaucheron, 2005; Holt, 1997). The separate determination of these different ions in the serum phase is not possible, the first ion equilibrium model in milk diffusate was proposed by Holt, Dalgleish, and Jenness (1981). Many models have been proposed and developed over the years by numerous authors describing the mineral equilibrium

in systems mimicking that of milk or milk diffusate. The recent mineral equilibrium model, (Holt, 2004; Mekmene, Le Graet, & Gaucheron, 2009) takes into account the micellar and serum phase. Mekmene, Le Graeet, and Gaucheron (2010) developed a model based on the function of milk pH during acidification. However, the basis of the models is on the assumption made regarding the nature of minerals present between the phases and the CCP.

The non-diffusible ions may not totally be part of calcium phosphate, suggesting colloidal calcium in milk to be a mixture of calcium caseinate (containing organic phosphate) and calcium phosphate (inorganic phosphate) (Gaucheron, 2005). It is not possible to separate the two forms of CCP thus, making it difficult to determine the composition of CCP experimentally. However, based on the Ca/P ratio analysis there are several structures of CCP (Gaucheron, 2005). The CCP could be of tricalcium phosphate with Ca/P ratio of 1.5 based on the assumption that the phosphate group of casein with bound calcium is not part of the calcium phosphate. However, if the phosphate group of casein with bound calcium were presumed to be an integral part of calcium phosphate, the Ca/P ratio would be close to 1.0 with CCP of more like a brushite type, which was further supported by x-ray absorption and infrared spectroscopy analysis (Le Graet & Brule, 1993). High-resolution electron microscopy and diffraction showed the structure of CCP to be of nanometer size having a high electron density of amorphous nature (Lucey & Horne, 2009). Figure 2.9 shows the schematic representation of mineral equilibrium between the ions species in the serum and colloidal phase.

Figure 2.9 Mineral equilibrium in milk representing the serum and micellar phase (Gaucheron, 2005).

2.3.1.2 Caseins micelles

The CCP is important for maintaining the structure and stability of casein micelles thus, it is crucial to understand both the structure and properties of caseins. Casein forms the protein component of milk representing about 80 % of the total milk proteins. Casein micelles contain 94 % protein and the remaining 4 % consists of calcium traces of citrate and magnesium, commonly stated as colloidal calcium phosphate (CCP). The micelles scatter light, which gives milk its white colour. Casein micelles are spheres, ranging In size from 50–500 nm with an average 120 nm as measured by electron microscopy and the mass ranging from 10^{6} to 10^{9} Da with an average of 10^{8} Da (Fox, 2008). The size of the casein micelle can be determined by the amount of κ–casein covering the surface, where the size is inversely proportional to the amount of κ–casein (Dalgleish, 2011).

There are four types of casein molecules: α_{s1}-casein, α_{s2}-casein, β-casein and κ-casein in approximate comparative quantities of 4:1:3.5:1.5, respectively (Dalgleish & Corredig, 2012). The casein molecules are highly flexible due to a high level of proline in the amino acid residue. The phosphate groups in the 8-9, 11 and 5 phosphoserine residues of the α_{s1}-caseins, α_{s2}-casein, β-casein respectively are negatively charged and serves as the binding site for cations especially Ca^{2+} (Gaucheron, 2005). As a result α_{s1}-, α_{s2}-, β-caseins are sensitive to calcium concentration and precipitates, whereas κ-casein has only one phosphoserine

residue making it insensitive to calcium. The κ-casein are highly glycosylated (50%) resulting in a hydrophilic C-terminal. This characteristic of κ-casein is important in the stabilization of micellar structure (Dalgleish, 2011). κ-casein interacts with calcium and stabilizes other casein molecules forming a stable colloidal phase (Qi, 2007). Moreover, κ-casein is found on the surface of the micelles, extending from the surface forming a "hairy layer" stopping aggregation through steric stabilization (De Kruif & Zhulina, 1996). According to Dalgleish (1998) the micellar surface is not completely surrounded by κ-casein and aggregation is prevented through steric stabilization. Typically, casein micelle structure consists of 15 % κ–casein while the remaining 85 % is of calcium sensitive α_{s1}-caseins, α_{s2}-casein, β-casein. How is it possible for such a small portion of κ –casein to stabilize the micelle structure? The best explanation is the arrangement of κ–casein on the surface covering the calcium-sensitive caseins, similar stabilization of a lipid emulsion by emulsifiers (Fox, 2008). The micelles bind water and can hydrate around 2-3 g H_2O/g protein and concentrations of 104-1016 micelles/ml in milk (Horne, 2008). There are various models proposed for casein micelles structure, most of which suggests that the CCP forms an integral part of casein micelle providing stability to the micellar structure. There have been numerous studies regarding the micelle structure however, the following three models are often proposed.

The submicelles model first proposed by Morr (1967), in which the subunits consisting of a core of α_{s1}-, α_{s2}-, β-caseins covered by κ–casein in the casein micelles are linked together by the CCP. However, this model has evolved and undergone many changes over the years. Slattery and Evard (1973) proposed that κ–casein on the submicelles surface is localized creating separate κ–casein deficient (hydrophobic) and κ –casein rich (hydrophilic) regions. The hydrophobic bond links the submicelles together and inhibits aggregation of subunits by complete coverage of κ–casein on the surface. Conversely, this model does not state the role of CCP in casein micelle stability. Schmidt (1980) further postulated the model; the submicelles regions not covered by κ–casein comprised of phosphoserine residues, which associates with CCP forming aggregates. Walstra (1999) improved the model; the CCP is present not only on the surface but also inside the submicelles. While most

of the studies on the submicelles model were based on the electron microscopy, McMahon and McManus (1998) debated this method as it is easier to produces artefacts during sample preparation.

Nanocluster model, (Holt, 1992, 1996); here the casein submicelles with a flexible web-like 3D structure called the "hairy layer" on the outside are held together by nanoclusters of CCP. These hairy layers of 5-10 nm in thickness are extended outward from the hydrophilic C-terminal of κ–casein preventing aggregation of the micelles. The hairy layer serves as an ionic brush preventing aggregation through steric stabilization (Fox, 2008). The calcium phosphate nanoclusters are a few nanometres in size and are made up of a calcium phosphate core and a casing of casein phosphopeptide (Gaucheron, 2005). Farrell, Malin, Brown, and Qi (2006) suggests that the formation of CCP nanoclusters occurred after the formation of casein super-molecules in the Golgi vesicles through a series of events.

The recent casein micelle structure of the dual-binding model (Horne, 1998, 2006, 2008), the assembly and structure of micelles involve a polymerization process where casein molecules are linked via hydrophobic regions and through bridging of CCP nanoclusters. The casein molecule functions as block copolymer with distinct hydrophobic and hydrophilic regions. The phosphoserine clusters make the hydrophilic regions negatively charged and prevent further aggregation via electrostatic repulsion. However, the net negative charges are neutralized by the CCP nanoclusters which creates a multitude of hydrophobic interactions upstream and downstream of the nanocluster link (Horne, 2008). (Dalgleish, 2011) proposed casein micelles have an open structure with the presence of water channels and nanoclusters within the micelles structure. The binding of α-caseins and β-caseins with CCP nanoclusters inside the micelles prevents uncontrolled CCP growth and precipitation, while the κ–casein on the surface provides stabilization through electrostatic repulsion.

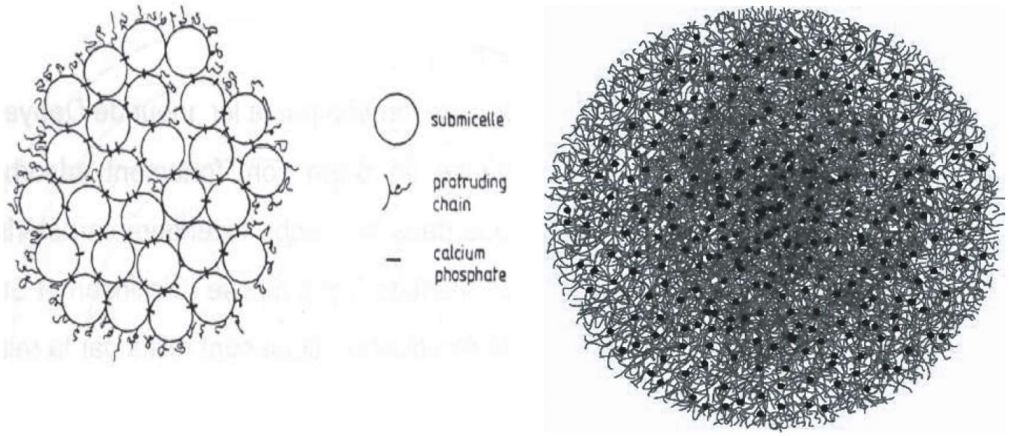

(a) (b)

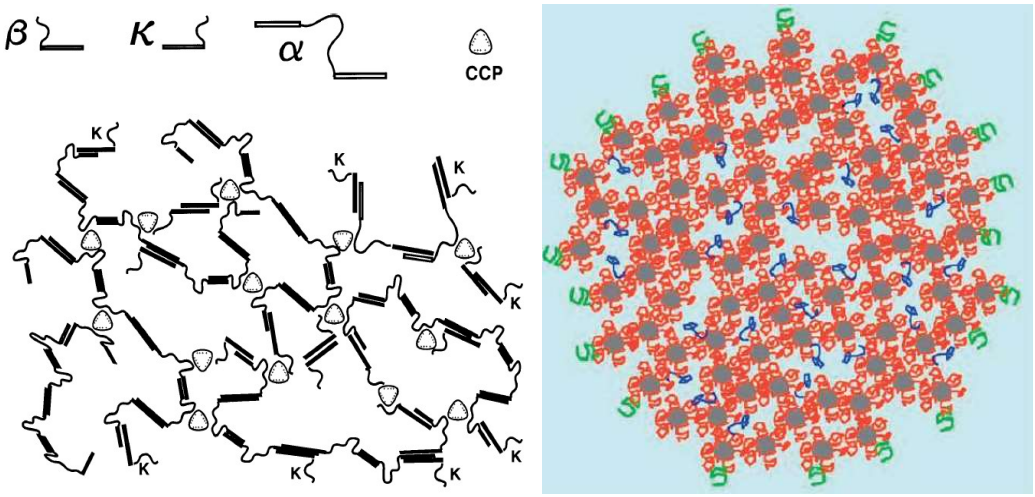

(c) (d)

Figure 2.10 (a) Casein submicelle model (HA thesis) (b) Casein nano cluster model from (Holt, 1992) (c) Dual binding model from (Horne, 1998) (d) Casein micelle structure with calcium phosphate nanoclusters (grey) with attached caseins (red) and κ-casein (green) on the surface. In the interior of the micelle the "hydrophobically bound" is the mobile β-casein (blue) inside the water channels adapted from (Dalgleish, 2011).

The common element in all the above three casein structure models is the surface role of κ–casein in providing a stabilizing effect and the binding role of CCP while, the difference is mainly in relation to the internal structure of the micelle (Fox,

2008). Most of the models emphasize the importance of hydrophobic bonding and CCP's role in the casein micelle's structure and stability.

2.3.1.2 Factors influencing milk salts equilibrium and casein micelle stability

Various factors affect the mineral balance between the serum and colloidal phase, which, in turn, affect the stability of casein micelle as well as the functional properties of milk products. Thus, the impact of various processing parameters are reviewed.

Temperature

Casein micelles are relatively stable during the heating process, which is of significance to the dairy industry in manufacturing high heat-treated milk products. However, the solubility of CCP increases during heat treatment. This is due to the reduction in pH of the milk during the heating process as shown in the reaction (Lucey & Horne, 2009).

$$3Ca^{2+} + 2HPO_4^{2-} \longrightarrow Ca_3(PO_4)_2 \text{ (precipitate)} + 2H^+$$

The change in mineral balance depends on the heating conditions, for example, less than 95°C for a few minutes and high heat treatment at 120°C for 20 min causes irreversible changes to both the milk salts and casein micelles (Gaucheron, 2005). While the change in salt equilibrium during moderate heating is restored by cooling, however, some hysteresis occurs during cooling. Thus, during freezing as the water component of milk freezes, there is less solvent for the same concentrations of solutes, thus the soluble calcium phosphate precipitates as $Ca_3(PO_4)_2$ (Fox, 2008). On the other hand high heat treatment results in dephosphorylation and dissociation of κ–casein and interaction of κ–casein with whey proteins (Singh, 2004). This dissociation of κ–casein is strongly dependent on the pH of milk, just as dissociation increases with increasing pH. Thus, κ–casein depleted micelles forms aggregates and precipitates during storage (Huppertz, Fox, & Kelly, 2018).

pH

During acidification, there is a reduction in milk pH, resulting in protonation of citrate ions and inorganic phosphate ions. As a result, the micellar calcium phosphate, citrate, magnesium associated with the micellar phase dissociates into the serum phase, increasing the ionic calcium concentration (Gaucheron, 2005). The solubilisation of CCP is pH dependent. Le Graet and Brule (1993) studied the effect of acidification on mineral equilibrium in skim milk. Their study showed that upon acidification, the CCP completely solubilized at pH 5.2 and the calcium bound to the casein micelles solubilized completely at pH 3.5. This change caused by acidification is irreversible, even upon neutralization process the milk had reduced buffering capacity and showed increased ionic calcium concentrations (Lucey & Horne, 2009).

Addition of Calcium

The effect of calcium addition is significant from a fortification point of view and milk stability during heat processing. Adding calcium in milk changes the mineral equilibrium by increasing the calcium content in both the micellar and serum phase of milk. The study by Philippe, Gaucheron, Le Graet, Michel, and Garem (2003) demonstrated a decrease in the pH of milk from 6.75 to 6.30 upon supplementation of 13.5 mmol/kg $CaCl_2$. This reduction in pH consequently resulted in an increased ionic calcium from 1.56 to 6.94 mM. However, upon adjustment of pH back to 6.7, it showed 80 % of the added calcium bound to casein micelles and 20 % in the ultra-filtrate. Philippe, Le Graet, and Gaucheron (2005) added different cations of Fe, Cu, Ca, Zn and Mg with an additional rate of 2.5–8.0 mmol/kg of cations. The study demonstrated a similar increase in association with these cations with the casein micelle showing a linear relationship between, the added cations and inorganic phosphate ultra-filtrate. On the physiochemical changes of casein micelles, the net negative charge of the casein micelles decreases probably due to the shielding effect created by the binding of the ionic calcium with casein micelles. The decrease in hydration capacity of casein micelles was observed with the release of water, however, the size of the casein micelles remains unaffected, thus, decreasing the heat stability of casein micelles (Philippe et al., 2003).

Calcium chelators or sequestering

From the industrial perspective, calcium in milk is removed to improve the heat stability, storage of milk and prevention of fouling of the plate heat exchangers through calcium phosphate deposition (Gaucheron, 2005). Calcium can be removed using calcium chelating agents having a high affinity towards calcium, such as ethylene diamine tetra acetic acid (EDTA), citrate or oxalates salts or ion exchange resins. The calcium chelator salts form complexes with the free calcium ions and deplete the CCP in milk disrupting the mineral equilibrium (Kaliappan & Lucey, 2011). In addition, the hydrophobic repulsion between the micelles increases resulting in dissociation of casein micelles. This dispersion of casein micelles causes changes like an increase in volume and higher hydration properties of the micelles (de Kort, Minor, Snoeren, van Hooijdonk, & van der Linden, 2011). In ion exchange resin removal of calcium, showed higher rennet coagulation time and ethanol stability, increase in the average size of casein micelle and higher negative zeta potential (Lin et al., 2006). The total mineral content is affected by different calcium removal methods, for instance, the use of chelating salts does not affect the total mineral content, whereas the use of ion exchange resin causes a decrease in total calcium and magnesium content by replacing with monovalent ions such as sodium or potassium (Deeth & Lewis, 2015). The calcium binding capacity of the chelating salts affects the stability of casein micelle. The structures of phosphate molecule determine the calcium binding capacity, for example, polyphosphate have higher chelating properties than orthophosphate (De Kort, Minor, Snoeren, Van Hooijdonk, & Van Der Linden, 2009).

2.3.2 Significance of calcium during processing

Apart from providing nutritional benefit to the new born, the milk salts component particularly calcium is said to play a significant role in various functional properties such as the structure and stability of casein micelles (Holt, 2011) and textural properties of cheese and yoghurt (Lucey & Horne, 2009). The role of calcium during dairy products processing is imperative in understanding the changes in the functional properties of the products.

2.3.2.1 Acid-induced gels

Acidification of milk can be brought about by microbial cultures or the addition of acids. During acidification, the negatively charged casein micelles are neutralized which causes aggregation of casein micelles forming a network of gel structure (Lucey & Singh, 1997). In the dairy industry, acidification process mainly applies to the manufacture of fermented products like yoghurt. Yoghurt preparation involves high heat treatment prior to acidification process. During the heat treatment, denaturation of whey proteins occurs, which associates with the κ-casein via hydrophobic bonds and disulphide linkages (Lucey & Singh, 1997). The role of CCP in acid-induced gels properties is important since CCP solubilizes at pH 5.2. Thus, calcium chelators are used to increase the firmness of acid-induced gels (Lucey & Horne, 2009). The addition of tri sodium citrate (TSC) increased the gel strength at lower concentrations of TSC while a higher concentration above 20 mM showed an opposite effect. The high flexibility of the micellar structure has attributed to the increased formation of cross-links between the strands at the low levels of CCP removal (Ozcan-Yilsay, Lee, Horne, & Lucey, 2007). Anema (2009) indicated the role of CCP in the formation of gel during early stages of acidification. The CCP continues to solubilize with the reducing pH, and solubilizes completely producing a viscous gel. Acidification at an elevated temperature shifted the gelation pH to the higher side, gave high $G_{shoulder}$ and the tan δ_{max}, because of more CCP in the residual casein micelles, while removal of CCP prior to heat treatment and acidification showed no change in gelation pH giving a diminished $G_{shoulder}$ and an increased tan δ_{max}.

2.3.2.2 Rennet induced gels

Coagulation of milk by rennet is important in the production of wide varieties of cheese. Rennet coagulation is a two-step process, the enzymatic cleavage of the κ-casein at the Phe 105–Met 106 bond (Lucey, 2011) into N-terminal, para-κ-casein which is still associated with the casein micelle and C-terminal peptide, also known as the glycomacropeptide (GMP), which goes with whey protein (Anema, Lee, & Klostermeyer, 2007). The hydrolysis of the κ-casein decreases the net negative charge and reduces the steric repulsion forces, which is required for micellar stability leading to the second step of aggregation. However, the aggregation of the

altered micelles takes place only in the presence of free calcium ions and consequent gelation is dependent on the amount of CCP present (Lucey, 2011).

The addition of $CaCl_2$ is a routine process during the manufacture of cheese. The addition of calcium reduces the rennet coagulation time (RCT) and increases curd firmness. The calcium ions shield the negative charge of the casein micelles, resulting in the micelles aggregation and causing the casein micelles to aggregate and formation of calcium bridges (Kethireddipalli & Hill, 2015). The addition rate from 0.1 mol L^{-1}up to 10 mol L^{-1} reduces the RCT and increases the curd strength. However, the reduction of CCP by 30 % inhibits curd formation, probably due to a change in micellar structure which is unable to precipitate (Lucey, 2011). A similar effect was observed by Udabage, McKinnon, and Augustin (2001), where the removal of 33 % CCP by EDTA lead to inhibition of gelation. There could be a possible reformation of the removed CCP upon addition of $CaCl_2$ back to the calcium-depleted milk which, resulted in the formation of the coagulum. The effect of CPP on the rennet induced coagulum properties was demonstrated by Choi, Horne, and Lucey (2007). The CCP content was reduced by the application of calcium chelator prior to gelation. The microstructure of the gels showed weak gels with reduced cross-linking between the casein micelles.

2.3.3 Calcium fortification in milk

2.3.3.1 Role of calcium in the human body

Calcium is the most abundant mineral in the body accounting to 1-2 % of the human body weight, of which 99 % is found in the bones and teeth for growth and structural maintenance of the skeleton (Flynn, 2003; Theobald, 2005). The remaining 1 % is found in the extracellular fluids and soft tissues performing various vital functions in the body (Gurr, 2000). Bone is comprised of an organic phase of collagen fibers and a mineral phase of Hydroxyapatite and other ions (Flynn, 2003). Apart from providing strength and structure, calcium is present in the form of ions on the bone surface. The ions serve as an ion exchanger with ions of body fluids, serving as a reserve of calcium and an ability to maintain constant of blood calcium

concentration needed for vital body functioning. Bone turnover is a process of continuous breakdown and formation of bones by the bone forming cells. This turn over process is mostly constant but is said to differ in the early and later stages of life (Gurr, 2000). The bone mass continues to increases from the early ages reaching peak bone mass in the middle age (at 25 years of age). The bone mass stays constant after reaching the peak for about another ten years after which the bone mass starts to reduce. Starting from infancy the body calcium content increases from around 28 g to 1200 g in adult men and women (Gurr, 2000). This reduction in bone mass is particularly important in calcium deficiency related diseases such as osteoporosis.

2.3.3.2 Calcium deficiency

Low calcium intake increases the bone turnover process or lower bone mass. Osteoporosis is the main bone disease related to calcium deficiency, which is characterized by bones becoming fragile leading to fractures commonly in the hip, spine, wrist and other skeletal parts (Cashman, 2006). Other calcium related disease includes hypertension, colon, breast cancer and cardiovascular diseases. As per the United Nations Department of Economic and Social Affairs and Population Division (2015) the population of the world is aging and the population over the age of 60 is predicted to increase 56 % by 2030. Bone related disease osteoporosis is also expected to increase because osteoporosis is known to occur mostly in elderly people particularly postmenopausal women. The decrease in bone mass is related to increased bone turn over time, failure in reaching the peak bone mass. Peak bone mass is affected by several factors such as nutrition, genetics, lifestyle, smoking, alcohol, hormone production and certain medications (Caroli, Ricotta, Cocchi, Poli, & Banfi, 2011; Lucey & Horne, 2009; Theobald, 2005).

Intervention through dietary calcium intake is one of the means in preventing osteoporosis (Rafferty et al., 2007). Several studies have demonstrated the increase in bone mass and body mass index in children and adolescents supplemented with calcium. In older people, calcium supplementation cannot stop bone loss fully but can retard the progress of bone loss. Apart from healthy nutrition, physical exercise (weight bearing exercise) is equally important for maintaining bone health (Weaver,

2006). However, the absorption of calcium from dietary products is dependent on the bioavailability of calcium. One-third of calcium is absorbed from foods and the rest is excreted from the body in the form of faeces, and minor losses of calcium can also occur from the skin, hair, and sweat (Gurr, 2000). The components in the foods and calcium interaction with the food component also affect calcium bioavailability. For example, phytic and oxalic acids form insoluble complexes with calcium, lowering calcium absorption (Gurr, 2000). Calcium absorption from bovine milk and milk products is 32 % and from human milk is approximately 60–70 % thus, it is recommended for mothers to feed the baby for at least six months of infancy (Weaver, 2006).

In addition to calcium supplementation, it is important to meet the recommended calcium intake values. There is a wide variation on recommended calcium intake depending on country of origin and different age groups. The calcium requirements are higher during the early stages of growth (children and adolescence), during pregnancy and older stages after 50 years of age (Cashman, 2006). For example, the recommended dietary allowance (RDA) for different age groups is "800 to 900 mg for adults, 1000 mg for pregnant and lactating women, and 1200 mg for adolescents and elderly persons" (Gaucheron, 2011).

Table 2.5 shows the RDA of calcium as developed by Food and Nutrition Board (FNB) at the Institute of Medicine of the National Academies.

Age	Male	Female	Pregnant	Lactating
0–6 months*	200 mg	200 mg		
7–12 months*	260 mg	260 mg		
1–3 years	700 mg	700 mg		
4–8 years	1,000 mg	1,000 mg		
9–13 years	1,300 mg	1,300 mg		
14–18 years	1,300 mg	1,300 mg	1,300 mg	1,300 mg
19–50 years	1,000 mg	1,000 mg	1,000 mg	1,000 mg
51–70 years	1,000 mg	1,200 mg		
71+ years	1,200 mg	1,200 mg		

* Adequate Intake (AI)

2.3.3.3 Calcium fortification and technological challenges

Bovine milk contains 1200 mg/L of calcium mineral (Gaucheron, 2011). Milk and dairy products are known for their good source of calcium providing 40 % of dietary calcium in adults (Theobald, 2005). Even with a high calcium content in milk, calcium is added to milk and other dairy products to further enhance the technological, functional and nutritional enhancement (Philippe et al., 2003). The increasing awareness of the role of dietary calcium in human health and higher consumer demand prompts production of calcium supplemented food products. There are various types of calcium used for fortification; (i) inorganic salts such as calcium carbonate and calcium phosphate, (ii) calcium from animal source (calcium phosphate from milk), plant origin (calcium carbonate from seaweed) and (iii) organic salts such as, tricalcium citrate, calcium lactate and calcium lactate gluconate. The choice of different calcium sources is dependent on factors such as cost, solubility, calcium content, sensorial properties and bioavailability (Munchbach & Gerstner, 2010; Rafferty et al., 2007). Most of the calcium salts used as fortificants exhibit good absorbility by the intestine (Rafferty et al., 2007).

Calcium absorption is optimum while in ionic form and there is a misconception pertaining to the relationship between solubility of salts and bioavailability. However, insoluble calcium like calcium carbonate is said to be absorbed well by the intestine (Gurr, 2000).

Fortification of calcium in milk is challenging because the serum phase of milk is saturated with calcium (On-Nom, Grandison, & Lewis, 2012) and further addition of calcium salts can lead to instability during processing. Heating is the common processing treatments in the manufacture of most dairy products such as pasteurized, UHT, sterilized milk, cheese, and yoghurt. During fortification the added calcium salts dissociate into ions, increasing the ionic calcium, decreasing the pH and causing destabilization of casein micelle structure leading to reduced heat stability (Munchbach & Gerstner, 2010).

Omoarukhe et al. (2010) reported a reduction in pH and increase in ionic calcium resulting in poor heat and ethanol stability by soluble calcium salts like calcium chloride, calcium lactate and calcium gluconate in milk when 30 mM was added and subjected to UHT treatment. A similar observation was reported by Kaushik, Sachdeva, and Arora (2015); the addition of 500 mg/L of calcium chloride and calcium gluconate in milk lead to a decrease in pH and low heat stability. On the sensorial properties of milk, calcium gluconate gave neutral taste and low mouthfeel as compared to normal milk while the increasing calcium chloride addition rate gave a more salty taste. Calcium lactate in large concentrations is bitter and insoluble calcium salts lead to grittiness (Munchbach & Gerstner, 2010). Calcium chelators allow fortification of soluble calcium salts by improving the heat stability, however, addition at higher rates of chelators lead to destabilization of casein micelles leading to instability as described in the previous section 2.3.1.2 (factors influencing milk equilibrium). Hence, according to Munchbach and Gerstner (2010), the best option for the manufacture of heat stable calcium fortified milk products is by addition of insoluble calcium salts. Omoarukhe et al. (2010) showed that insoluble calcium salts like calcium carbonate, calcium phosphate, and calcium citrate did not show any change in pH and ionic calcium demonstrating better ethanol and heat stability with

small amounts of sedimentation. Hydroxyapatite is commonly used in insoluble calcium salts as a source of calcium supplementation commercially because of its similarity to minerals found in bone and teeth and high thermodynamic stability (Tercinier, Ye, Anema, Singh, & Singh, 2013). However, one draw back of insoluble calcium salts is sedimentation of calcium salts during storage causing chalky and gritty mouthfeel mentioned earlier the application of insoluble calcium salts lead to sedimentation because of their less solubilization property (Munchbach & Gerstner, 2010).

One of the means to solve this sedimentation drawback is by improving the dispersibility of insoluble calcium salts. Gerhart and Schottenheimer (2013) suggested the application of microsized calcium salts for better dispersion and improved mouthfeel, for example, microsized tricalcium citrate salt. Nano sized HA with diverse structures can be produced from different production methods mentioned in the earlier section (2.2.1 production and physiochemical properties of HA). Thus, the addition of HA nano particles (nHA) in milk has improved the dispersibility. However, the application of nano sized ingredients in food systems has given rise to increasing questions pertaining to the implications in health and environment from both the regulatory organizations and consumers. It is believed that during ingestion the acidic condition in the stomach will result in dissolution of the nHA, if not, there could be possible chances of nHA translocation into other organs through the GI tract.

2.4 Gastrointestinal digestion

2.4.1 Physiology of digestive tract

Digestion is a process of breaking down large food molecules into simpler molecules for ease of absorption by the human body. The digestion process is a complex process involing a mechanical and chemical break down of food (Bornhorst, 2017). Furthermore, this process can be divided into subprocesses corresponding to the human digestive system such as the oral process in the mouth, the gastric process

in the stomach and the intestinal process in the small intestine and fermentation in the large intestine (Mike, 2016).

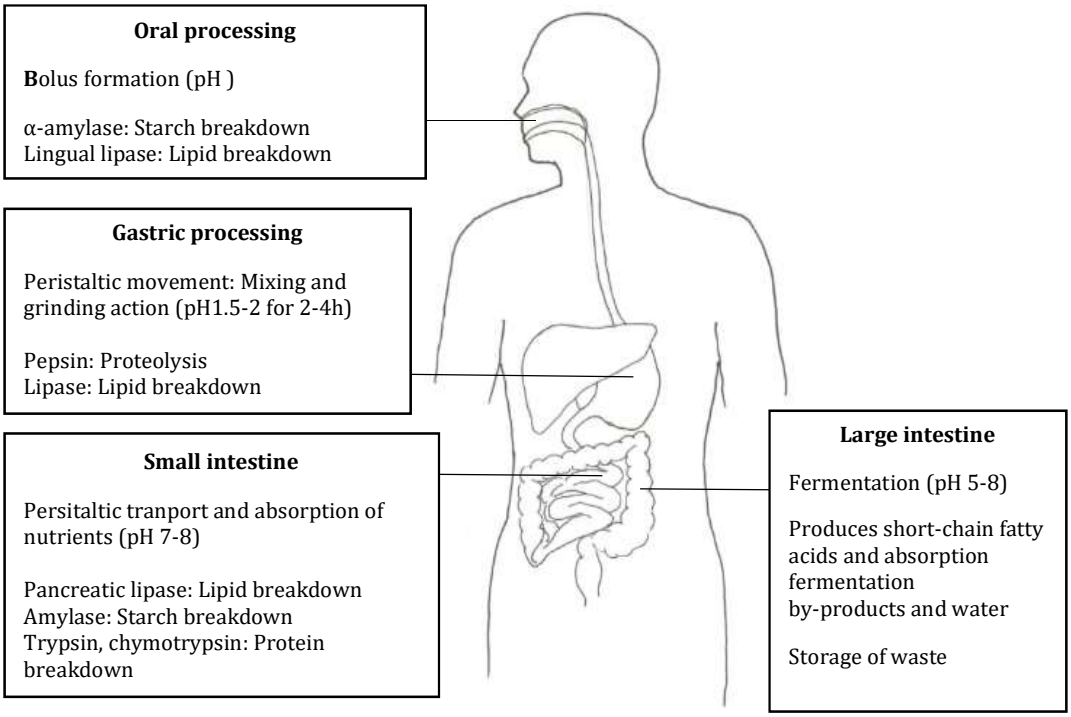

Figure 2.11 Overview of digestion process.

Oral digestion

In the mouth the food is broken down into smaller pieces forming a bolus by the mechanical grinding action of the teeth and binding action of the salivary mucins. The formation of the bolus is important for the ease of swallowing the food along the GI esophagus without causing any damage to the mucosa (Mike, 2016). This mastication process depends on the biting force of a number of teeth in functional occlusion. The saliva contains enzymes like α-amylase which hydrolyzes starch present in the food. The pH of saliva is in the range of 6.5-7.4, and this neutral pH also serves as a buffering solution preventing demineralization of dental teeth. Apart from α-amylase enzyme, saliva also contains lingual lipase for break down of lipids however, it is not of significance in healthy humans but of significant importance with people suffering from insufficieny of producing pancreatic lipase

(Pedersen, Bardow, Jensen, & Nauntofte, 2002). The resident time in the mouth is dependent on the particle size during mastication, which, in turn, is dependent on the nature of food like solid food takes a longer time when compared to liquid and semi-solid food (Bornhorst & Singh, 2014; Singh, Ye, & Ferrua, 2015). The oral processing has a significant influence on the subsequent digestion of food along the GI path such as the gastric emptying rate (Kong & Singh, 2008).

Gastric digestion

Once the bolus passes through the esophagus, it enters the stomach where further break down of food takes place, lasting usually up to one to two hours. Based on the structure and functions, the stomach is divided into three main parts, being the cardia, fundus/body and antrum (Bornhorst, 2017). The cardia is located at the upper part of the stomach where the food enters the stomach after passing through the esophagus. The fundus forms the largest part of the stomach representing 75 % of the gastric surface area. The cardia consists of mucin secreting cells while the fundus consists of parietal cells secreting acid HCl and enzymes and the antrum cells secretes mucosa (Bornhorst, 2017). The enzymes include pepsinogen and lipase which hydrolyzes proteins and lipids respectively. The acid provides the acidic environment required for the activation of inactive pepsinogen to active pepsin enzyme and has a bactericidal effect on most of the ingested bacteria (Kong & Singh, 2008). This production of acid makes the stomach highly acidic with a pH <2 (Mike, 2016). The gastric fluid has a high ionic strength of >150 mM and, as a result, the ions diffuse in and out of the food particles causing disintegration of the food network. This diffusion of ions is determined by the structural properties of food (Singh et al., 2015). The secretion of gastric fluid is initiated by the food entering the stomach. The gastric fluid secretion in the stomach is around 2-3 L in a day. The epithelial cells of the gastric tract are protected by the mucous layer forming the highly acidic environment of the stomach (Bornhorst & Singh, 2014).

Further, the stomach can be divided into two parts the upper proximal (fundus) and the lower distal section (antrum and pylorus). The proximal part is able to

accumulate up to 4 L of food because of its flexibility (Kong & Singh, 2008). Thus, the upper fundus serves a as reservoir for undigested food whereas in the lower distal section the food is broken down and mixed by the peristaltic movements of the stomach (Mike, 2016). The average speed of contraction is 1.5–3 mm s^{-1} and an average frequency of 2.6–3 cycles per min (Bornhorst & Singh, 2014). The propagation of food (92.5 mm/sec) increases as it moves from the upper to the lower part of the stomach (Kong & Singh, 2010). After the gastric digestion process, the digesta is emptied from the stomach via the pylorus. During gastric emptying the pylorus functions as a sieve allowing only digesta particles less than 0.5-2.0 mm in size to pass through (Mike, 2016). The gastric emptying rate is affected by various factors such as composition and structure of the food ingested, nutrient content, gastric motility and gender (Bornhorst, 2017; Mike, 2016). For instance solids, viscous and fatty foods have longer gastric emptying time when compared to liquid, no viscous and watery foods (Schneeman, 2002).

Intestinal digestion

The intestinal digestion is crucial in the further break down of the digesta to ensure absorption of nutrients through the intestinal walls into the bloodstream. The small intestine has an increased surface area because of its highly convoluted length of 6-7 m long, consisting of three separate regions; duodenum, jejunum and ileum . In the duodenum, the pancreas secretes enzymes, bile salts, and bicarbonates. The bicarbonates are important in neutralizing the acidic conditions after the gastric process and for the optimum activity of the enzymes. The enzyme is known as the pancreatic which hydrolyzes fat, carbohydrates, and proteins. The activity of the pancreatic enzyme is dependent on bile salts and calcium. The bile salts facilitates the break down of fats by emulsifying the fats. The jejunum and ileum functions like a reactor allowing enzymatic hydrolysis into simple molecules for absorption. The absorption of nutrients takes place in the jejunum and completes in the ileum region. The only absorption of vitamin B_{12} and bile takes place in the distal 100cm of the ileum. The peristaltic movement facilitates transport of chyme at a rate of 2–25 cm/s and absorption of nutrients along the intestinal walls (Bornhorst & Singh, 2014).

Fermentation

The large intestine is colonized with 10^{12} bacteria of diverse microflora of mostly beneficial microbes and a few microbes related to intestinal diseases (Schneeman, 2002). The composition of the microflora differs across individuals and these anaerobic microflora ferment the undigested digesta producing short-chain fatty acids and methane. As the digesta pass along the colon, the water from the digesta is absorbed which is important in maintaining electrolyte balance and water in the body (Mike, 2016) and the waste is excreted from the body.

2.4.2 Digestion Models

Digestion is a vital physiological process for providing nutrients and energy to the body for growth and repair of cells. From an industrial standpoint, a proper understanding of various physiochemical changes occurring during digestion is crucial in assessment of digestibility of food components, bioaccessibility and bioavailability of nutrients and in the development of food products with novel properties such as delivery of bioactive compounds (Lucas-Gonzalez, Viuda-Martos, Perez-Alvarez, & Fernandez-Lopez, 2018). Numerous studies on human digestion process are available which includes both *in vivo* and *in vitro* experimental models.

In vivo studies usually includes testing on live animals in the laboratory or through human trials. *In vivo* models are considered "gold standards" for digestion related studies for producing accurate results (Minekus et al., 2014). However, there are limitations and drawbacks such as technical challenges in analyzing the complex process during animal or human digestion, ethical issues while using harmful substances, time consuming and economically expensive (Boisen & Eggum, 1991; Guerra et al., 2012). Hence, a wide range of *in vitro* gastrointestinal model as an alternative to the *in vivo* method, have been developed over the years starting from a single simple static system to more complex dynamic systems. In comparison to vivo models, *in vitro* models are cheaper, requiring less labor, and have no ethical objections and concerns (Coles, Moughan, & Darragh, 2005; Minekus et al., 2014)

allowing rapid screening and reproducible conditions (Kong & Singh, 2008; Minekus et al., 2014).

The *in vitro* digestion models differ with respect to experimental procedures such as the choice of digestion sequences like oral, gastric, and small and large intestine, the composition of chemicals and enzymes used for digestive fluids, application of mechanical forces and flow rates of fluid flow. The choice of experimental operation is dependent on the food matrix, the intended objective of the study like digestibility, release, and absorption of bioactive compounds and structural changes (Hur, Lim, Decker, & McClements, 2011). In the studies pertaining to liquid and semi-liquid foods, the oral processing step can be left out and proceed to the gastric and intestinal step. This is because oral digestion functions mostly in the formation of bolus while ingesting solid foods and in the case of foods other than solid in nature, the residence time in the mouth is short and it does not have a significant effect on the digestion of the food components (Alegria, Garcia-Llatas, & Cilla, 2015; Mackie & Rigby, 2015).

Food properties are the main component while considering and designing *in vitro* parameters such as enzyme composition, enzyme concentration and digestion time. For example, the type of enzymes used depends on the investigative aspects of the food component, like application of amylase, proteinase and lipase enzyme in the digestion study of carbohydrate, protein and fat respectively and, accordingly, increase the enzyme concentration and digestion time of the content of target component (Hur et al., 2011). During the simulation of *in vitro* digestion, it is important to take into account the digestive enzyme's activity as well as the microbial activity in the GI tract (Boisen & Eggum, 1991). In order to simulate the digestion process, the enzymes are added in sequence rather than altogether, such as pepsin in gastric digestion and pancreatic in intestinal digestion (Boisen & Eggum, 1991). In preparation of the enzyme, it is preferable to prepare it fresh for individual study because enzyme activity is lost or decreases over time (Hur et al., 2011).

In vitro static model is the simplest digestion model consisting of a continuous shaking bioreactor kept under controlled temperature and pH for a particular period mimicking physiological digestion conditions. The homogenized food sample is subjected to sequential simulated gastric and intestinal fluids maintained under a specific temperature (37^{o}C) and pH (1-2 gastric and 6-7 intestinal) for a specified time period inside an enclosed bioreactor (Alegria et al., 2015; Guerra et al., 2012; Lucas-Gonzalez et al., 2018). The static model is cost effective allowing rapid screening and reduction in sample size (Alegria et al., 2015; Lucas-Gonzalez et al., 2018). Recently, a standardized static digestion method was proposed by COST INFOGEST, which could be applied to various studies improving the comparability of the results among the studies (Minekus et al., 2014). However, the static model lacks the ability to simulate the *in vivo* dynamic environments such as the peristaltic movements and continual biochemical changes (Kong & Singh, 2008; Lucas-Gonzalez et al., 2018) simplifying the actual dynamic *in vivo* conditions (Kong & Singh, 2010). Therefore, several dynamic models have been developed over the years to overcome the static model limitations. Dynamic models are applicable incomplete digestion studies, release, and bioaccessibility of bioactive compounds, the study of food matrix effect on the delivery of nutrients and fermentation studies and have better correlation with *in vivo* studies (Lucas-Gonzalez et al., 2018). The design of different dynamic models are based on the following parameters (i) the geometry of the stomach such as vertical, horizontal and beaker, (ii) the physical forces exerted to simulate gastric mixing and movement and (iii) biochemistry related to the addition of digestive fluids over time (Thuenemann, Mandalari, Rich, & Faulks, 2015). Thus, following dynamic models, designs are available (i) dynamic gastric stimulator (DGS, (ii) human gastric simulator (HGS) and (iii) TNO gastrointestinal model (TIM). The detailed description of DGS is presented by Thuenemann et al. (2015) and TIM model by Minekus (2015).

The peristaltic movement in the DGM model fails to simulate the actual forces applied while the TIM model lacks the actual antral contraction movements. Thus, the Human Gastric stimulator (HGS) was designed to simulate realistic *in vivo* peristaltic movement (Kong & Singh, 2010). The HGS design is such that it allows

adjustment and control of motor activity producing different mechanical forces and frequencies, which can be applied in studying the effect of gastric motility (Ferrua & Singh, 2015) under dissimilar physiological conditions like age, health, and gender (Kong & Singh, 2010). According to Kong and Singh (2010) HGS has a tapered design at the bottom stimulating actual stomach shape generating increased antral contractions forces as the rollers proceed downward which, renders the model more effective in mimicking actual gastric disintegration of food as compared to the shaking bath method. The main area of interest related to the *in vitro* dynamic model is the HGS which is applied in this study. Thus, a detailed description and working of the HGS according to Kong and Singh (2010) is presented below.

The HGS model consists of a cylindrical stomach chamber of 5.7 L of 20 cm height and 10.2 cm width, having a tapered shape at the bottom of 13 cm high and 2.5 cm diameter. The stomach is made out of a latex material that can be inserted from the top into the stainless steel ring of 10.2 cm height and 15.2 cm width. This ring is held by the four legs which is welded to the base and placed opposite to each other at 90 degrees. The chamber is insulated to maintain the temperature at 37 ^{o}C and controlled by a thermostat. In order to generate peristaltic movement, there are four conveyor belts with three rollers in each belt forming a pulley system. The Teflon rollers are placed on the conveyor belt (0.2 cm wide and 1.5 cm length) at a distance of 20 cm from each other. The rollers on the conveyor belts are powered by the motor and moves at 2/3rd of the total height along the side of the latex stomach wall, compressing the walls as it moves downwards. These compression forces increase as the roller approaches the tapered side of the stomach. This movement of the rollers creates the peristaltic contraction similar to that of a stomach. In order to avoid collision of the rollers as it passes along the bottom of the stomach, the opposite pairs of pulleys are placed at 3 cm higher than the other pairs. A polyester mesh bag of 1.5 mm pore size is placed in the inner lining of the latex stomach to mimic the sieving effect of digestion. The gastric fluids can be added into the stomach with the help of tubes and rate of addition can be controlled via a mini peristaltic pump.

2.4.3 Studies on *in vitro* digestion of milk

The behaviour of milk during gastric digestion shows the formation of a structural clot from the milk proteins particularly the casein molecules. This clot formation is important in the determination of gastric emptying rate for nutrient uptake as well for studying the behaviour of different commercial milk proteins during digestion for food design purposes. The mechanism for the formation of coagulum during gastric digestion is similar to that of rennet-coagulated milk, where the pepsin enzyme cleaves the κ-casein at Phe and Met bond (Lucey, 2011).

Boirie et al. (1997) proposed the concept of slow casein and fast whey protein during hydrolysis. The structure of the clot formed during gastric digestion is reported to be affected by various factors. Ye, Cui, Dalgleish, and Singh (2016b) demonstrated the effect of heat treatment on clot formation and subsequent rate of proteolysis. The study found that unheated raw milk gave a close-knit structured clot allowing less diffusion of pepsin enzyme, which slowed down the gastric emptying rate as compared to a loose crumbly structure obtained from heated milk ($90^{o}C/2$ min) using HSG (Figure 2.12). The heating process resulted in denaturation of whey proteins and its interaction with κ-caseins making the proteins more susceptible to pepsin action. The resultant changes in the structural conformation of proteins during the heating process attributed to the structural difference in the clot formed. Apart from the effect on proteolysis, the coagulum formation also has an impact on the lipolysis during gastric digestion and subsequent intestinal digestion. In another study by Ye, Cui, Dalgleish, and Singh (2016a) the clot structure of heated and unheated whole milk was similar to that of their previous study in skim milk (Ye et al., 2016b). The release of milk fat in the form of fatty acid was faster from heated milk coagulum due to its open loose structure. The release of fat was in linearity to that of proteolysis, which showed entrapment of fat in the coagulum and gradual release with the breakdown of the coagulum matrix. Ye, Cui, Dalgleish, and Singh (2017) further investigation into lipid digestion reported that in homogenized milk, the lipid droplets covered by casein were embedded into the loose casein matrix, whereas in untreated whole milk the oil droplets were found entrapped within the firm clot matrix. The rate of proteolysis was higher from a loose crumbled clot, which led to the faster release of fat into the digesta.

A similar clot structure was observed in Mulet-Cabero, Mackie, Wilde, Fenelon, and Brodkorb (2018) during gastric digestion of pasteurized milk and UHT milk (comparatively more open knit structure) using semi-dynamic *in vitro* model. The further investigation related to the influence of milk processing showed phase separation in UHT homogenized milk unlike raw non-homogenized milk (sedimentation) caused by the action of pepsin on the milk fat globule membrane protein. The entrapped fat droplet in the homogenized milk gave a finer dispersion of aggregates in comparison to larger aggregates in non-homogenized milk leading to sedimentation.

Wang, Ye, Lin, Han, and Singh (2018) investigated the clot formation behaviour from different types of protein; skim milk powder (SMP), milk protein concentrate (MPC) calcium depleted MPC, sodium caseinate and whey protein isolate (WPI) during gastric digestion. The clot formation was found to be dependent on the type of protein, processing conditions and micellar integrity. The initial clot formation in skim milk powder (SMP) and milk protein concentrate (MPC) was observed at 10 min of digestion time whereas in calcium-depleted MPC and sodium caseinate, the clot formation took place after 40 min of digestion time. Moreover, the clot structure of SMP had a looser crumbled structure as compared to MPC with "integrated ball like structure". Loose fragments with large open structure clot in the case of calcium depleted MCP and sodium caseinate, whereas WPI showed no clot after 220 min of digestion time. The dissimilarity in clotting behaviour of calcium depleted MPC and sodium caseinate is due to loss of intact casein micelle structure and presence of individual casein molecules.

In conclusion, one important aspect from all the studies taken in milk digestions includes clot formation and its consequent influence on the digestibility and absorption of milk components.

Figure 2.12 Structured clot formation during gastric digestion; top row clot obtained from unheated milk and bottom row clot obtained from heated milk from (Ye et al., 2016b).

2.4.4 Correlation between *in vivo* and *in vitro* digestion

The *in vivo* digestion is a complex process governed by different physiological parameters. Bohn et al. (2017) mentioned that various *in vitro* models are able to provide appropriate information required in understanding the fate of food components for interpreting the health effects from ingested good. *In vitro* models provides a cheaper option for understanding the digestion behaviour of different food systems and components. However, it is challenging to accurately simulate *in vivo* digestive conditions. Therefore, a correlation of *in vitro* and *in vivo* digestion model is important in validating *in vitro* studies from the food industries' viewpoint in the development of novel food designs as well as consumers health aspects. According to Bohn et al. (2017) static *in vitro* data demonstrates a good correlation with *in vivo* in terms of macronutrients; simple food mixtures such as in protein and starch digestibility while, the knowledge on digestion of micronutrients is limited.

As mentioned earlier in the study of Egger et al. (2016) where they emphasized on the need for vivo correlation studies. Subsequently, Egger et al. (2017) studied the correlation between the INFOGEST protocol with an *in vivo* pig study. They compared the data from INFOGEST *in vitro* static and dynamic *in vitro* protocol with *in vivo* pig protein digestibility of skim milk powder. The comparison of data from both *in vitro* protocols showed appropriate correlation with *in vivo* results. In the case of *in vitro* dynamic models, due to the availability of different models, the validation of results model and foods does not imply its relevancy with other types of food. A comprehensive description of the availability of different *in vitro* dynamic models and its validation was presented recently by Dupont et al. (2018).

2.5 Conclusion

Insoluble calcium phosphate salts have higher heat stability in terms of interactions with food components compared to soluble calcium salts. Therefore, insoluble calcium phosphate such as Hydroxyapatite is used for calcium fortification in dairy products. One drawback related to insoluble calcium salts is sedimentation causing undesirable gritty texture. Thus, hydroxyapatite nano particles (nHA) are used for better dispersion during fortification. Recently, there has been an increasing trend of nHA supplementation of milk products. The main concerns arising from the application of nano-sized ingredients is the probability of translocation from the gastrointestinal tract to other organs in the body. Thermodynamically, it is known that in comparison to the bulk micro sized materials the nano-sized materials would dissolve much faster. HA is soluble in water but is known to dissolve at pH < 4 and it is mostly assumed that HA would dissolve under the acidic condition of the stomach. However, there is a lack of research studies on the behavior of nHA after ingestion through food and does not accurately simulate the human GI tract environment. Therefore, the main aim of the study is to examine the dissolution behavior of nHA when supplemented in milk during *in vitro* gastrointestinal digestion process. The dissolution behavior of nHA would help in understanding the fate of NPs during the digestion process.

Chapter 3 Materials and methods

3.1 Materials

In this study, the reference food grade needle shaped nano hydroxyapatite (nHA) powder was purchased from Hebei Shunye Import and Export Limited Company, China as obtained from the previous study of Schoepf et al. (2017). As per their study, the particle size of HA powder was 30 ± 5 nm (width) by 131 ± 25 nm (length) and aggregate size of 141–1786 nm as measured from TEM micrographs using Image J soft ware.

Pasteurised skim milk was obtained from a local super market and stored under refrigerated temperature until further analysis. The milk composition was taken as mentioned on the packaging label in Table 3.1.

Table 3.1 Skim milk composition as derived from the packaging label.

Components	**250ml**
Fat	0.3 g
Protein	10.0 g
Sugar	12.4 g
Calcium comtent	320 mg

The enzyme for gastric study was procured from Sigma-Aldrich Co (St.Louis, MO, California). Pepsin powder was obtained from porcine gastric mucosa (EC-232-629-2 P-7000) with ≥250 units/mg solids. Bile extract porcine (B8631) contained glycine, taurine conjugates of hyodeoxcholic acid and other bile salts. The enzyme for intestinal study was procured from MP Biomedicals, LLC (Santa Ana, California, USA). Pancreatin obtained from porcine pancreas (02193976) with 8 X UPS specification contained lipase, amylase and protease. All the chemicals were of analytical grade and were purchased from Sigma Chemical Co. (St. Louis, MO) or BDH Chemicals (BDH Ltd., Poole, England). Water purified by treatment with a Milli-

Q apparatus (Millipore Corp., Bedford, MA) was used for all experiments and reagent preparation.

3.2 Digestion sample preparation

For this study, the digestion samples was prepared as follows:

i. nHA blank

   The nHA blank digestion solution/dispersion was prepard by adding 420mg of nHA powder into 250ml Milli Q water.

ii. nHA_{milk}

   According to European Union RDA, the maximum amount of fortification of calcium in milk is 500 mg/250 ml. Thus, nHA was added based on the calcium content in the skim milk sample to increase the calcium content to 500 mg/250 ml. 420 mg of nHA powder was added into 250 ml of skim milk. The supension was mixed using a stirrer bar for 120 min at room temperature to ensure proper dispersion and equilibrium (Tercinier et al., 2014b). The solution/dispersion was prepared before the start of each digestion experiment.

iii. $Milk_{blank}$

   The $milk_{blank}$ digestion sample was prepared with 250ml of the skim milk alone without the addition of nHA powder.

3.3. Simulated gastric and intestinal fluid preparation

3.3.1 Simulated gastric fluid (SGF)

The simulated gastric fluid was prepared according to Minekus et al. (2014) harmonized INFOGEST protocol with minor modifications. In order to obtain a SGF mixture of 1.25 X concentrate in final the volume of 1 L. SGF was prepared by mixing KCl (6.9 mmol/L), KH_2PO_4 (0.9 mmol/L), $NaHCO_3$ (25 mmol/L), NaCl (47.2 mmol/L), $MgCl_2(H_2O)_6$ (0.1 mmol/L), $(NH_4)_2CO_3$ (0.5 mmol/L) in 800 ml deionzed water. The final concentration of SGF was obtained with an addition of pepsin, $CaCl_2$ (0.15 mmol/L) and the rest of the deionzed water. The final pH of SGF mixture was adjusted to 1.5 with the use of 1 M NaOH and 6 M HCl. Pepsin (3.2 g/L) and $CaCl_2$ (0.15 mmol/L) was added before the start of the digestion process.

3.3.2 Simulated intestinal fluid (SIF)

The simulated intestinal fluid was prepared according to Minekus et al. (2014) harmonized INFOGEST protocol with minor modifications. In order to obtain a SIF mixture of 1.25 X concentrate in the final volume of 1 L. SIF was prepared by mixing KCl (6.8 mmol/L), KH_2PO_4 (0.8 mmol/L), $NaHCO_3$ (85 mmol/L), NaCl (38.4 mmol/L), $MgCl_2(H_2O)_6$ (0.3 mmol/L) in 800ml deionzed water. The final concentration of SGF was obtained with the addition of $CaCl_2$ (0.05 mmol/L) and the rest of the deionzed water. The final pH of SIF mixture was adjusted to pH 7.5 with the use of 1 M NaOH and 6 M HCl. Pancreatin, bile salats and $CaCl_2$ was added before the start of intestinal digestion process.

3.4 *In vitro* gastrointestinal digestion

For *in vitro* gastric digestion, a freshly prepared suspension of nHA_{milk} (250 ml) was heated to 37°C with the help of a water bath to bring the temperature to that of human physiological conditions. The HGS chamber temperature was achieved with the application of a heater and was maintianed at 37°C with the of help of a thermostat. Before the start of the digestion study, the HGS machine was started 30 min earlier in order for the HGS temperature to reach 37°C. The peristaltic pumps for the dispensing of SGF and pepsin ezyme were calibrated before each digestion expertiment to maintain a flow rate of 2 ml/min and 0.5 ml/min respectively. The gastric contraction frequency was maintained at 3 times/min. The digestion experiment was initiated with the dispensing of the SGF and enzyme into the latex stomach chamber. The total digestion time lasted for 240 min and the samples were taken at specified digestion interval time.

For in vitro intesinal digestion, the gastric digesta sample at the end of the digestion experiment was taken (240 min digesta sample). The pH of the digesta sample was adjusted to 7.0 with the use of 0.1 M NaOH. The digesta sample was mixed with SIF in 1:1 ratio and incubated at 37°C in a flask with the help of the magnetic stirrer bar maintained at 95 RPM for 120 min time. The temperature was maintained at 37°C in the water bath that circulated hot warm water to the double-jacketed flask during

the whole intestinal digestion process. The digesta was taken at the end of 120 min digestion time.

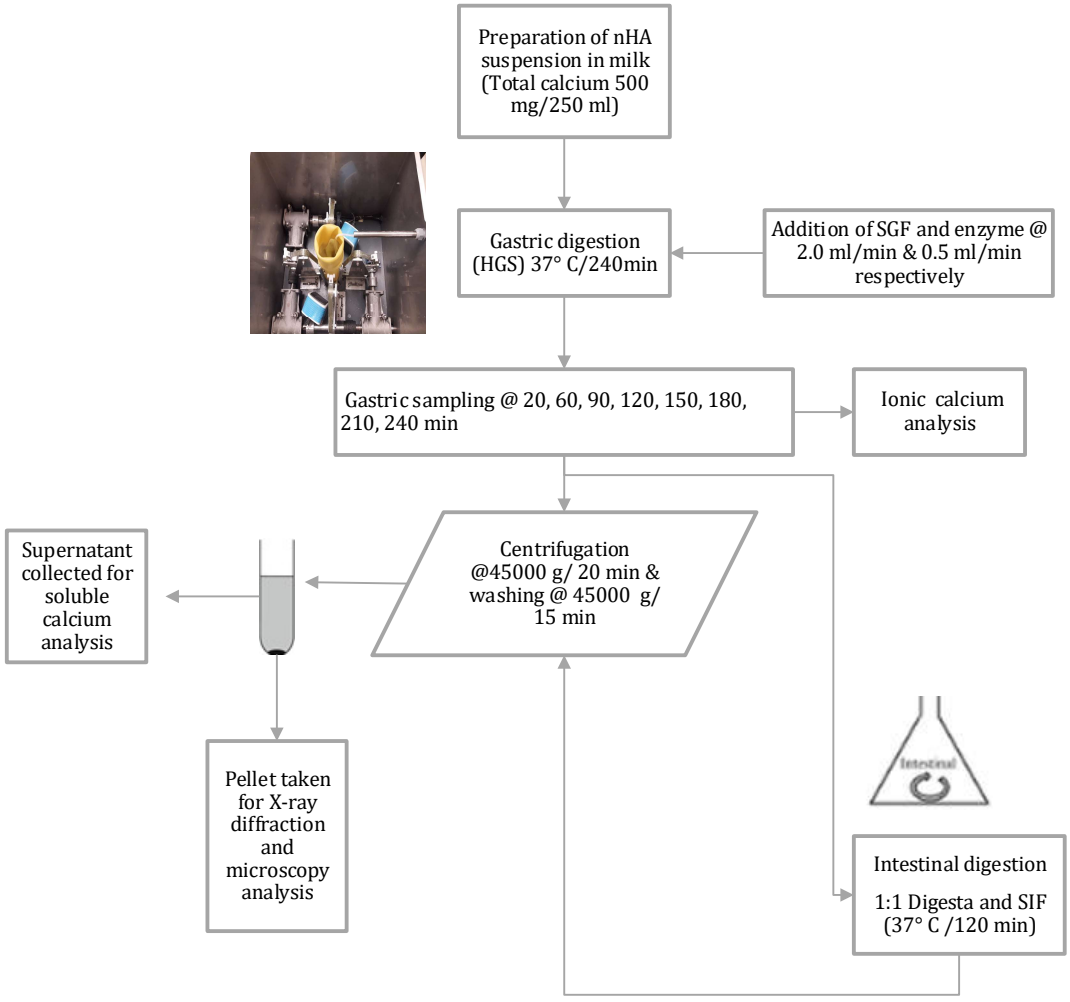

Figure 3.1 Schematic representation of sequence of gastrointestinal digestion.

3.4.1 Sampling procedure and sample preparation

The gastric digestion samples were taken at different digestion interval; during the first stages of digestion time, the sample was taken at 20 min and at 60 min after which sampling was done at every 30 min until the end of digestion process (Table 3.2). The digesta was taken out at the rate of 3 ml/min equating the gastric emptying rate as mentioned in previous report of Ye et al. (2016b) with the help of bottle sampler from the bottom outlet of the HGS chamber. The digesta sample after

sampling was filtered through a stainless steel (SS) mesh pore size of 1mm to mimic gastric sieving. Usually, inactivation of pepsin is achieved through an adjustment of pH back to neutrality and heating in boiling water for a few min. However, due to the complex chemical nature of calcium phosphate salts (nHA) to pH used in this specific digestion study, there is probability of changing the phosphate into different forms with the change in pH like in the tripotic equilibrium mentioned earlier in Figure 2.6.

Table 3.2 Digesta sample sampling points for different measurements.

	Gastric								
Time (min)	**20**	**60**	**90**	**120**	**150**	**180**	**210**	**240**	**Intestinal**
pH	x	x	x	x	x	x	x	x	x
Temperature (^{o}C)	x	x	x	x	x	x	x	x	x
Ionic Calcium	x	x	x	x	x	x	x	x	x
Soluble Calcium		x		x		x		x	x
TEM		x		x		x		x	x
X-Ray diffraction		x		x		x		x	x
EDS		x		x		x		x	x

It was assumed that the HA particles would precipitate during centrifugation from the digesta solution. Thus, the inactivation of pepsin enzyme was achieved through the centrifugation of the digesta immediately after sampling and through the centrifugation-washing step. High-speed centrifuge (Sorvall R6, Thermo scientific, UK) was used for centrifugation of the digestion solution. 35 ml digesta solution was taken in 50 ml capacity centrifuge tubes in duplicates. The centrifugation was carried out at 45000 g/20 min. The supernatant after centrifugation was collected for soluble calcium analysis while the pellet obtained after centrifugation was washed with MIlliQ water (centrifugation at 45000 g/15 min) containing 0.2% Na-

Azide to wash off any residual pepsin enzyme. Precaution was taken during collection of the supernatant to avoid any breakage and loss of the pellet obtained. The pellet obtained was stored at refrigerated temperature for X-ray diffraction (XRD) analysis and for microscopy. The digesta pH and temperature was determined immediately after sampling. For ionic calcium measurement, a small aliquot (10 ml) was taken before subjecting the digestion solution to centrifugation process.

3.5 pH measurement

The pH measurement of the digestion sample was carried out immediately after filtering the digestion solution through the mesh with the help of CyberScan pH 510 pH/mV Meter (Eutech Instruments-Thermo Scientific). The pH electrode was calibrated before the start of each experiment using standard buffer solutions (pH 4.0, pH 7.0 and pH 10.0).

3.6 Characterization and identification of nHA in digesta

3.6.1 Electron microscopy

The identification and detection of nHA in the digetsa was carried out with the help of TEM (An FEI Tecnai G2 Spirit BioTWIN, Czech Republic) at Manuwatu Microscopy Centre, Massey University.

The pellet obtained after centrifugation of the digesta was prepared for TEM analysis as depicted in Figure 3.2. The samples obtained from Figure 3.1 was subjected to negative staining grid method of Schoepf et al. (2017) with some minor modifications before TEM analysis as follows:

1. With a help of glass bulb pipette a drop (approx. 80ul) of sample was placed on a glass petri dish lined with parafilm.
2. A copper formvar/carbon coated 200 mesh copper grid (Agar Scientific, coated in the lab) was placed (film upside down) on to the sample with a contact time of 5 min.
3. Whatman No1 filter was used to drain off excess sample solution.

4. The grid was placed on the TEM holder for analysis.

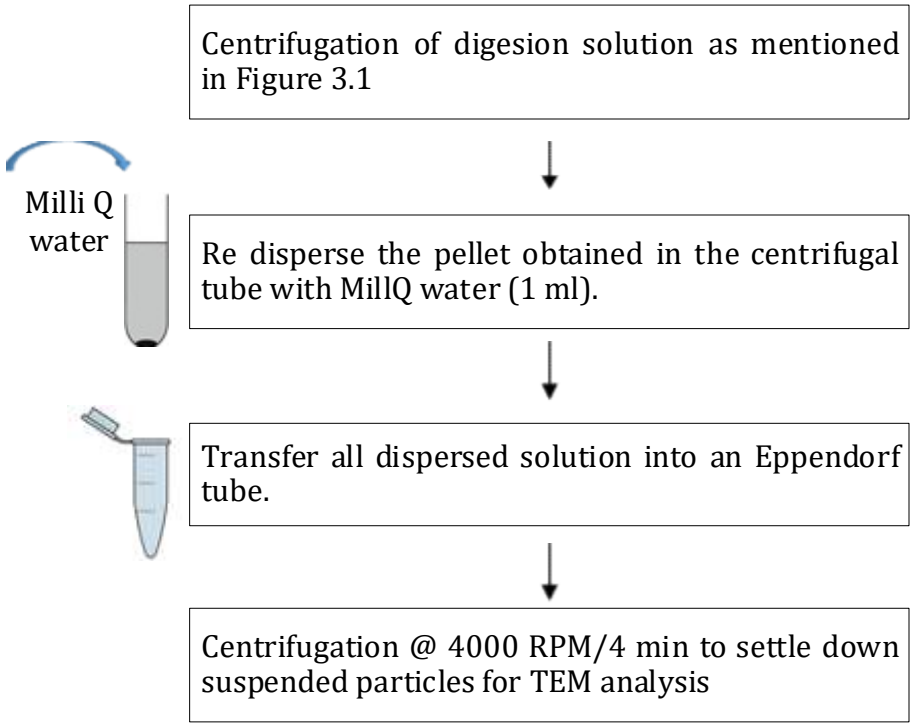

Figure 3.2 Sample preparation for TEM analysis.

For TEM analysis, the same procedure was applied to all the digesta samples including both gastric and intestinal.

3.6.2 X ray diffraction (XRD)

X ray diffraction is a technique applied mainly for the study of crystal structure by deflecting x-rays off the atomic planes of a substance. This technique has been applied since the early 1960s for crystallographic determination. The advantage of this technique is that it requires minimal sample treatment. In addition, it can be used to analyse small samples, smears, and traces of a substance (Benson, 2013). X-ray diffractometers consist of three basic elements: X-ray tube, a sample holder, and an X-ray detector. X- ray diffraction is based on the constructive interference of monochromatic radiation produced by the x ray tube on the crystalline sample. The

constructive interference created by diffracted rays is based on Bragg's law ($n\lambda = 2dsin\ \theta$).

XRD was performed using X-ray diffractometer (Rigaku, Spider, Japan) for the detection of any undissolved crystalline nHA particles after gastrointestinal digestion process. For XRD analysis, the following procedure was followed:

i. The concentrated pellet obtained after centrifugation process was placed directly on the sample holder.
ii. The generation of diffracted rays was achieved through use of diffractometer with a monochromatic Cu–Kα radiation at 40 kV and 30 mA.
iii. The sample was scanned at 2θ values from 10° to 70° for a period of 60s.

3.6.3 Energy dispersive spectroscopy (EDS)

EDS was applied for the elemental analysis of the digested samples, mainly for the detection of calcium and phosphate. The pellet obtained after centrifugation was sent to the Nutrition Laboratory, Massey University, for freeze-drying. The freeze-dried samples were then prepared for EDS analysis in the School of Agriculture & Environment, Soil and earth Sciences, Massey University.

The freeze-dried digesta sample was placed in a mould and epoxy resin was added to embed the sample. The epoxy was left to air dry overnight and the hardened epoxy was taken out the next day from the mould. The epoxy was then grinded manually using silicon carbide powder of starting form 220-400-600-1200 gritt to expose the epoxy surface with the samples embedded inside but care was taken as not it lose the samples during grinding. After grinding, the mould was polished using a diamond paste of 6 and 1 micron fine polishing on a Planopol-3 (Struers) polishing machine until a fine polished surface of exposed sample particles could be seen under the microscope.

This polished epoxy with the exposed sample particles was sent to the Manuwatu Microscopy Centre, Massey University for analysis. For EDS analysis, the samples were carbon coated and analysed using FEI Quanta 200 200 SEM (FEI, Eindhoven, Netherlands) with spectra taken by a silicon EDAX unit (NJ, USA) on EDAX Genesis (Ametek, NJ, USA) software.

3.7 Calcium analysis

3.7.1 Ionic Calcium

The ionic calcium concentration was measured using a calcium selective electrode (Orion 9720BNWP, Thermo Scientific, USA) with a CyberScan pH 510 pH/mV Meter (Eutech Instruments-Thermo Scientific, USA. The Ag/AgCl single junction electrode, reference electrode was filled with 4 M KCl. Calibration standard solutions of 1, 2, 4, 6, 8 and 10 mM Ca^{2+} was prepared from successive dilutions of the stock solution. A stock solution of 10 mM $CaCl_2$ was prepared in 51 mM KCl. As per the Nernst equation, there exists a linear relationship electrical output (mV) obtained from the electrode for the calibration solutions and log of Ca^{2+} concentration of the standard solutions. The theoretical slope for the linear equation should be around 29 mV (Lewis, 2011). The calibration was carried out every time before the start of each digestion experiment. The electrode should not take any longer than 5 min to give a stable reading. The calibration was considered correct if the slope was between 27 and 31 mV. The linear equation given by the standard was then used to convert the measured electrode mV to Ca^{2+} concentration.

3.7.2 Soluble calcium

The supernatant obtained after centrifugation of the digestion solution at different sampling time interval was sent to the Nutrition Laboratory, Massey University for a measurement of the soluble calcium concentration. The samples were centrifuged and analysed directly on the Daytona Plus Clinical Analyser (Randox laboratories limited, UK). The basis of analysis is that the calcium ions bind specifically with Arsenazo III forming a coloured complex. The amount of calcium is directly proportional to the intensity of the coloured complex formed.

Calcium + Arsenazo III $\longrightarrow$ Coloured complex.

The change in absorbance is directly proportional to the calcium concentration and was measured photometrically.

3.8 nHA dissolution (%) calculation

The percentage of nHA dissolved at each sampling time was calculated based on calcium concentration results, the SGF addition rate of 2.5 ml/min and gastric emptying rate of 3 ml/min. For nHA $_{milk}$ samples, soluble calcium results were used for the calculation whereas for nHA $_{blank}$ samples, ionic calcium results were used. Since pH decreased slowly in nHA $_{milk}$ digesta, the ionic calcium results were much lower than soluble calcium at 60 min (Figure 4.1). From 120 min to 240 min the ionic calcium and soluble calcium, results were similar due to sufficient ionization of calcium at low pH. As for nHA $_{blank}$ digesta, since the pH at 60 min were already lower than 120 min in nHA $_{milk}$, we assumed that pH would not affect ionic calcium results as in nHA $_{milk}$ samples. Therefore, the ionic calcium would give good indication of nHA dissolution in nHA $_{blank}$.

3.8.1 Dissolution (%) of nHA in nHA $_{blank}$

$$D_{t_{1-2}} = \frac{m_{t2} - m_{\text{carryover } t_2}}{m_{total}} \times 100\%$$

$$m_{t2} = (C_{HA\ blank}\ t_2 - C_{SGF}\ t_2) \times V_{t2} \times M$$

$$m_{\text{carryover t1}} = (C_{HA\ blank}\ t_1 - C_{SGF}\ t_1) \times V'_{t1} \times M$$

3.8.2 Dissolution (%) of nHA in nHA $_{milk}$

$$D_{t_{1-2}} = \frac{m_{t2} - m_{\text{carryover } t_2}}{m_{total}} \times 100\%$$

$$m_{t2} = (C_{HA\ milk}\ t_2 - C_{milk\ blank}\ t_2) \times V_{t2} \times M$$

$$m_{\text{carryover t1}} = (C_{HA\ milk}\ t_1 - C_{milk\ blank}\ t_1) \times V'_{t1} \times M$$

Where:

D_{t1-2} - Dissolution rate between time t_1 and t_2

t – Digestion time

m_t – Weight of calcium dissolved from HA at time t

$m_{carryover\ t}$ – Weight of carryover calcium dissolved from HA at time t

C_t – Ionic calcium concentration at time t

V_t – Volume of digesta at time t (before sampling)

V'_t – Volume of digesta at time t (after sampling)

M – Molecular mass of calcium

m_{total} – Weight of total calcium in added HA

3.9 Statistical analysis

All the experiments was conducted at least in triplicates or duplicates using freshly prepared samples and chemicals required for the experimental work. The results are reported as calculated means or standard deviation. T –test and One way Anova using SPSS 25.0 package (IBM, Armonk, New York) and Tukey multiple range test were used to determine the significant difference ($P<0.05$).

Chapter 4 Results and discussion

4.1 Gastrointestinal digestion

4.1.1 pH profile

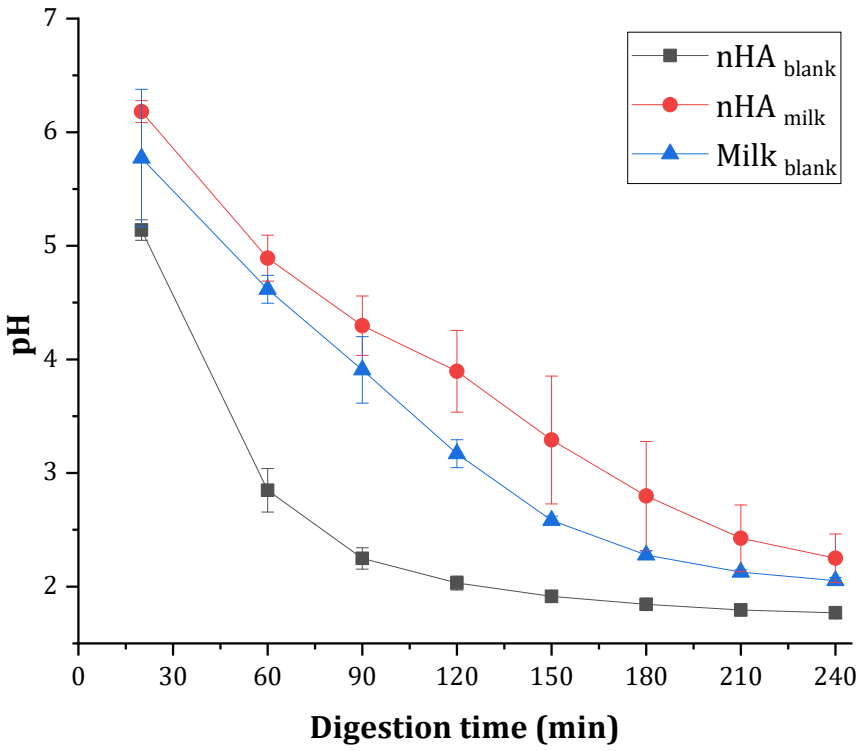

Figure 4.1 pH profile (mean ± SD) as a function of gastric digestion time for different digesta samples.

The pH of nHA $_{blank}$ digesta decreased rapidly while the pH of nHA $_{milk}$ and milk $_{blank}$ digesta decreased gradually with progression of gastric digestion as depicted in Figure 4.1. The pH of nHA $_{blank}$ decreased from initial 5.14 ± 0.09 at 20 min to 2.85 ± 0.19 at first 60 min, then decreased slowly to pH 1.77± 0.04 at 240 min. The initial pH for nHA $_{milk}$ and milk $_{blank}$ was taken to that of skim milk at zero time. The pH decreased gradually from initial pH 6.7 to pH 2.25 ± 0.21 and pH 2.05 ± 0.02 for nHA $_{milk}$ and milk $_{blank}$ respectively at 240 min. The pH values at each sampling time among the three digesta samples were found to be significantly different ($P<0.01$).

The overall changes of pH in nHA $_{milk}$ and milk $_{blank}$ digesta during digestion were similar except from 120 to 150 min which differed significantly ($P<0.05$). Both the digestion samples containing milk had significantly different ($P<0.01$) pH in comparison to nHA $_{blank}$ during the entire digestion period.

4.1.2 Calcium

The determination of the ionic calcium content was carried out from the non-centrifuged digesta, while the soluble calcium content was obtained from the supernatant after centrifugation of the digestion solution at specific digestion times.

4.1.2.1 Ionic calcium

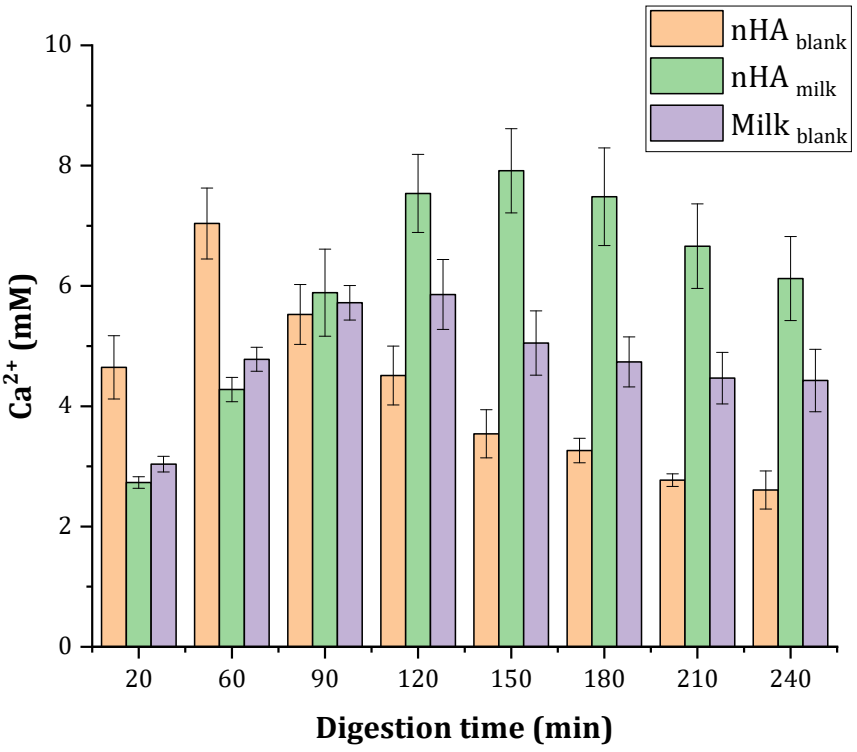

Figure 4.2 Ionic calcium concentration (mM) in the three different gastric digesta samples.

In general, there was a gradual increase in the release of calcium in the form of ionic calcium with digestion time followed by a gradual decrease after reaching the

highest concentration in all the digesta samples (Figure 4.2). The ionic calcium concentration for nHA $_{blank}$ increased sharply from of 4.65 ± 0.59 mM at 20 min reaching a maximum concentration of 7.04 ± 0.66 mM at 60 min. For nHA $_{milk}$ digesta samples, the Ca^{2+} concentration increased gradually from 2.73 ± 0.10 mM at 20 min to the highest Ca^{2+} concentration value of 7.95 ± 0.70 mM at 150 min. Similarly, for milk $_{blank}$ digesta samples the concentration of Ca^{2+} increased gradually from 3.04 ± 0.13 mM (20 min) reaching 5.86 ± 0.58 mM (120 min). The Ca^{2+} concentration values between the three different digesta were significantly different ($P<0.01$) with an exception at 90 min. The digestion time taken for the attainment of maximum concentration of Ca^{2+} was different for all the digesta; from the initial 20 min the maximum concentration of Ca^{2+} was reached at 60 min for the nHA $_{blank}$, 150 min for nHA $_{milk}$ and, 120 min for Milk $_{blank}$ digesta. After the attainment of the maximum Ca^{2+} concentration, the Ca^{2+} started to decrease gradually in all the digestion solutions reaching ~6.01 mM, ~4.43 mM and ~2.61 mM for nHA $_{milk}$, milk $_{blank}$ and nHA $_{blank}$ respectively at the end of the 240 min digestion process.

4.1.2.2 Soluble Calcium

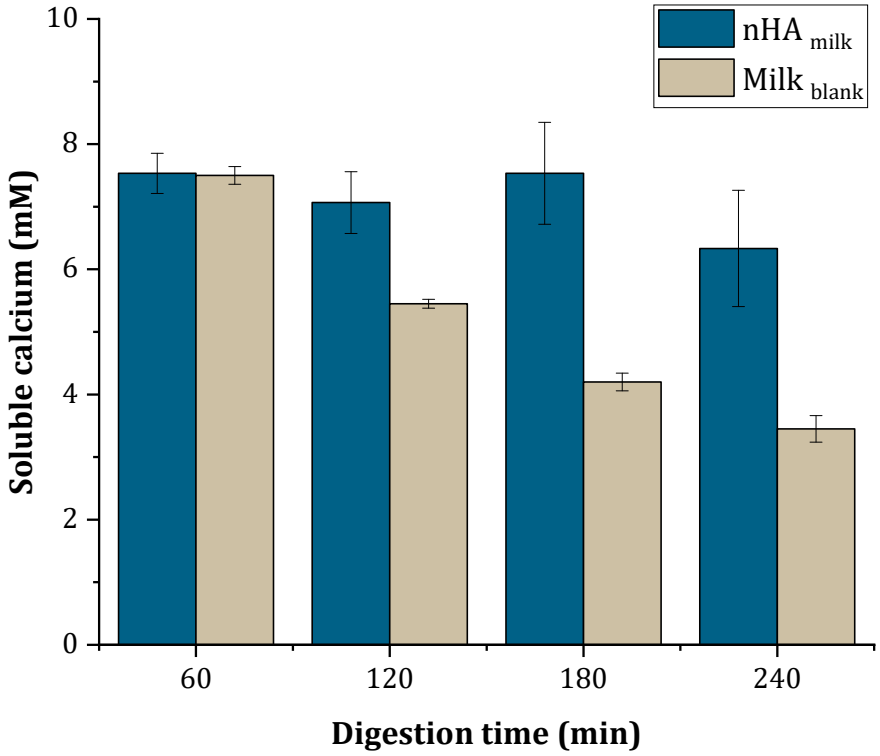

Figure 4.3 Soluble calcium concentration of nHA $_{milk}$ and milk $_{blank}$

The soluble calcium concentration decreased gradually in both nHA $_{milk}$ and milk $_{blank}$ digesta (Figure 4.3). The soluble calcium concentration values for nHA $_{milk}$ (7.53 ± 0.32 mM) and milk $_{blank}$ (7.50 ± 0.14 mM) are similar during the first 60 min of digestion time. After 60 min of digestion time, the soluble calcium concentration in nHA $_{milk}$ was significantly higher ($P < 0.05$) than the milk $_{blank}$ digesta. The soluble calcium concentration decreased with the progression of digestion time reaching to 6.33 ± 0.93 mM and 3.45 ± 0.21 mM respectively for at nHA $_{milk}$ and milk $_{blank}$ digesta at 240 min gastric digestion.

4.1.2.3 Ionic calcium vs. Soluble Calcium

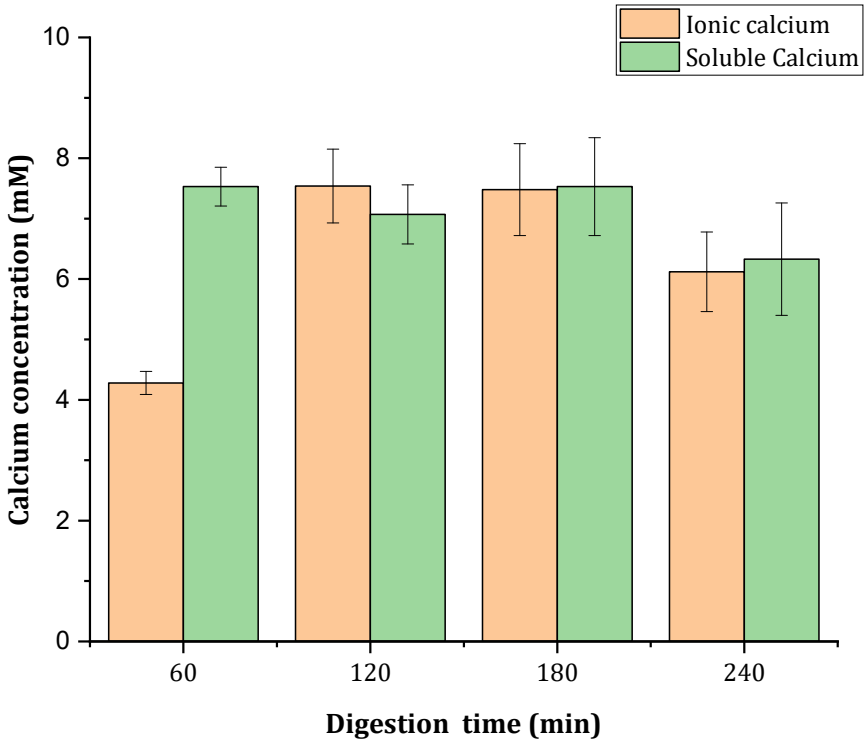

Figure 4.4 Ionic calcium vs. soluble calcium at each digestion sampling time for nHA $_{milk}$ digesta samples.

The comparison between the ionic and soluble calcium results in nHA $_{milk}$ showed that initially at 60 min of gastric digestion, the soluble calcium concentration ~ 7.53 mM in the digesta was considerably higher than the ionic calcium concentration ~4.28 mM. After 60 min the ionic calcium and soluble calcium, results are found to be in similar range to each other until 240 min of digestion except at 120 min (Figure 4.4).

4.1.2.4 Calcium in the intestinal digesta

After gastric digestion of 240 min the digesta collected was subjected to intestinal digestion for a period of 120 min in 1:1 ratio of gastric digesta and SIF. After 120 min of intestinal digestion, the digsta was collected for determination of both ionic and soluble calcium concentration.

Table 4.1 Ionic and soluble calcium concentration after 120 min of intestinal digestion.

Samples	**Ionic calcium concentration (mM)**		**Soluble calcium concentration (mM)**	
	Gastric digestion (240 min)	**120 min intestinal digestion**	**Gastric digestion (240 min)**	**120 min intestinal digestion**
nHA $_{blank}$	2.61 ± 0.35	0.48 ± 0.36	2.65 ± 0.21	1.20 ± 0.00
nHA $_{milk}$	6.01 ± 0.70	0.93 ± 0.25	6.33 ± 0.93	1.80 ± 0.28
Milk $_{blank}$	4.43 ± 0.52	0.98 ± 0.01	3.45 ± 0.21	2.00 ± 0.00

Table 4.2 demonstrates the ionic calcium and soluble calcium concentration of the three different digesta after 120 min of intestinal digestion. In all the three digetsa samples, both the ionic calcium and soluble calcium concentration decreased after 120 min of intestinal digestion when compared to the gastric (240 min) ionic calcium and soluble calcium concentration.

The ionic and soluble calcium concentration after intestinal digestion was similar for nHA $_{milk}$ and milk $_{blank}$. In nHA blank digesta, both the ionic calcium and soluble calcium content was comparatively lower than that from digesta of milk as the dispersing medium.

4.1.3 Determination of the dissolution rate of nHA

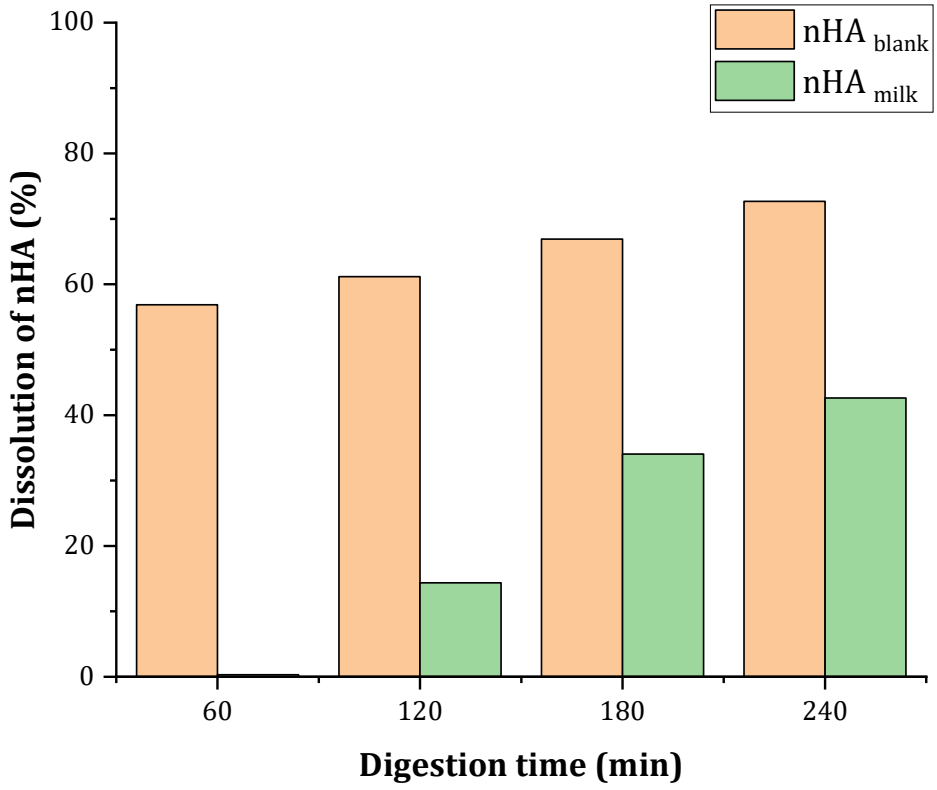

Figure 4.5 Dissolution (%) of nHA $_{milk}$ as a function of digestion time in SGF.

In general, the dissolution of nHA $_{blank}$ and nHA $_{milk}$ digesta increased with the progression of digestion. The dissolution of the digesta increased from an initial 57 % at 20 min to 73 % for nHA $_{blank}$ and from 0.30 % at 20 min to 43 % for nHA $_{milk}$ after 240 min of the gastric digestion process respectively. The dissolution trend observed in Figure 4.5 corresponds to the trend observed in the ionic calcium concentration in Figure 4.2.

Table 4.2: nHA dissolved (%) in a digestion time interval of 60 min.

	nHA $_{blank}$	**nHA $_{milk}$**
Digestion time (min)	**nHA dissolved (%) in time interval of 60 min**	**nHA dissolved (%)in time interval of 60 min**
0-60	56.7	0.3
60-120	4.3	14.1
120-180	5.8	19.8
180-240	5.8	8.9

Table 4.2 represents the rate of dissolution of nHA in nHA $_{milk}$ and nHA $_{blank}$ digesta sampled with 60 min time gap of digestion time before the next digestion sampling time. In the nHA $_{blank}$ digesta, the dissolution rate was rapid increasing to 56.7 % in one hour time gap (0-60 min) that relates to the attainment of the highest dissolution rate of nHA $_{milk}$ and decreased gradually thereafter. However, for nHA $_{milk}$ digesta the dissolution was lower (0.3 %) during first one hour time gap of 0-60 min. The percentage dissolution of nHA increased gradually and reached the highest 19.8 % at 120-180 min after which, the dissolution rate slowed down. At the last 60 min time gap (180-240 min) of the gastric digestion process, the percentage of dissolution was 5.8 % and 8.9 % for nHA $_{blank}$ and nHA $_{milk}$ respectively.

4.1.4 Detection and identification of undissolved nHA during gastrointestinal digestion

The determination of the presence of undissolved nHA during gastrointestinal digestion was carried out using techniques generally recognized for the characterisation of NPs such as TEM, XRD and EDS. The paste like pellet obtained after the centrifugation of digesta was subjected to TEM and XRD analysis. For EDS analysis, the pellet was freeze dried and crushed into a powder for determination of calcium and phosphate content.

4.1.4.1 TEM analysis

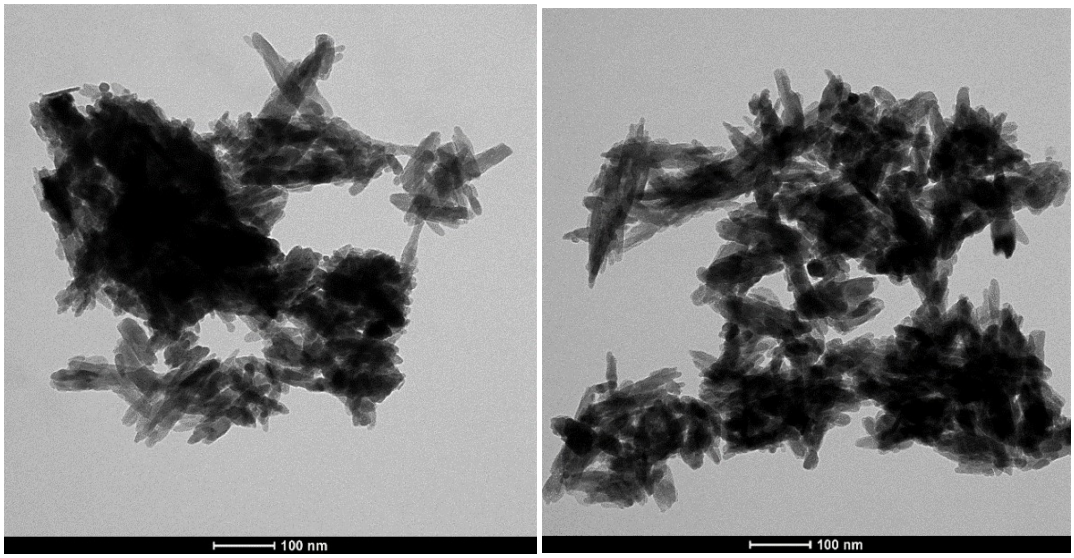

Figure 4.6 TEM micrographs of reference nHA powder (1% suspension solution) @ 105kx magnification.

The TEM micrographs in Figure 4.6 demonstrated that the structure of reference nHA powder was typically of rod-shaped needle-like nano sized HA crystals as per supplier's specification. The dark field in the images showed that the nHA crystal were present in the form of aggregates, which overlapped each other creating a darker shade in the TEM micrographs.

After 240 min of gastric digestion, the TEM micrographs indicated the presence of undissolved nHA in the digesta of both nHA_{blank} (Figures 4.7 and 4.8) and nHA_{milk} (Figures 4.9 and 4.10). During gastric digestion, the sharp needle-like structure of nHA crystals as seen in reference TEM micrographs were reduced with the progression of the digestion process.

For $nHA_{blank,}$ the dissolution/dissociation of nHA particles increased with the progression of digestion. After 60 min of gastric digetsion the presence of undissolved nHA on the TEM grid was difficult to find with the progression of digestion process. The dissociation of nHA was evident from the TEM images (Figures 4.7 and 4.8) at different digestion times showing the presence of lesser and fewer numbers of nHA aggregates. By the end of the digestion process, there were higher numbers of single nHA particles as compared to the first 60 min of digestion.

For nHA_{milk} the presence of larger aggregates of undissolved nHA were still seen during the first 120 min of the digestion process as shown in Figures 4.9 and 4.10. Similar to the nHA_{blank} digesta, the dissociation process could be seen at the initial 60 min. However, more dissociation of nHA was observed at 120 min as at 60 min some intact clusters of undissolved nHA particles similar to the reference nHA TEM images in Figure 4.6 were found. Although after 120 min the presence of undissolved nHA was still observed, it became harder to find the undissolved nHA from 180 to 240 min of the digestion process.

A clearer representation of the nHA dissolution process showing the dissociation of nHA into smaller aggregates or individual nHA is depicted in Figure 4.11 A and B for nHA_{blank} and nHA_{milk} digesta respectively.

The TEM micrographs in Figure 4.12 showed the presence of undissolved nHA after 120 min of intestinal digestion in both nHA_{blank} and nHA_{milk} digesta.

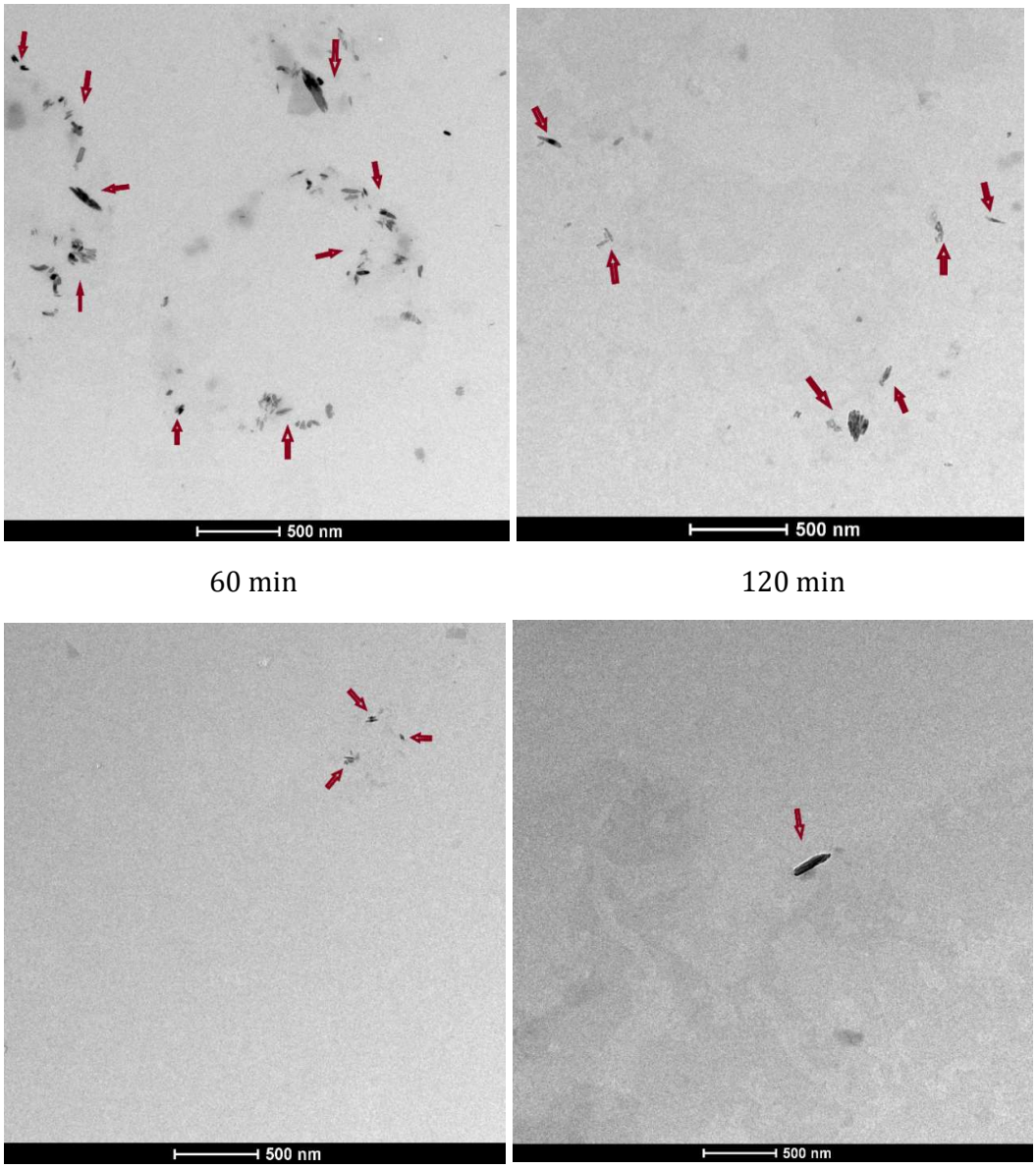

60 min 120 min

180 min 240 min

Figure 4.7: TEM micrographs of nHA $_{blank}$ digesta at different digestion times, red arrows indicate the presence of undissolved nHA @26500x magnification.

60 min 120 min

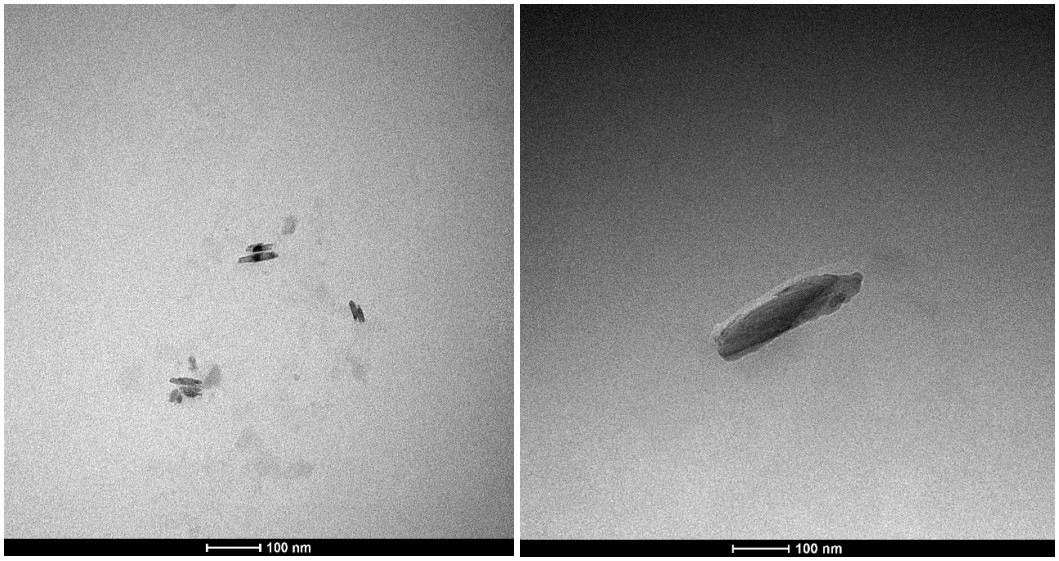

180 min 240 min

Figure 4.8: TEM micrographs of nHA $_{blank}$ digesta at different digestion times, demonstrates the presence of undissolved nHA @105Kx magnification.

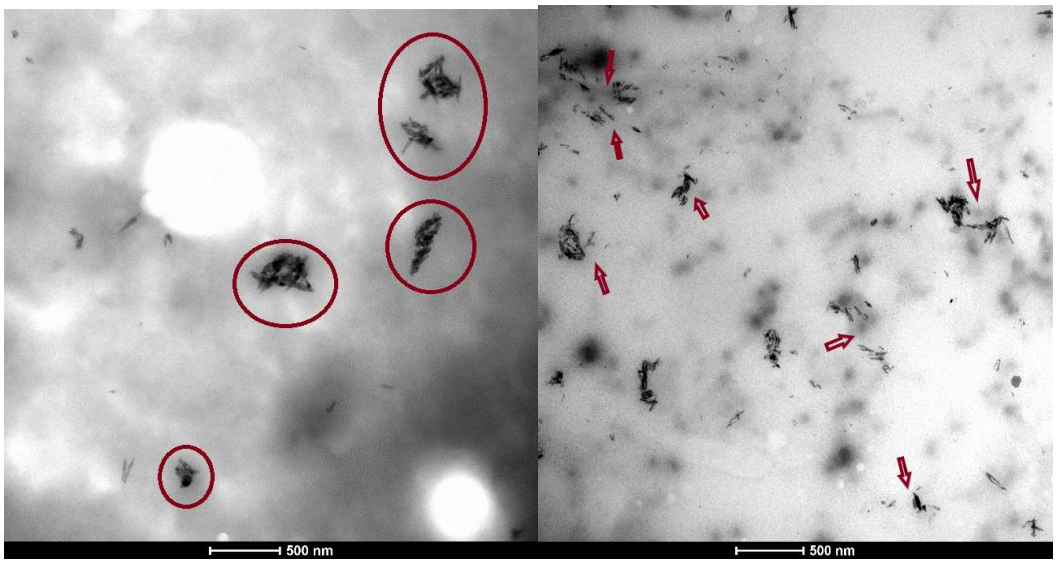

60 min 120 min

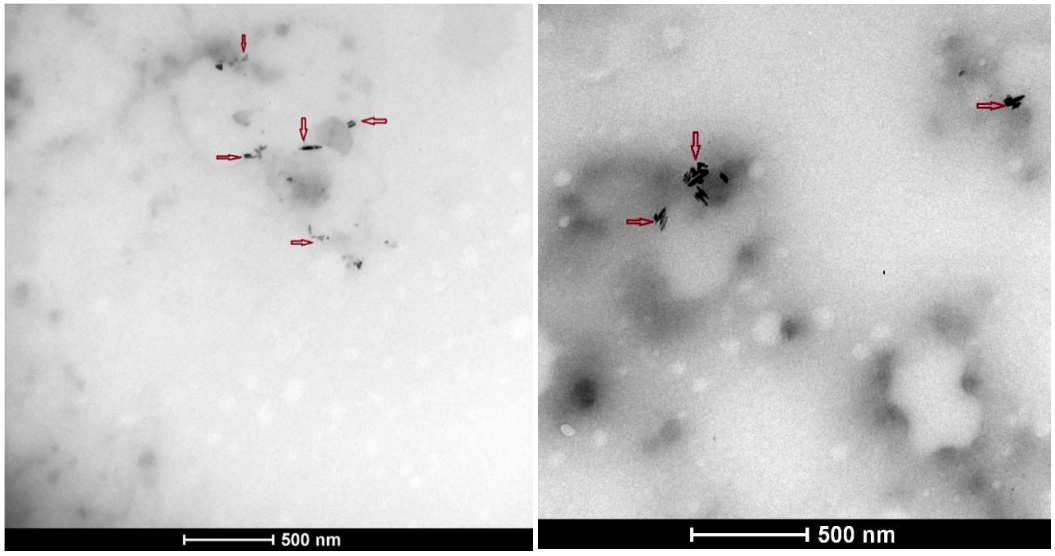

180 min 240 min

Figure 4.9: TEM micrographs of nHA $_{milk}$ digesta at different digestion times, red circles and arrows indicate the presence of undissolved nHA @26500x.

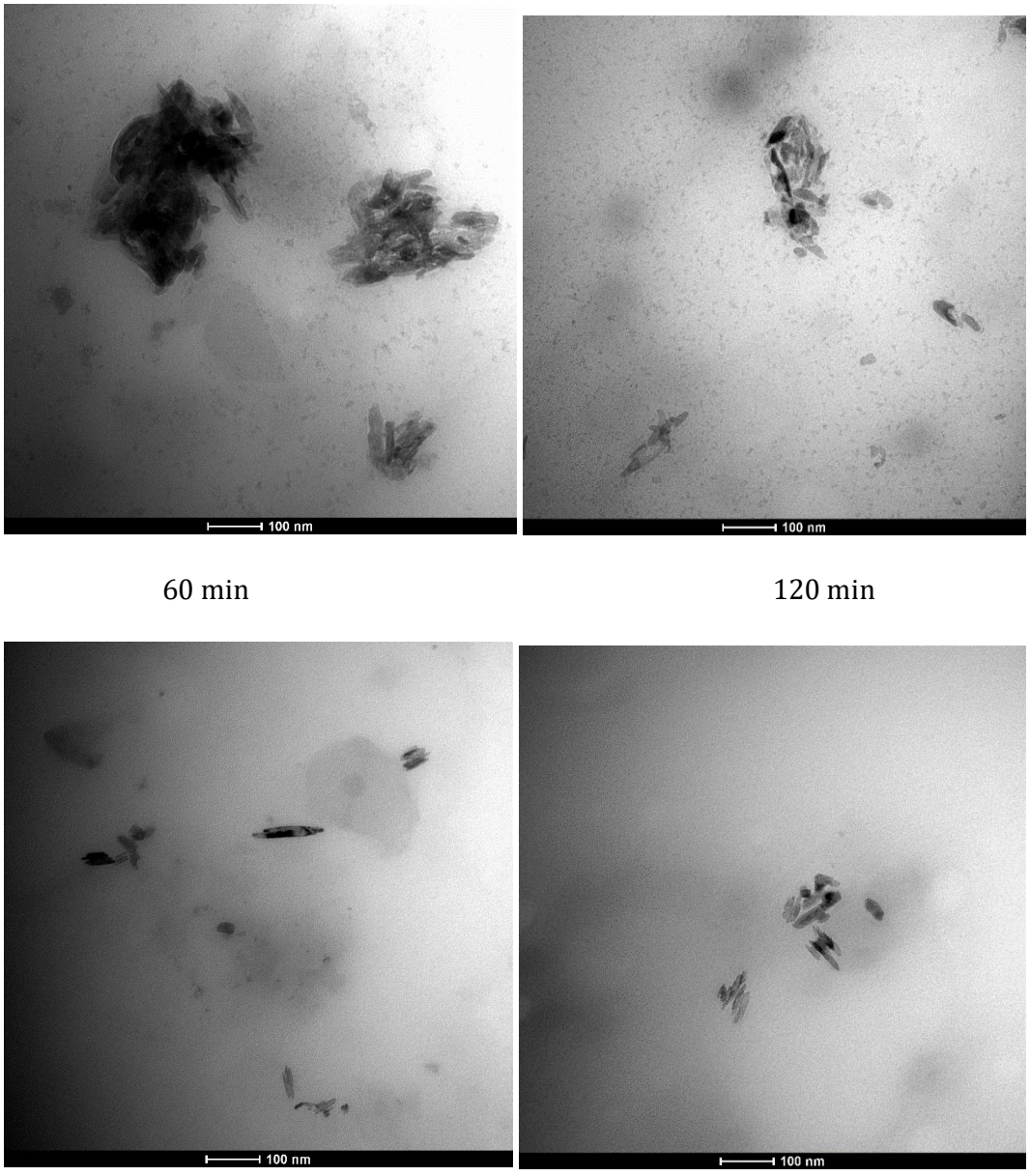

60 min 120 min

180 min 240 min

Figure 4.10: TEM micrographs of nHA $_{milk}$ digesta at different digestion times, demonstrates the presence of undissolved nHA @105Kx magnification.

60 min 120 min

(A)

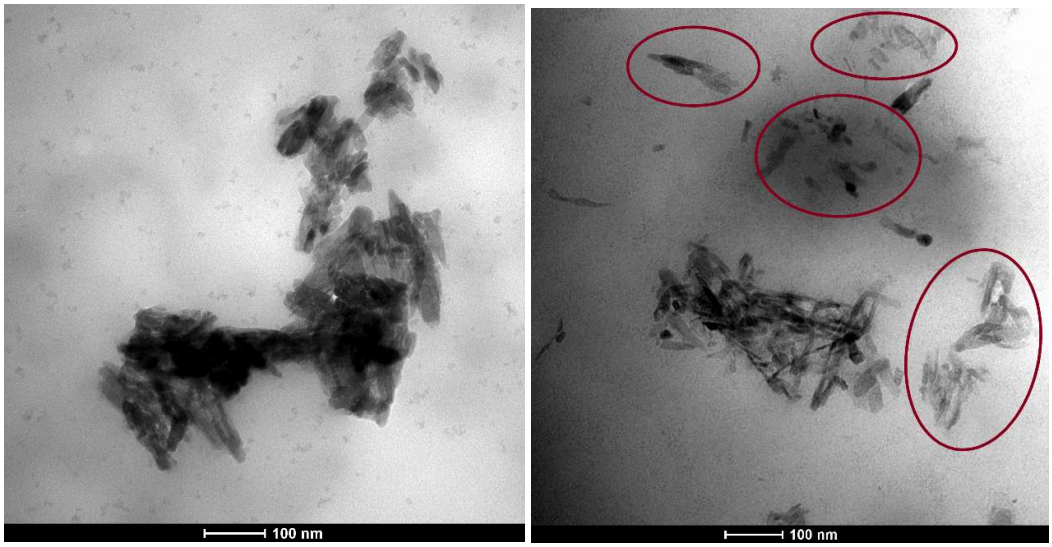

60 min 120 min

(B)

Figure 4.11 TEM micrographs showing dissociation of nHA aggregates marked with red circles (A) nHA $_{blank}$ digesta at 60 min and 120 min of digestion time and (B) nHA $_{milk}$ digesta at 60 min and 120 min of digestion time @105kx magnification.

(A)

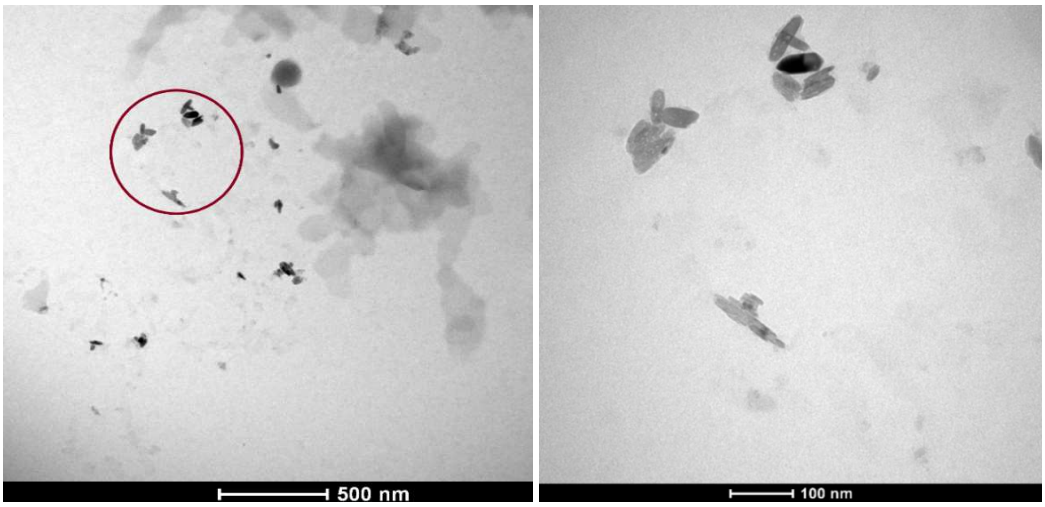

(i) **(ii)**

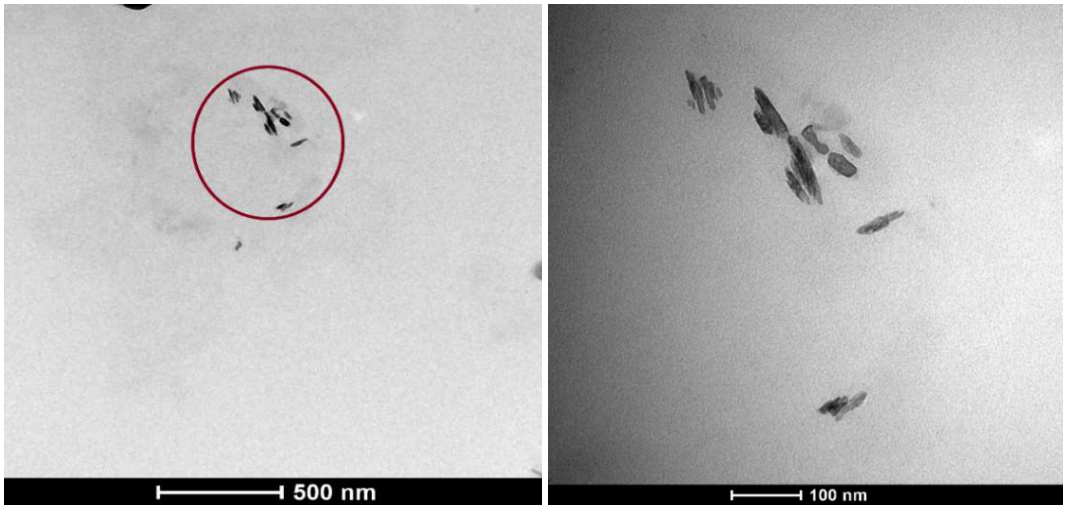

(B)

(i) **(ii)**

Figure 4.12 TEM micrographs after 120 min of intestinal digestion (A) nHA $_{blank}$ and (B) nHA $_{milk}$ represented by (i) Red circles represent nHA particles @ 26500x magnification and (ii) 105kx magnification.

4.1.4.2 XRD analysis

The XRD diffraction peaks of reference nHA were sharp showing the presence of a crystalline structure. The reference nHA generated peaks in the range of 25 to 60 2Θ degrees; the most prominent peak was in between 30-35 2Θ degrees followed by the peaks in between 25- 30 2Θ degrees and from 40 to 60 2Θ degrees (Figure 4.13).

In the nHA $_{blank}$ digesta samples, there was no generation of diffraction peaks similar to that of reference diffraction peaks. However, for the nHA $_{blank}$ the occurrence of a small peak and a curve like peak (bump) can be noticed between 2Θ degrees of 20 and 25 (Figure 4.13). This small peak was first observed at 60 min to 180 min however, at 240 min it is difficult to confirm the peak appearance and after intestinal digestion the peak seems to reappear.

For nHA $_{milk}$ digesta, the XRD diffraction peaks detected the presence of crystalline nHA during the initial 120 min of gastric digestion. However, at 240 min the diffraction peaks were not visible and is visible at the end of intestinal digestion. The XRD diffraction peaks at 60 and 120 min was similar to that of the reference nHA diffraction peaks at 2Θ degrees starting from 25 to 55 as depicted in Figure 4.14. On the other hand, the diffraction peaks produced showed a decrease in peak sharpness at 60 min and 120 min of digestion time when compared to reference nHA diffraction peaks. In addition to the diffraction peaks similar to reference nHA, the occurrence of the same small peak and curve, as in the case of nHA $_{blank}$ was also observed between 2Θ degrees of 20 and 25 starting from 120 min to 180 min. At 240 min the peak was not detected but was again observed during intestinal digestion.

The XRD peaks of milk $_{blank}$ digesta samples did not show any sharp peaks of crystalline nHA (Figure 4.15). Similarly, the new 2Θ degrees peaks between 20 and 25 were also noticed in both the gastric and intestinal digesta.

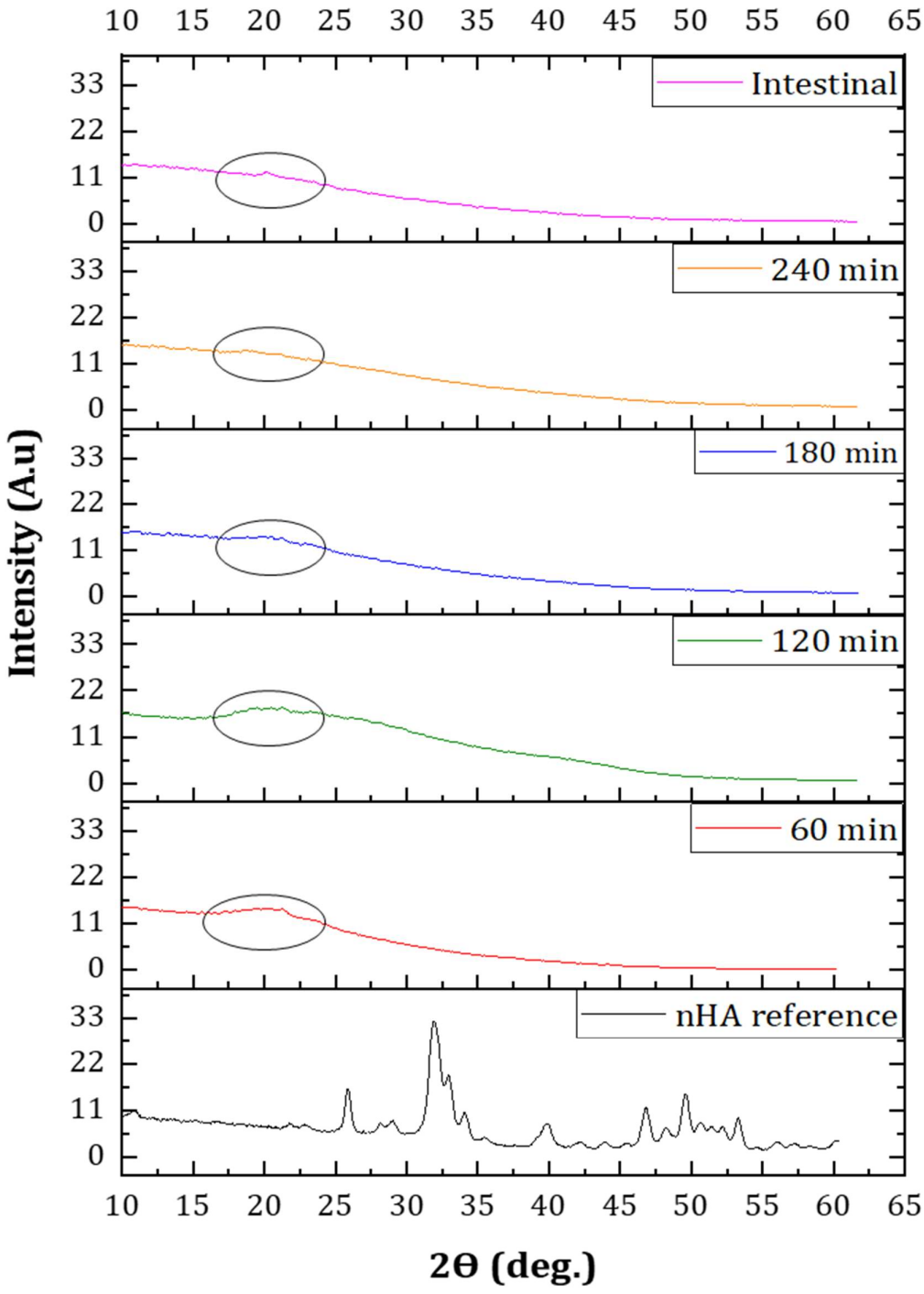

Figure 4.13: XRD pattern from pellets collected from nHA $_{blank}$ at different gastrointestinal digestion times.

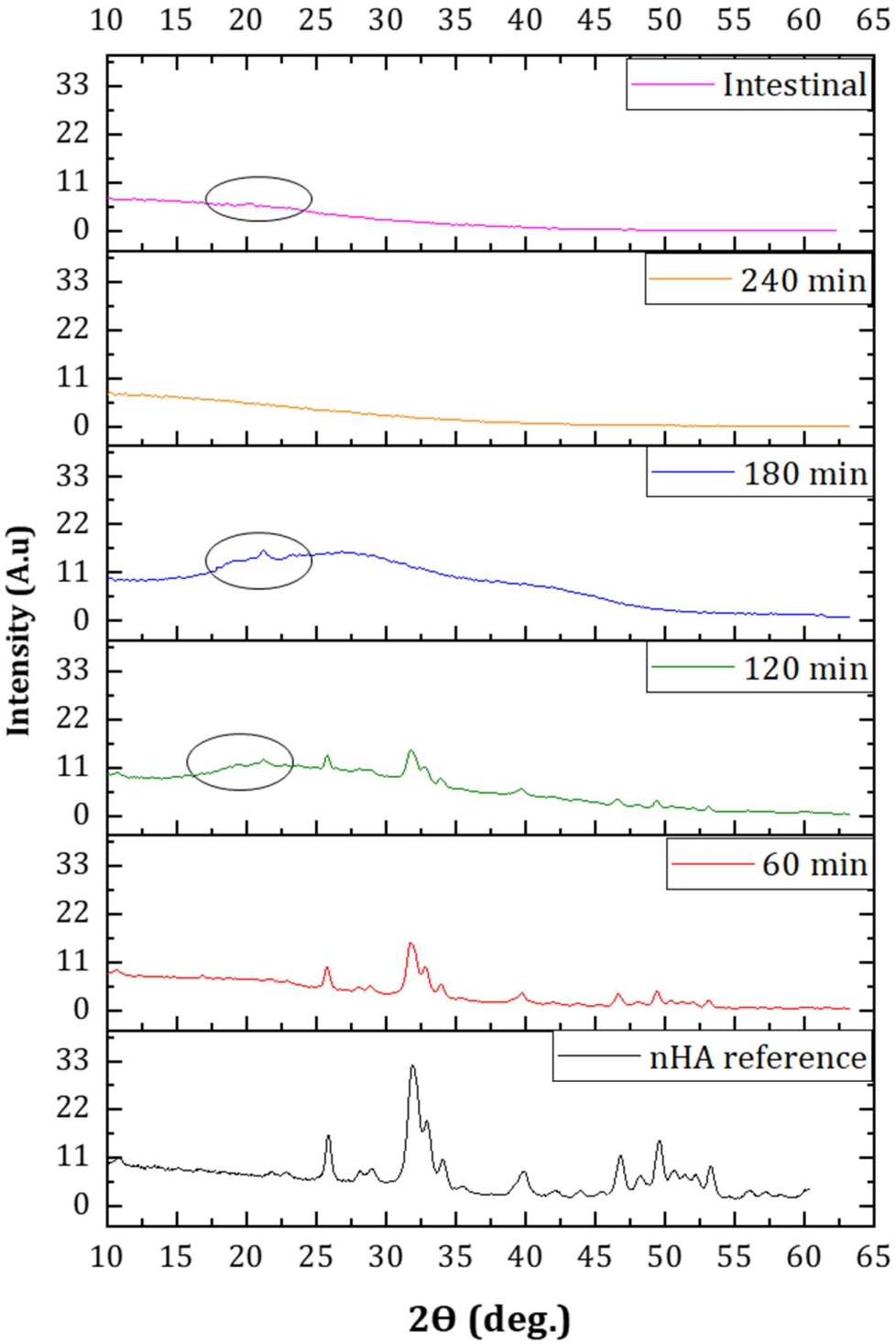

Figure 4.14: XRD pattern from pellets collected from nHA $_{milk}$ at different gastrointestinal digestion times.

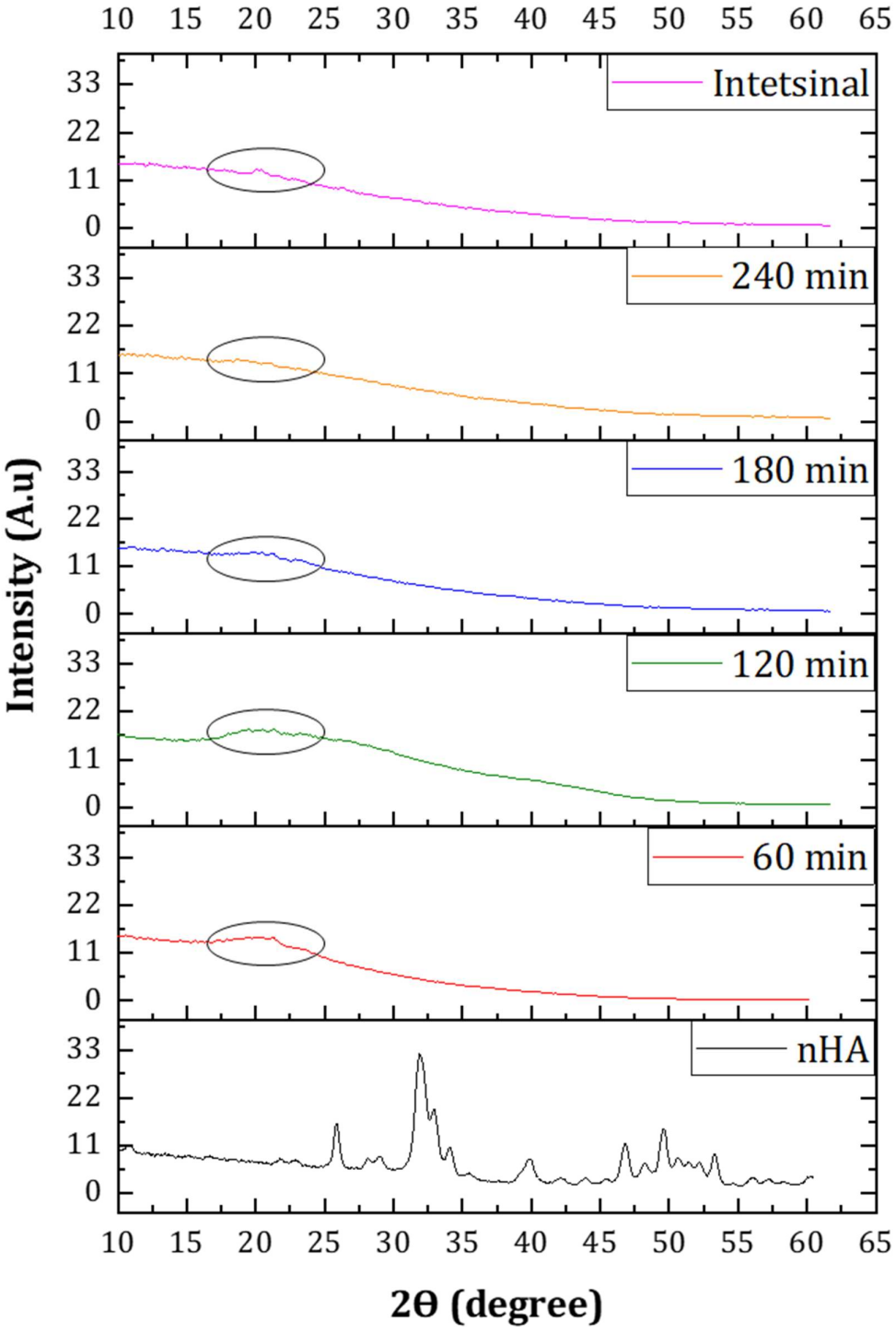

Figure 4.15: XRD pattern from pellets in milk $_{blank}$ at different gastrointestinal digestion times.

4.1.4.3 Energy dispersive spectroscopy analysis

The presence of calcium and phosphate elements in the pellets obtained at different digestion times were measured using the energy dispersive spectroscopy.

Table 4.2: EDS results of freeze-dried digesta pellet from nHA $_{milk}$ samples at different gastric digestion times.

Element	Reference nHA powder		Gastric digestion						Intestinal digestion
			60 min		120 min		180 min	240 min	
	Avg. Wt. %	Ca/P	Avg. Wt. %	Ca/P	Avg. Wt. %	Ca/P	Avg. Wt. %	Avg. Wt. %	Avg. Wt. %
P K	8.41 ± 3.08	1.67 ± 0.22	8.49 ± 0.63	1.86 ± 0.02	9.09 ± 1.30	1.70 ± 0.05	< 1	< 1	< 1
Ca K	14.54 ± 6.87		15.86 ± 1.24		16.2 ± 1.89		< 1	< 1	< 1

During gastric digestion, the EDS results in Table 4.3 demonstrates the presence of calcium and phosphate content in freeze dried powder of nHA $_{milk}$ digesta at 60min and 120 min. From 180 min to the end of intestinal digestion process the concentration of calcium and phosphate is too low (<1%). The Ca/P ratio of reference nHA powder is 1.67, while for the nHA $_{milk}$ digesta the Ca/P is 1.86 and 1.78 at 60 min and 120 min respectively.

4.2 Discussion

4.2.1 Dissolution of nHA in nHA $_{blank}$

For nHA $_{blank}$ digesta, the pH decreased rapidly from an initial ~ 5.14 at 20 min to ~ 2.85 at 60 min and then decreased gradually as shown in Figure 4.1. These changes in pH were brought about by the addition of SGF at the rate 2.5 ml/min. The rapid decrease in pH during the first 60 min could be due to a lack of buffering constituents in nHA $_{blank}$ unlike digestion samples prepared with milk. Consequently, with the reduction in pH, the ionic calcium concentration increased until attainment of the highest ionic calcium concentration. In Figure 4.2, the maximum value of ionic calcium concentration (7.04 ± 0.66 mM) were achieved at 60 min of digestion time. This could be attributed to the changes in the pH values with digestion time. The rapid reduction in pH during the first 60 min of digestion corresponded to the highest concentration of Ca^{2+}. After reaching the maximum level, the Ca^{2+} concentration decreased gradually even with the gradual decrease in pH. This could be due to the dilution effect caused by the subsequent addition of SGF and sampling out of the digesta samples.

Figure 4.5 showed an increased dissolution of nHA with a progression of digestion time. On average 73 % of total nHA dissolved at the end of 240 min gastric digestion time. The incomplete dissolution of nHA was observed in the TEM micrographs taken at different digestion times. The percentage of nHA dissolution in the nHA $_{blank}$ samples are similar to the dissolution result in the study of Schoepf et al. (2017). They reported a dissolution of >60 % of needle like HA when performed under 2 h of static digestion at pH 1.6. The dissolution of nHA within a one hour time gap showed that the maximum dissolution (57 %) was achieved within first 0-60 min of digestion time. This highest dissolution value observed in Table 4.2 corresponds to the highest values observed in the ionic calcium concentration in Figure 4.2.

It is well known that hydroxyapatite is insoluble in water but dissolves in acidic solution below pH 4 (Dorozhkin & Epple, 2002). The Ostwald–Freundlich equation of dissolution expresses solubility as a function of interfacial tension and particle size and predicts the solubility to increase with the decrease in particle size (Borm et al., 2006; Wang et al., 2011). Theoretically, this states that the dissolution of a

smaller size crystal is faster. However, it was interesting to note that experimentally in this study; the nHA $_{blank}$ sample prepared in water without the matrix effect did not dissolve completely even under acidic conditions as low as pH 1.77 ± 0.04. The TEM micrographs clearly showed the presence of undissolved nHA during the entire 240 min of gastric digestion time (Figures 4.7 and 4.8). This suggests involvement of other mechanisms that inhibit the dissolution process. Thus, we suggest the following possible mechanisms that could inhibit the dissolution process of nHA such as (i) critical size effect, (ii) diffusion mechanism and (iii) ion binding property of nHA.

4.2.1.1 Critical size effect

The incomplete dissolution behaviour of nHA could be attributed to the critical size effect. As the nHA particle size is reduced and approaches the critical length value, the free energy required to overcome the value is higher which slows down the dissolution process. Under acidic conditions, the dissolution of crystal is initiated with the formation of pits on the surface followed by spreading of the dissolution steps on the surface as mentioned in the etch pit dissolution model (Dorozhkin, 2012). The spreading of dissolution steps results in an increase in step length that increases the Gibbs Thompson free energy (L. Wang et al., 2011). Tang, Nancollas, and Orme (2001) emphasized the role of critical size during the dissolution of sparingly soluble CPs. They stated that the formation and spreading of active etch pits on the surface leads to dissolution and the pits size need to be larger than the critical size/value for continuous dissolution. However, when crystallite sizes are the same as the critical value, it leads to inhibition of dissolution. This size effect is further enhanced for sparingly soluble NPs (Tang et al., 2004a). They demonstrated the role of critical length value in dissolution of hydroxyapatite using constant composition technique and found that the dissolution of HA crystals was suppressed when the size of the crystal reached the critical length of the active pit sites.

4.2.1.2 Diffusion mechanism

The dissolution process is a spontaneous process continuing until equilibrium is reached between the nHA surface and the liquid phase or until all the solid phase is dissolved. Dissolution takes place through the diffusion of molecules from the dissolving solids to the bulk solution through a diffusion layer. The diffusion layer region consists largely of solvated ions and solute molecules (Borm et al., 2006). The driving force for diffusion is governed by the concentration gradient between the solute surface and bulk solution phase and on the solubility of the material themselves in the given environment (Borm et al., 2006; Misra, Dybowska, Berhanu, Luoma, & Valsami-Jones, 2012). During the digestion process, the dissolution of nHA takes place through detachment and transport of atoms from the surface to the solution that leads to formation of a diffusion layer on the surface. In our study, 73 % of nHA was dissolved after 240 min of digestion, of which the majority of nHA was dissolved during the first 60 min of digestion due to the rapid decline in pH. During the remaining part of the digestion until 240 min, the dissolution of nHA at every 60 min was approximately 5-6 %. The continuous addition of SGF diluted the digesta, creating the concentration gradient between nHA and the liquid phase, preventing complete inhibition of the dissolution process.

4 .2.1.3 Ion binding property of nHA

HA is highly susceptible to substitution on its crystal lattice that allows binding of other ions and atoms from the surrounding medium on the HA surface. This is because the surface of HA is not homogenous containing both positive and negative charges; the P-sites are negatively charged, formed by the oxygen atoms associated with phosphate while, the C-sites are positively charged formed by the Ca^{2+} on the crystal lattice (Gorbunoff & Timasheff, 1984). However, in water HA is negatively charged because of greater number of exposed P-sites than C-sites on the HA surface (Tercinier et al., 2014b). From the surrounding medium, both the cations and anions can bind on to the respective negatively charged P-sites and positively charged C-sites of HA surface. This ion binding ability of nHA on its surface leads to the inhibition of nHA dissolution; the mechanism is known as the self-inhibition model (Mafe et al., 1992). In this model, apatite is dissolved by the removal of calcium ions

and phosphate ions from the surface to the solution. However, the Ca^{2+} ions can strongly adsorb back on the apatite surface forming a layer of calcium at the solid interface. Owing to its low permeability this calcium rich layer was found to restrict the diffusion of calcium and phosphate ions into the bulk solution ultimately slowing down the dissolution process (Thomann, Voegel, & Gramain, 1990). Similarly, during the dissolution of nHA, the higher adsorption of detached Ca^{2+} ions back on the larger number of negatively charged P-sites leads to the formation of this calcium rich layer, which could ultimately inhibit the dissolution process.

Another ion binding effect during digestion of nHA $_{blank}$ could be the adsorption of the molecules from the surrounding SGF medium on the nHA surface owing to high susceptibility of HA to substitution on the crystal lattice. The adsorption of the cations and anions from the SGF on the nHA surface would lead to an increase in the diffusion layer slowing down the dissolution process. Misra et al. (2012) stated that composition of the surrounding dissolution medium such as the organic and inorganic components could interact with the NPs affecting the solubility of NPs either by promoting or by inhibiting dissolution.

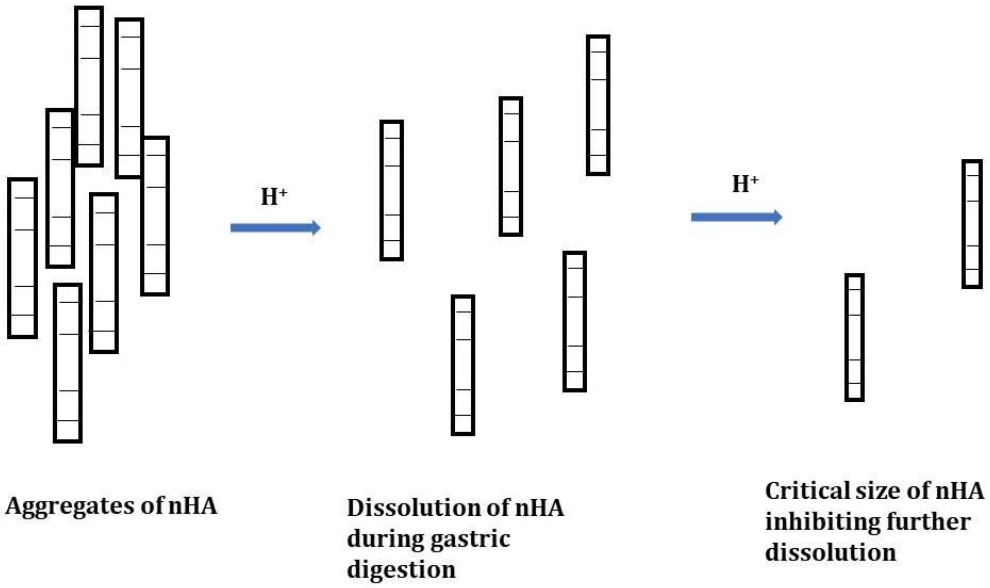

Figure 4.16 Schematic representation of dissolution of nHA by the action of acid during gastric digestion, leading to critical size effect.

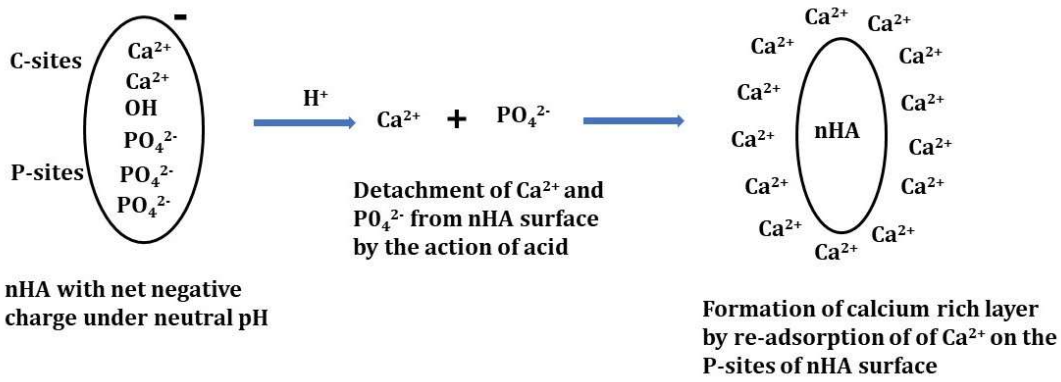

Figure 4.17 Schematic diagram showing the formation of calcium rich layer on nHA surface during gastrc digestion inhibiting nHA dissolution.

4.2.2 Dissolution of nHA in nHA $_{milk}$

During gastric digestion of nHA $_{milk}$ sample, it is observed that the pH decreased gradually (Figure 4.1) resulting in gradual increase in ionic calcium concentration until the maximum peak value (Figure 4.2). The time taken to reach the maximum ionic calcium concentration was slower when compared to the blank samples (nHA $_{blank}$ and milk $_{blank}$). The calculated percentage dissolution of nHA from nHA $_{milk}$ digesta after 240 min of gastric digestion was low standing at 43 % when compared to nHA $_{blank}$ (73 %). The presence of undissolved nHA during gastric digestion was confirmed from the TEM micrographs (Figures 4.9 and 4.10) as well as from the XRD diffraction peaks at 60 and 120 min of digestion (Figure 4.14).

Based on the slower dissolution of nHA in nHA $_{milk}$ digesta when compared with nHA $_{blank}$ digetsa, we can conclude that the milk components have a detrimental effect on the dissolution of nHA during the digestion process. Thus, we propose that during gastric digestion, the delayed decrease in pH, the presence of ions and protein binding ability of HA and formation of clot may have played a crucial role in slowing down the dissolution of nHA.

4.2.2.1 pH

During gastric digestion, there is a gradual decrease in pH for nHA $_{milk}$ digesta compared to nHA $_{blank}$ digesta (Figure 4.1). The gradual reduction in pH with increasing digestion time was brought about by the buffering capacities of milk components and nHA. Milk components such as proteins and salts (phosphate, carbonate, citrate and lactate) are known to increase the buffering capacity (Salaun, Mietton, & Gaucheron, 2005). Hydroxyapatite is chemically a calcium phosphate salt containing 40 % calcium. Milk is saturated with calcium phosphate salts and the addition of calcium salts, in an already saturated milk system, results in an increased buffering capacity (Salaun et al., 2005).

The ionic calcium concentration increased until the maximum concentration with simultaneous reduction in pH and the progression of digestion time. Tsioulpas, Lewis, and Grandison (2007) demonstrated a linear relationship between pH and log (Ca^{2+}). As expected, the concentration of ionic calcium (Ca^{2+}) from nHA $_{milk}$ is the

highest followed by the HA blank and least by the milk $_{blank}$ (Figure 4.2). The presence of free ionic calcium and calcium in milk and the simultaneous detachment of calcium from nHA with the decreasing pH results in higher ionic calcium concentration in nHA $_{milk}$ digesta. For nHA $_{milk}$ digesta the buffering capacity of milk components results in delayed reduction in pH in comparison to nHA $_{blank}$, leading to slower detachment of Ca^{2+} from the nHA surface. Similar to nHA $_{blank}$, the Ca^{2+} concentration decreased after the maximum value, presumably due to the dilution effect.

4.2.2.2 Ion and protein binding property of nHA

As mentioned earlier in section 4.2.2.1 HA is highly susceptible to substitution on its crystal lattice due to its positively charged C-site and negatively charged P-site. This HA surface charge density is dependent on pH and salt ions present in the suspension. The point of zero charge (PZC) for HA is at pH 7.3 ± 0.1, when the PZC > pH the zeta potential is negative and when the PZC < pH the zeta potential is positively charged (Harding, Rashid, & Hing, 2005; Luo & Andrade, 1998). The variation of zeta potential as a function of pH is attributed to the different degrees of protonation of phosphate ions on the HA surface like PO_4^{3-}, HPO_4^{2-}, H_2PO^{4-} (Tercinier et al., 2014b). At the pH of milk HA is negatively charged, a large number of P-sites on the surface than the C-sites (Tercinier et al., 2014b) explains the negative charge.

Ion binding

During the initial stages of digestion the release of Ca^{2+} is slow in nHA $_{milk}$ when compared to milk $_{blank}$ from ionic calcium results (Figure 4.2). This was probably related to the ion binding property of nHA. The negatively charged nHA serves as a calcium chelator binding Ca^{2+} on the P-sites of nHA surface that reduces the number of free ionic Ca^{2+} available in the digesta. The chelating effect of HA has been demonstrated by Tercinier et al. (2014a). They found that the addition of HA in skim milk leads to the binding of Ca^{2+} on HA that disrupts mineral salt balance affecting

the casein micelle stability. This binding of Ca^{2+} would lead to an increased diffusion layer and formation of a calcium rich layer that might further delays the dissolution process when compared to nHA_{blank}.

Protein binding

The milk proteins are negatively charged at the natural pH of milk. It has been reported that the amino groups of proteins adsorb on the P-sites via electrostatic interactions while the carboxyl or phosphoserine groups of proteins forms complexes on the C-sties of the HA surface (Gorbunoff & Timasheff, 1984; Reynolds & Black, 1987). The binding on the C-sites of HA is reported to be greater than the binding on the P-sites (Luo & Andrade, 1998) because the complexes formed at the C-sites are held together by stronger bonds as compared to electrostatic interactions at the P-sites (Tercinier et al., 2013). In addition the adsorption of calcium ions on HA surface is shown to give a positive charge enhancing the number of protein adsorption sites (Tercinier et al., 2014a).

The binding of proteins on the nHA can act as a protective shield against the action of acid subsequently inhibiting the dissolution of nHA during gastric digestion. We propose that as per the Langmuir model, the adsorbed proteins forms a layer on the HA surface preventing detachment of PO_4^{3-} and Ca^{2+} away from nHA surface by increasing the diffusion layer. Barbour, Shellis, Parker, Allen, and Addy (2008) suggested that formation of layer of casein on HA surface that acts as a shield preventing HA dissolution rate by 50 % in soft drinks. They also mentioned that the inhibitory effect was enhanced further when calcium was added externally at low concentrations. The gradual reduction in pH during digestion changes the zeta potential of nHA to positive charge and similarly the proteins in milk also bears a positive charge at their isoelectric point. These two positively charged nHA and proteins should lead to repulsion but the adsorption of the positively charged proteins on the nHA surface at low pH could be probably through hydrophobic interactions as mentioned in Barbour et al. (2008). The protective effect of protein adsorption on the HA demineralization/dissolution has been shown in previous studies (Reynolds & Black, 1987, 1989; Reynolds & Del Rio, 1984); they reported the anticariogenicity properties of casein, whey proteins and caseinate on rat tooth

enamel. In addition, several investigators have identified casein-derived peptides such as caseinomacropeptide (Setarehnejad, Kanekanian, Tatham, & Abedi, 2010), caseinophoshopeptide (Kanekanian, Williams, Brownsell, & Andrews, 2008), and proteose-peptone (Grenby, Andrews, Mistry, & Williams, 2001) to be effective in preventing dental erosion due to acid attack .

4.2.2.3 Clot formation

One of the distinguishing behaviour of milk during digestion is the formation of a clot in the stomach. The hydrolytic action of pepsin enzyme leads to formation of a structured clot usually at the first 20 min of digestion time (Ye et al., 2016b). In several previous studies, this structured clot plays a crucial role in the rate of protein digestibility and absorption of milk proteins and fats during digestion process (Ye et al., 2016a, 2016b). Similarly, during digestion it is possible that the clot formation would also hinder the dissolution rate of nHA.

In this study the clot formed during digestion is likely to have a close-knit structure similar to unheated milk as reported in the study of Ye et al. (2016b). The digestion sample of nHA $_{milk}$ was prepared from pasteurised skim milk; pasteurization involves heating of milk at 72^{o}C for 15s, which is relatively mild heat treatment as compared to heating at 90^{o}C or ultra-heat treatment. During clot formation, the breaking of κ-casein "hairy layer" by the action of pepsin enzyme exposes the inner hydrophobic casein molecules. This allows more adsorption of the exposed casein molecules (β-casein and α_s-(α_{s1}- and α_{s2}-) caseins) due to higher phosphoserine content on the nHA surface as compared to κ-casein and whey proteins. The entrapment of nHA inside the close-knit structured clot formed restricts nHA dissolution by affecting the diffusion of acid inside during gastric digestion.

In addition to the protein binding and clot formation, we propose there is a synergistic effect from the binding of the proteins on nHA surface and the entrapment of nHA in the clot that contributes to the slower dissolution of nHA during gastric digestion. The adsorption of milk proteins on the nHA surface leads to active incorporation of nHA inside the clot. In milk, the β-casein and α_s-casein has stronger binding affinity on nHA surface than the κ-casein and whey proteins.

During digestion, the κ-casein is cut off exposing the inner hydrophobic core of the casein micelles especially the β-casein and α_s-casein. Thus, β -casein and α_s -casein would be more accessible during gastric providing stronger binding effect and greater incorporation of nHA inside the clot structure comparing to in natural milk. The higher absorption of β-casein and α_s-casein was reported by Tercinier et al. (2013), the casein molecules adsorbed on HA surface in the order β-casein > α_s-casein > κ-casein and β-lactoglobulin > α-lactalbumin in whey proteins. The stronger adsorption of caseins on HA surface than the whey proteins is because the phosphoserine clusters of casein molecules would serve as anchor points for the binding on HA surface through complexation of phosphate group of phosphoserine residue with the C-sites on HA surface (Tercinier, Ye, Anema, Singh, & Singh, 2017). In addition, α_s-casein can self-associate as oligomers and β-casein can form micellar type and can competitively displace whey proteins forming a thick layer of closely packed protein on the HA surface (Tercinier et al., 2017).

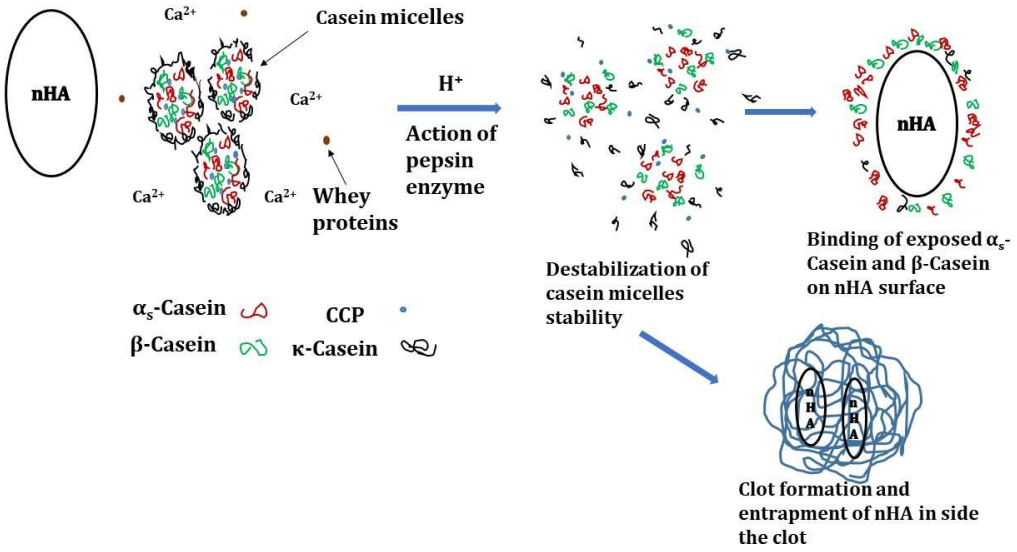

Figure 4.18 Schematic diagram showing binding of milk proteins on nHA surface and entrapment of nHA inside the clot.

4.2.4 Detection and identification of nHA in the gastric and intestinal digesta

The incomplete dissolution of nHA for nHA_{blank} and nHA_{milk} were confirmed through the detection of nHA crystals in the TEM micrographs at different digestion times. The dissolution of nHA were observed in TEM micrographs; for nHA_{blank} initially at 60 min, the maximum dissociation of nHA is seen via breaking down or dissociation of large aggregates of nHA into smaller aggregates leading to fewer small aggregates or single crystals of nHA by the end of digestion time. However, the TEM images of nHA_{milk} at 60 min mostly demonstrates clusters of nHA aggregates similar to that of reference nHA TEM images followed by more occurrence of nHA dissociation at 120 min (Figure 4.9). The traces of undissolved nHA were also seen in the TEM micrographs (Figure 4.12) of intestinal digesta of both nHA_{blank} and nHA_{milk} digesta.

The XRD analysis shows that for nHA_{blank} digesta, there is no generation of XRD peak similar to reference nHA after 60 min of digestion, whereas for nHA_{milk} digesta the XRD peak corresponding to reference nHA were seen until 120 min digestion time. The broadening of the diffraction peaks at 60 min and 120 min for nHA_{milk} digesta with digestion time comparing to nHA reference XRD peak shows loss of crystallinity of nHA and this is consistent with TEM images showing the dissociation of nHA aggregates with a reduction in definite needle like structures. The discrepancies between TEM and XRD results in the presence of nHA in the digesta from 60 min (nHA_{blank}) and 180 min (nHA_{milk}) of gastric digestion time is probably because the concentration of nHA in the centrifuged pellet was too low to be detected by the XRD technique. The concentration of nHA is low due to the dissolution of nHA as evident from calcium results and TEM analysis and the simultaneous dilution effect caused by the addition of SGF. The occurrence of XRD peaks similar to reference nHA was observed until the digestion time taken to reach the maximum Ca^{2+} values. The absence of XRD peaks resembling nHA reference were noticed at 60 min and 180 min for nHA_{blank} nHA_{milk} respectively. The emergence of new diffraction patterns similar to a curve without definite sharp peak and a small definite sharp peak at 20 to 25 2θ degrees were noticed during different gastrointestinal digestion time. For nHA_{blank}, this new peak was observed from the

initial 60 to 180 min of gastric digestion and seem to reappear at the end of intestinal digestion. While for nHA $_{milk}$ digesta the new peak was noticed during 60 to 180 min of digestion time. At 240 min and after intestinal digestion the appearance of this new peak is difficult to confirm. For milk $_{blank}$ the small new peak were also seen form the initial 60 min of gastric digestion until the end of intestinal digestion. The formation of this new diffraction curve peak at 20 to 25 2θ degrees might be from the presence of non-crystalline amorphous calcium phosphate phase and the formation of small sharp definite peak could be from the presence of calcium phosphate solids phases. The curved XRD peak observed suggesting amorphous calcium phosphate is in the similar range (25 to 35 2θ degrees) observed by Drouet (2013).

From the EDS results (Table 4.3), the higher content of calcium and phosphate during 60 min and 120 min of gastric digestion could be related to the generation of XRD peaks at that digestion time similar to that of nHA reference. After 120 min of gastric digestion the concentration of calcium and phosphate in freeze-dried nHA $_{milk}$ digesta was negligible (<1%), which corresponded to the disappearance of nHA peaks in XRD graph. Elevated Ca/P ratio at 60 min (1.86) and 120 min (1.78) in comparison to reference nHA (1.67) was probably due to higher attachment of Ca^{2+} on nHA surface. The ionic calcium absorption on HA surface leading to HA crystal growth has been reported by Tercinier et al. (2014a). The higher adsorption of Ca^{2+} in comparison to other elements because of larger numbers of negatively charged P-sites (Tercinier et al., 2014b).

4.2.5 Intestinal digestion

After intestinal digestion, the ionic calcium concentration decreases as compared to the initial concentration after gastric digestion (Table 4.1). The change in the pH profile from acidic gastric environment to neutral conditions of the intestine resulted in decreased solubility of calcium. Goss, Lemons, Kerstetter, and Bogner (2007) the solubility of calcium salts decreased with the increase in pH to that of intestinal environment demonstrated the pH dependency of calcium solubility.

The primary concern of intestinal digestion was whether nHA can recrystallize when subjected to the alkaline pH of the intestinal phase. From the result of this study, there is no evidence that the nHA can form again after its dissolution in the gastric phase. The TEM images of Figure 4.12 depicted the presence of nHA after intestinal digestion. However, based on TEM images the recrystallization of nHA cannot be concluded because the observed nHA crystals in TEM micrographs can probably be the traces of undissolved nHA after gastric digestion entering the intestinal phase. The XRD results (Figures 4.13, 4.14 and 4.15) did not demonstrate the presence of peaks similar to that of nHA reference peaks suggesting the absence of nHA. However, there is a formation of two new diffraction patterns similar to that during gastric digestion, a curve without definite sharp peak and another with a small definite sharp peak at 20 to 25 2θ degrees. The curve like diffraction pattern suggests the presence of amorphous calcium phosphate phase while the new sharp peak suggests the formation of a calcium phosphate solid phase other than nHA. Moreover the production of nHA mostly involves complex process conditions such as calcification at high temperature above 100^{o}C and milling (Sadat-Shojai et al., 2013). Thus, under the simple intestinal conditions the probability of reformation of nHA is very low.

Chapter 5 Conclusion

The study demonstrated the presence of undissolved nHA crystals under the acidic conditions of the stomach that were observed subsequently even after intestinal digestion in both nHA $_{blank}$ and nHA $_{milk}$ digesta samples. After 240 min of simulated gastric digestion using HGS, the percentage dissolution of nHA was 43 % and 73 % for nHA $_{blank}$ and nHA $_{milk}$ digesta samples respectively.

In both nHA $_{blank}$ digesta and nHA $_{milk}$ digesta, the presence of undissolved nHA crystals were confirmed visually through TEM micrographs. The dissolution of nHA was faster in nHA $_{blank}$ digesta and there was no generation of XRD peaks similar to nHA reference XRD peaks until the end of gastrointestinal digestion process. For nHA $_{milk}$ digesta, XRD peaks similar to nHA reference were observed only at 60 and 120 min of gastric digestion indicating slower dissolution of nHA. On the contrary,

in both the nHA $_{blank}$ and nHA $_{milk}$ digesta there was an appearance of a new diffraction peaks similar to a curve without definite sharp peak and a small definite sharp peak at 20 to 25 2θ degrees at different gastrointestinal digestion times. This new peak could probably be due to formation of calcium phosphate solid phases and curve represents the amorphous calcium phosphate phases other than nHA.

We propose that the incomplete dissolution of nHA in nHA $_{blank}$ could be due to following mechanisms:

i. The critical size effect.
ii. The diffusion layer thickness restricts the detachment of ions form the nHA surface to the bulk solution.
iii. Self-inhibition through re-adsorption of Ca^{2+} on nHA surface forming a calcium rich layer.
iv. The presence of other inorganic cations in the SGF and the enzymes would also attach on the surface of nHA creating the same inhibitory effect (diffusion layer and self-inhibition).

The dissolution of nHA in nHA $_{milk}$ under gastric conditions in comparison to nHA $_{blank}$ was slower we propose the following mechanisms to explain this effect.

i. The delayed reduction in pH due to the buffering capacity of milk components leads to slower dissolution rate of nHA during early digestion time.
ii. Ion binding and protein binding property of nHA results in the formation of a protective layer on the nHA surface.
iii. The formation of a clot during gastric digestion entrap the nHA inside the colt protecting from the action of acid.
iv. The synergistic effect between the adsorbed proteins on nHA surface and simultaneous entrapment of nHA in clot further slows downs nHA dissolution process.

The dissolution of any nHA in a biological environment is a complex process where the size effect and the possible interaction of the nHA with the inorganic and organic components should be taken into consideration.

5.1 Recommendations and future research

The study indicates the presence of undissolved nHA after *in vitro* gastrointestinal digestion. From nano toxicity perspective the cellular uptake of NPs through different mechanisms (Choi, Lee, Jeong, & Choy, 2013) can be associated with generation of reactive oxygen species causing inflammation and cell damage (Elsaesser & Howard, 2012). The pathological prevalence of calcium has been attributed to the calcification of calcium phosphate in the formation of urinary stones and atherosclerosis (Dorozhkin & Epple, 2002). Thus, further toxicological implication from the application of nHA needs to be verified using different intestinal cell models.

Apart from *in vitro* digestion models, additional work needs to be done to further validate and explore the dissolution behaviour of nHA *in vivo* systems, for example in rat or pig model.

References

Alegria, A., Garcia-Llatas, G., & Cilla, A. (2015). Static Digestion Models: General Introduction. In K. Verhoeckx, P. Cotter, I. Lopez-Exposito, C. Kleiveland, T. Lea, A. Mackie, T. Requena, D. Swiatecka, & H. Wichers (Eds.), *The Impact of Food Bioactives on Health: in vitro and ex vivo models* (pp. 3-12). Cham: Springer International Publishing.

Anema, S. G. (2009). Role of colloidal calcium phosphate in the acid gelation properties of heated skim milk. *Food Chemistry, 114*(1), 161-167. doi:https://doi.org/10.1016/j.foodchem.2008.09.031

Anema, S. G., Lee, S. K., & Klostermeyer, H. (2007). Effect of pH at heat treatment on the hydrolysis of κ-casein and the gelation of skim milk by chymosin. *LWT-Food Science and Technology, 40*(1), 99-106.

Arora, S., Rajwade, J. M., & Paknikar, K. M. (2012). Nanotoxicology and in vitro studies: The need of the hour. *Toxicology and Applied Pharmacology, 258*(2), 151-165. doi:https://doi.org/10.1016/j.taap.2011.11.010

Bai, H., & Liu, X. (2016, 2016 / 03 / 22 /). *Food nanotechnology and nano food safety*.

Barbour, M. E., Shellis, R. P., Parker, D. M., Allen, G. C., & Addy, M. (2008). Inhibition of hydroxyapatite dissolution by whole casein: the effects of pH, protein concentration, calcium, and ionic strength. *European Journal of Oral Sciences, 116*(5), 473-478. doi:doi:10.1111/j.1600-0722.2008.00565.x

Benson, A. K. (2013). X-ray diffraction. In: Salem Press.

Bohn, T., Carriere, F., Day, L., Deglaire, A., Egger, L., Freitas, D., . . . Dupont, D. (2017). Correlation between in vitro and in vivo data on food digestion. What can we predict with static in vitro digestion models? *Critical Reviews in Food Science and Nutrition*, 1-23. doi:10.1080/10408398.2017.1315362

Boirie, Y., Dangin, M., Gachon, P., Vasson, M.-P., Maubois, J.-L., & Beaufrere, B. (1997). Slow and Fast Dietary Proteins Differently Modulate Postprandial Protein Accretion. *Proceedings of the National Academy of Sciences of the United States of America*(26), 14930.

Boisen, S., & Eggum, B. O. (1991). Critical Evaluation of in Vitro Methods for Estimating Digestibility in Simple-Stomach Animals. *Nutrition Research Reviews, 4*(1), 141-162. doi:10.1079/NRR19910012

Borm, P., Klaessig, F. C., Landry, T. D., Moudgil, B., Pauluhn, J. r., Thomas, K., . . . Wood, S. (2006). Research Strategies for Safety Evaluation of Nanomaterials, Part V: Role of Dissolution in Biological Fate and Effects of Nanoscale Particles. *Toxicological Sciences, 90*(1), 23-32. doi:10.1093/toxsci/kfj084

Bornhorst, G. M. (2017). Gastric Mixing During Food Digestion: Mechanisms and Applications. *Annual Review of Food Science and Technology, 8*(1), 523-542. doi:10.1146/annurev-food-030216-025802

Bornhorst, G. M., & Singh, R. P. (2014). Gastric digestion in vivo and in vitro: How the structural aspects of food influence the digestion process. *Annual Review of Food Science and Technology, 5*(1), 111-132. doi:10.1146/annurev-food-030713-092346

Bouwmeester, H., Dekkers, S., Noordam, M. Y., Hagens, W. I., Bulder, A. S., de Heer, C., . . . Sips, A. J. A. M. (2009). Review of health safety aspects of nanotechnologies in food production. *Regulatory Toxicology and Pharmacology, 53*(1), 52-62. doi:https://doi.org/10.1016/j.yrtph.2008.10.008

Caballero-Diaz, E., & Valcarcel Cases, M. (2016). Analytical methodologies for nanotoxicity assessment. *TrAC Trends in Analytical Chemistry, 84*, 160-171. doi:https://doi.org/10.1016/j.trac.2016.03.007

Caroli, A., Ricotta, D., Cocchi, D., Poli, A., & Banfi, G. (2011). Invited review: Dairy intake and bone health: A viewpoint from the state of the art1. *Journal of Dairy Science, 94*(11), 5249-5262. doi:10.3168/jds.2011-4578

Cashman, K. D. (2006). Milk minerals (including trace elements) and bone health. *International Dairy Journal, 16*(11), 1389-1398. doi:https://doi.org/10.1016/j.idairyj.2006.06.017

Cashman, K. D. (2011). Milk Salts | Macroelements, Nutritional Significance A2 - Fuquay, John W. In *Encyclopedia of Dairy Sciences (Second Edition)* (pp. 925-932). San Diego: Academic Press.

Chellaram, C., Murugaboopathi, G., John, A., Sivakumar, R., Ganesan, S., Krithika, S., & Priya, G. (2014). Significance of nanotechnology in food industry. *APCBEE procedia, 8*, 109-113.

Chetty, A., Wepener, I., Marei, M. K., Kamary, Y., & Moussa, R. M. (2012). Synthesis, properties, and applications of hydroxyapatite. In: Nova Science Publishers.

Choi, J., Horne, D. S., & Lucey, J. A. (2007). Effect of Insoluble Calcium Concentration on Rennet Coagulation Properties of Milk. *Journal of Dairy Science, 90*(6), 2612-2623. doi:https://doi.org/10.3168/jds.2006-814

Choi, S.-J., Lee, J. K., Jeong, J., & Choy, J.-H. (2013). Toxicity evaluation of inorganic nanoparticles: considerations and challenges. *Molecular & Cellular Toxicology, 9*(3), 205-210. doi:10.1007/s13273-013-0026-z

Christoffersen, M. R., Dohrup, J., & Christoffersen, J. (1998). Kinetics of growth and dissolution of calcium hydroxyapatite in suspensions with variable calcium to phosphate ratio. *Journal of Crystal Growth, 186*(1), 283-290. doi:https://doi.org/10.1016/S0022-0248(97)00473-9

Chuang, H.-C., Hsiao, T.-C., Wu, C.-K., Chang, H.-H., Lee, C.-H., Chang, C.-C., & Cheng, T.-J. (2013). Allergenicity and toxicology of inhaled silver nanoparticles in allergen-provocation mice models. *International journal of nanomedicine, 8*, 4495.

Chung, S.-Y., Kim, Y.-M., Kim, J.-G., & Kim, Y.-J. (2008). Multiphase transformation and Ostwald's rule of stages during crystallization of a metal phosphate. *Nature Physics, 5*, 68. doi:10.1038/nphys1148

https://www.nature.com/articles/nphys1148#supplementary-information

Coles, L. T., Moughan, P. J., & Darragh, A. J. (2005). In vitro digestion and fermentation methods, including gas production techniques, as applied to nutritive evaluation of foods in the hindgut of humans and other simple-stomached animals. *Animal Feed Science and Technology, 123-124*, 421-444. doi:https://doi.org/10.1016/j.anifeedsci.2005.04.021

Cox, S. (2012). Synthesis method of hydroxyapatite. *Lucideon (formerly Ceram)*, 1-10.

Dalgleish, D. G. (1998). Casein Micelles as Colloids: Surface Structures and Stabilities. *Journal of Dairy Science, 81*(11), 3013-3018. doi:https://doi.org/10.3168/jds.S0022-0302(98)75865-5

Dalgleish, D. G. (2011). On the structural models of bovine casein micelles—review and possible improvements. *Soft Matter, 7*(6), 2265-2272.

Dalgleish, D. G., & Corredig, M. (2012). The structure of the casein micelle of milk and its changes during processing. *Annual Review of Food Science and Technology, 3*(1), 449-467. doi:10.1146/annurev-food-022811-101214

De Kort, E., Minor, M., Snoeren, T., Van Hooijdonk, T., & Van Der Linden, E. (2009). Calcium-binding capacity of organic and inorganic ortho- and polyphosphates. *Dairy Science & Technology, 89*(3-4), 283-299. doi:10.1051/dst/2009008

de Kort, E., Minor, M., Snoeren, T., van Hooijdonk, T., & van der Linden, E. (2011). Effect of calcium chelators on physical changes in casein micelles in concentrated micellar casein solutions. *International Dairy Journal, 21*(12), 907-913. doi:https://doi.org/10.1016/j.idairyj.2011.06.007

De Kruif, C., & Zhulina, E. B. (1996). κ-casein as a polyelectrolyte brush on the surface of casein micelles. *Colloids and Surfaces A: Physicochemical and Engineering Aspects, 117*(1-2), 151-159.

de la Fuente, M. A., Fontecha, J., & Juarez, M. (1996). Partition of Main and Trace Minerals in Milk: Effect of Ultracentrifugation, Rennet Coagulation, and

Dialysis on Soluble Phase Separation. *Journal of Agricultural and Food Chemistry, 44*(8), 1988-1992. doi:10.1021/jf9506949

De Matteis, V. (2017). Exposure to inorganic nanoparticles: routes of entry, immune response, biodistribution and in vitro/in vivo toxicity evaluation. *Toxics, 5*(4), 29.

Deeth, H. C., & Lewis, M. J. (2015). Practical consequences of calcium addition to and removal from milk and milk products. *International Journal of Dairy Technology, 68*(1), 1-10. doi:10.1111/1471-0307.12188

Demirchan, A. C., & Gshalaev, V. S. (2012). *Hydroxyapatite : Synthesis, Properties, and Applications*. Hauppauge, N.Y.: Nova Science Publishers, Inc.

Di Felice, G., & Colombo, P. (2017). Nanoparticle–allergen complexes for allergen immunotherapy. *International journal of nanomedicine, 12*, 4493.

Dorozhkin, S. V. (1997). Surface Reactions of Apatite Dissolution. *Journal of Colloid and Interface Science, 191*(2), 489-497. doi:https://doi.org/10.1006/jcis.1997.4942

Dorozhkin, S. V. (2002). A review on the dissolution models of calcium apatites. *Progress in Crystal Growth and Characterization of Materials, 44*(1), 45-61. doi:https://doi.org/10.1016/S0960-8974(02)00004-9

Dorozhkin, S. V. (2012). Dissolution mechanism of calcium apatites in acids: A review of literature. *World Journal of Methodology, 2*(1), 1-17. doi:10.5662/wjm.v2.i1.1

Dorozhkin, S. V., & Epple, M. (2002). Biological and Medical Significance of Calcium Phosphates. *Angewandte Chemie International Edition, 41*(17), 3130-3146. doi:doi:10.1002/1521-3773(20020902)41:17<3130::AID-ANIE3130>3.0.CO;2-1

Drouet, C. (2013). Apatite Formation: Why It May Not Work as Planned, and How to Conclusively Identify Apatite Compounds. *BioMed Research International, 2013*, 12. doi:10.1155/2013/490946

Dupont, D., Alric, M., Blanquet-Diot, S., Bornhorst, G., Cueva, C., Deglaire, A., . . . Van den Abbeele, P. (2018). Can dynamic in vitro digestion systems mimic the physiological reality? *Critical Reviews in Food Science and Nutrition*, 1-17. doi:10.1080/10408398.2017.1421900

Egger, L., Ménard, O., Baumann, C., Duerr, D., Schlegel, P., Stoll, P., . . . Portmann, R. (2017). Digestion of milk proteins: Comparing static and dynamic in vitro digestion systems with in vivo data. *Food Research International*. doi:https://doi.org/10.1016/j.foodres.2017.12.049

Egger, L., Ménard, O., Delgado-Andrade, C., Alvito, P., Assuncao, R., Balance, S., . . . Portmann, R. (2016). The harmonized INFOGEST in vitro digestion method: From knowledge to action. *Food Research International, 88*, 217-225. doi:https://doi.org/10.1016/j.foodres.2015.12.006

Ehrlich, H., Koutsoukos, P. G., Demadis, K. D., & Pokrovsky, O. S. (2009). Principles of demineralization: Modern strategies for the isolation of organic frameworks: Part II. Decalcification. *Micron, 40*(2), 169-193. doi:https://doi.org/10.1016/j.micron.2008.06.004

Elsaesser, A., & Howard, C. V. (2012). Toxicology of nanoparticles. *Advanced Drug Delivery Reviews, 64*, 129-137. doi:10.1016/j.addr.2011.09.001

Farrell, H. M., Malin, E. L., Brown, E. M., & Qi, P. X. (2006). Casein micelle structure: What can be learned from milk synthesis and structural biology? *Current Opinion in Colloid & Interface Science, 11*(2), 135-147. doi:https://doi.org/10.1016/j.cocis.2005.11.005

Ferraz, M. P., Monteiro, F. J., & Manuel, C. M. (2004). Hydroxyapatite Nanoparticles: A Review of Preparation Methodologies. *Journal of Applied Biomaterials and Biomechanics, 2*(2), 74-80. doi:10.1177/228080000400200202

Ferrua, M. J., & Singh, R. P. (2015). Human Gastric Simulator (Riddet Model). In K. Verhoeckx, P. Cotter, I. Lopez-Exposito, C. Kleiveland, T. Lea, A. Mackie, T. Requena, D. Swiatecka, & H. Wichers (Eds.), *The Impact of Food Bioactives on Health: in vitro and ex vivo models* (pp. 61-71). Cham: Springer International Publishing.

Flynn, A. (2003). The role of dietary calcium in bone health. *The Proceedings Of The Nutrition Society, 62*(4), 851-858.

Fox, J. L., Higuchi, W. I., Fawzi, M. B., & Wu, M.-S. (1978). A new two-site model for hydroxyapatite dissolution in acidic media. *Journal of Colloid and Interface Science, 67*(2), 312-330. doi:https://doi.org/10.1016/0021-9797(78)90016-4

Fox, P. F. (2008). Chapter 1 - Milk: an overview. In A. Thompson, M. Boland, & H. Singh (Eds.), *Milk Proteins* (pp. 1-54). San Diego: Academic Press.

Fulmer, M. T., Ison, I. C., Hankermayer, C. R., Constantz, B. R., & Ross, J. (2002). Measurements of the solubilities and dissolution rates of several hydroxyapatites. *Biomaterials, 23*(3), 751-755. doi:https://doi.org/10.1016/S0142-9612(01)00180-6

Gaucheron, F. (2005). The minerals of milk. *Reprod. Nutr. Dev., 45*(4), 473-483.

Gaucheron, F. (2011). Milk and Dairy Products: A Unique Micronutrient Combination. *Journal of the American College of Nutrition, 30*(sup5), 400S-409S. doi:10.1080/07315724.2011.10719983

Gerhart, M., & Schottenheimer, M. (2013). Mineral fortification in dairy. *Wellness Foods, 428*, 429.

Gorbunoff, M. J., & Timasheff, S. N. (1984). The interaction of proteins with hydroxyapatite: III. Mechanism. *Analytical Biochemistry, 136*(2), 440-445. doi:https://doi.org/10.1016/0003-2697(84)90241-0

Goss, S. L., Lemons, K. A., Kerstetter, J. E., & Bogner, R. H. (2007). Determination of calcium salt solubility with changes in pH and PCO2, simulating varying gastrointestinal environments. *Journal of Pharmacy and Pharmacology, 59*(11), 1485-1492. doi:doi:10.1211/jpp.59.11.0004

Grenby, T. H., Andrews, A. T., Mistry, M., & Williams, R. J. H. (2001). Dental caries-protective agents in milk and milk products: investigations in vitro. *Journal of Dentistry, 29*(2), 83-92. doi:https://doi.org/10.1016/S0300-5712(00)00061-0

Guerra, A., Etienne-Mesmin, L., Livrelli, V., Denis, S., Blanquet-Diot, S., & Alric, M. (2012). Relevance and challenges in modeling human gastric and small intestinal digestion. *Trends in Biotechnology, 30*(11), 591-600. doi:https://doi.org/10.1016/j.tibtech.2012.08.001

Gurr, M. (2000). Book reviews : Calcium in nutrition. *Food Science and Technology International, 6*(1), 75-75. doi:10.1177/108201320000600112

Hamad, A. F., Jong-Hun, H., Kim, B.-C., & Rather, I. A. (2017). The Intertwine of Nanotechnology with the Food Industry The Intertwine of Nanotechnology with the Food Industry. *Saudi journal of biological sciences*.

Handford, C. E., Dean, M., Henchion, M., Spence, M., Elliott, C. T., & Campbell, K. (2014). Implications of nanotechnology for the agri-food industry: Opportunities, benefits and risks. *Trends in Food Science & Technology, 40*(2), 226-241. doi:10.1016/j.tifs.2014.09.007

Harding, I. S., Rashid, N., & Hing, K. A. (2005). Surface charge and the effect of excess calcium ions on the hydroxyapatite surface. *Biomaterials, 26*(34), 6818-6826. doi:https://doi.org/10.1016/j.biomaterials.2005.04.060

He, X., & Hwang, H.-M. (2016). Nanotechnology in food science: Functionality, applicability, and safety assessment. *Journal of Food and Drug Analysis, 24*(4), 671-681. doi:https://doi.org/10.1016/j.jfda.2016.06.001

Henchion, M., Handford, C. E., Dean, M., Spence, M., Elliott, C. T., Campbell, K., & Henchion, M. *Implications of nanotechnology for the agri-food industry: Opportunities, benefits and risks*.

Holt, C. (1992). Structure and Stability of Bovine Casein Micelles. In C. B. Anfinsen, F. M. Richards, J. T. Edsall, & D. S. Eisenberg (Eds.), *Advances in Protein Chemistry* (Vol. 43, pp. 63-151): Academic Press.

Holt, C. (1996). The hairy casein micelle : evolution of concept and its implications for dairy technology. *Netherlands Milk and Dairy Journal, 50*, 85-111.

Holt, C. (1997). The milk salts and their interaction with casein. In *Advanced Dairy Chemistry Volume 3* (pp. 233-256): Springer.

Holt, C. (2004). An equilibrium thermodynamic model of the sequestration of calcium phosphate by casein micelles and its application to the calculation of the partition of salts in milk. *European Biophysics Journal, 33*(5), 421-434. doi:10.1007/s00249-003-0377-9

Holt, C. (2011). *Milk Salts: Interaction with Caseins*: Elsevier Inc.

Holt, C., Dalgleish, D. G., & Jenness, R. (1981). Calculation of the ion equilibria in milk diffusate and comparison with experiment. *Analytical Biochemistry, 113*(1), 154-163. doi:https://doi.org/10.1016/0003-2697(81)90059-2

Honarvar, Z., Hadian, Z., & Mashayekh, M. (2016). Nanocomposites in food packaging applications and their risk assessment for health. *Electronic Physician, 8*(6), 2531-2538. doi:10.19082/2531

Horne, D. S. (1998). Casein Interactions: Casting Light on the Black Boxes, the Structure in Dairy Products. *International Dairy Journal, 8*(3), 171-177. doi:https://doi.org/10.1016/S0958-6946(98)00040-5

Horne, D. S. (2006). Casein micelle structure: Models and muddles. *Current Opinion in Colloid & Interface Science, 11*(2), 148-153. doi:https://doi.org/10.1016/j.cocis.2005.11.004

Horne, D. S. (2008). Chapter 5 - Casein micelle structure and stability A2 - Thompson, Abby. In M. Boland & H. Singh (Eds.), *Milk Proteins* (pp. 133-162). San Diego: Academic Press.

Huppertz, T., Fox, P. F., & Kelly, A. L. (2018). 3 - The caseins: Structure, stability, and functionality. In R. Y. Yada (Ed.), *Proteins in Food Processing (Second Edition)* (pp. 49-92): Woodhead Publishing.

Hur, S. J., Lim, B. O., Decker, E. A., & McClements, D. J. (2011). In vitro human digestion models for food applications. *Food Chemistry, 125*(1), 1-12. doi:https://doi.org/10.1016/j.foodchem.2010.08.036

Jain, A., Ranjan, S., Dasgupta, N., & Ramalingam, C. (2018). Nanomaterials in food and agriculture: An overview on their safety concerns and regulatory issues. *Critical Reviews In Food Science And Nutrition, 58*(2), 297-317. doi:10.1080/10408398.2016.1160363

Kaliappan, S., & Lucey, J. A. (2011). Influence of mixtures of calcium-chelating salts on the physicochemical properties of casein micelles. *Journal of Dairy Science, 94*(9), 4255-4263. doi:https://doi.org/10.3168/jds.2010-3343

Kanekanian, A. D., Williams, R. J. H., Brownsell, V. L., & Andrews, A. T. (2008). Caseinophosphopeptides and dental protection: Concentration and pH studies. *Food Chemistry, 107*(3), 1015-1021. doi:https://doi.org/10.1016/j.foodchem.2007.09.013

Kaushik, R., Sachdeva, B., & Arora, S. (2015). Heat stability and thermal properties of calcium fortified milk. *CYTA - Journal of Food, 13*(2), 305-311. doi:10.1080/19476337.2014.971346

Keller, A. A., McFerran, S., Lazareva, A., & Suh, S. (2013). Global life cycle releases of engineered nanomaterials. *Journal of Nanoparticle Research, 15*(6), 17. doi:10.1007/s11051-013-1692-4

Kethireddipalli, P., & Hill, A. R. (2015). Rennet coagulation and cheesemaking properties of thermally processed milk: Overview and recent developments. *Journal of Agricultural and Food Chemistry, 63*(43), 9389-9403.

Kolmas, J., Groszyk, E., & Kwiatkowska-Rozycka, D. (2014). Substituted Hydroxyapatites with Antibacterial Properties. *BioMed Research International, 2014*, 178123. doi:10.1155/2014/178123

Kolter, M., Ott, M., Hauer, C., Reimold, I., & Fricker, G. (2015). Nanotoxicity of poly(n-butylcyano-acrylate) nanoparticles at the blood–brain barrier, in human whole blood and in vivo. *Journal of Controlled Release, 197*, 165-179. doi:https://doi.org/10.1016/j.jconrel.2014.11.005

Kong, F., & Singh, R. P. (2008). Disintegration of Solid Foods in Human Stomach. *Journal of Food Science, 73*(5), R67-R80. doi:10.1111/j.1750-3841.2008.00766.x

Kong, F., & Singh, R. P. (2010). A Human Gastric Simulator (HGS) to Study Food Digestion in Human Stomach. *Journal of Food Science, 75*(9), E627-E635. doi:10.1111/j.1750-3841.2010.01856.x

Kour, H., Malik, A. A., Ahmad, N., Wani, T. A., Kaul, R. K., & Bhat, A. (2015). Nanotechnology -New Lifeline For Food Industry. *Critical Reviews In Food Science And Nutrition*, 0-0.

Laborda, F., Bolea, E., Cepriá, G., Gómez, M. T., Jiménez, M. S., Pérez-Arantegui, J., & Castillo, J. R. (2016). Detection, characterization and quantification of inorganic engineered nanomaterials: A review of techniques and methodological approaches for the analysis of complex samples. *Analytica Chimica Acta, 904*, 10-32. doi:https://doi.org/10.1016/j.aca.2015.11.008

Le Graet, Y., & Brule, G. (1993). *Effects of pH and ionic strength on distribution of mineral salts in milk*.

Lefebvre, D. E., Venema, K., Gombau, L., Valerio, L. G., Raju, J., Bondy, G. S., . . . Stone, V. (2015). Utility of models of the gastrointestinal tract for assessment of the digestion and absorption of engineered nanomaterials released from food matrices. *Nanotoxicology, 9*(4), 523-542. doi:10.3109/17435390.2014.948091

Legeros, R. Z., Ito, A., Ishikawa, K., Sakae, T., &, & Legeros, J. P. (2010). Fundamentals of Hydroxyapatite and Related Calcium Phosphates. In *Advanced Biomaterials*.

Lewis, M. J. (2011). The measurement and significance of ionic calcium in milk - A review. *International Journal of Dairy Technology, 64*(1), 1-13. doi:10.1111/j.1471-0307.2010.00639.x

Liao, F., Chen, C., & Subramanian, V. (2005). Organic TFTs as gas sensors for electronic nose applications. *Sensors and Actuators B: Chemical, 107*(2), 849-855.

Lin, M.-J., Grandison, A., Chryssanthou, X., Goodwin, C., Tsioulpas, A., Koliandris, A., & Lewis, M. (2006). Calcium removal from milk by ion exchange. *Milchwissenschaft-Milk Science International, 61*(4), 370-374.

Linse, S., Cabaleiro-Lago, C., Xue, W.-F., Lynch, I., Lindman, S., Thulin, E., . . . Dawson, K. A. (2007). Nucleation of protein fibrillation by nanoparticles. *Proceedings of the National Academy of Sciences of the United States of America, 104*(21), 8691-8696. doi:10.1073/pnas.0701250104

Liu, Q., Huang, S., Matinlinna, J. P., Chen, Z., & Pan, H. (2013). Insight into Biological Apatite: Physiochemical Properties and Preparation Approaches. *BioMed Research International, 2013*, 13. doi:10.1155/2013/929748

López-Huertas, E., Teucher, B., Boza, J. J., Martínez-Férez, A., Majsak-Newman, G., Baró, L., . . . Fairweather-Tait, S. (2006). Absorption of calcium from milks enriched with fructo-oligosaccharides, caseinophosphopeptides, tricalcium phosphate, and milk solids. *The American Journal of Clinical Nutrition, 83*(2), 310-316. doi:10.1093/ajcn/83.2.310

Lopez-Macipe, A., Gomez-Morales, J., & Rodriguez-Clemente, R. (1998). The Role of pH in the Adsorption of Citrate Ions on Hydroxyapatite. *Journal of Colloid and Interface Science, 200*(1), 114-120. doi:https://doi.org/10.1006/jcis.1997.5343

Lucas-Gonzalez, R., Viuda-Martos, M., Perez-Alvarez, J. A., & Fernandez-Lopez, J. (2018). In vitro digestion models suitable for foods: Opportunities for new fields of application and challenges. *Food Research International, 107*, 423-436. doi:https://doi.org/10.1016/j.foodres.2018.02.055

Lucey, J. A. (2011). Cheese | Rennet-Induced Coagulation of Milk. In J. W. Fuquay (Ed.), *Encyclopedia of Dairy Sciences (Second Edition)* (pp. 579-584). San Diego: Academic Press.

Lucey, J. A., & Horne, D. S. (2009). Milk Salts: Technological Significance. In P. McSweeney & P. F. Fox (Eds.), *Advanced Dairy Chemistry: Volume 3: Lactose, Water, Salts and Minor Constituents* (pp. 351-389). New York, NY: Springer New York.

Lucey, J. A., & Singh, H. (1997). Formation and physical properties of acid milk gels: a review. *Food Research International, 30*(7), 529-542. doi:https://doi.org/10.1016/S0963-9969(98)00015-5

Luo, Q., & Andrade, J. D. (1998). Cooperative Adsorption of Proteins onto Hydroxyapatite. *Journal of Colloid and Interface Science, 200*(1), 104-113. doi:https://doi.org/10.1006/jcis.1997.5364

Lynn, A. K., & Bonfield, W. (2005). A Novel Method for the Simultaneous, Titrant-Free Control of pH and Calcium Phosphate Mass Yield. *Accounts of Chemical Research, 38*(3), 202-207. doi:10.1021/ar040234d

Mackie, A., & Rigby, N. (2015). InfoGest Consensus Method. In K. Verhoeckx, P. Cotter, I. Lopez-Exposito, C. Kleiveland, T. Lea, A. Mackie, T. Requena, D. Swiatecka, & H. Wichers (Eds.), *The Impact of Food Bioactives on Health: in vitro and ex vivo models* (pp. 13-22). Cham: Springer International Publishing.

Mafe, S., Manzanares, J. A., Reiss, H., Thomann, J. M., & Gramain, P. (1992). Model for the dissolution of calcium hydroxyapatite powder. *The Journal of Physical Chemistry, 96*(2), 861-866. doi:10.1021/j100181a062

McMahon, D. J., & McManus, W. R. (1998). Rethinking casein micelle structure using electron microscopy1. *Journal of Dairy Science, 81*(11), 2985-2993.

Mekmene, O., Le Graeet, Y., & Gaucheron, F. (2010). Theoretical model for calculating ionic equilibria in milk as a function of pH: comparison to experiment. *Journal of Agricultural and Food Chemistry, 58*(7), 4440-4447.

Mekmene, O., Le Graet, Y., & Gaucheron, F. (2009). A model for predicting salt equilibria in milk and mineral-enriched milks. *Food Chemistry, 116*(1), 233-239.

Mike, B. (2016). Human digestion – a processing perspective. *Journal of the Science of Food and Agriculture, 96*(7), 2275-2283. doi:doi:10.1002/jsfa.7601

Minekus, M. (2015). The TNO Gastro-Intestinal Model (TIM). In K. Verhoeckx, P. Cotter, I. López-Expósito, C. Kleiveland, T. Lea, A. Mackie, T. Requena, D. Swiatecka, & H. Wichers (Eds.), *The Impact of Food Bioactives on Health: in vitro and ex vivo models* (pp. 37-46). Cham: Springer International Publishing.

Minekus, M., Alminger, M., Alvito, P., Ballance, S., Bohn, T., Bourlieu, C., . . . Brodkorb, A. (2014). A Standardised Static in Vitro Digestion Method Suitable for Food - an International Consensus.

Misra, S. K., Dybowska, A., Berhanu, D., Luoma, S. N., & Valsami-Jones, E. (2012). The complexity of nanoparticle dissolution and its importance in nanotoxicological studies. *Science of The Total Environment, 438*, 225-232. doi:https://doi.org/10.1016/j.scitotenv.2012.08.066

Montero, M. L., Saenz, A., & Castano, V. M. (2009). Synthesis of nano-hydroxyapatite from silica suspensions through chemical compensation. *Journal of Experimental Nanoscience, 4*(2), 193-202. doi:10.1080/17458080902774663

Mulet-Cabero, A.-I., Mackie, A. R., Wilde, P. J., Fenelon, M. A., & Brodkorb, A. (2018). Structural mechanism and kinetics of in vitro gastric digestion are affected by process-induced changes in bovine milk. *Food Hydrocolloids*. doi:https://doi.org/10.1016/j.foodhyd.2018.03.035

Munchbach, M., & Gerstner, G. (2010). Calcium fortification in dairy products. *Food Market Technology,* 4-8.

Nayak, A. K. (2010). Hydroxyapatite synthesis methodologies: an overview. *International Journal of ChemTech Research, 2*(2), 903-907.

Omoarukhe, E. D., On-Nom, N., Grandison, A. S., & Lewis, M. J. (2010). Effects of different calcium salts on properties of milk related to heat stability. *International Journal of Dairy Technology, 63*(4), 504-511. doi:10.1111/j.1471-0307.2010.00613.x

On-Nom, N., Grandison, A., & Lewis, M. J. (2012). Heat stability of milk supplemented with calcium chloride. *Journal of Dairy Science, 95*(4), 1623-1631.

Orme, C. A., & Giocondi, J. L. (2007). Model systems for formation and dissolution of calcium phosphate minerals. *Handbook of Biomineralization Vol, 2*.

Ozcan-Yilsay, T., Lee, W.-J., Horne, D., & Lucey, J. (2007). Effect of trisodium citrate on rheological and physical properties and microstructure of yogurt. *Journal of Dairy Science, 90*(4), 1644-1652.

Pan, H., Chen, Z., & Darvell, B. (2010). Solubility of sparingly-soluble electrolytes–a new approach. *Analytical Methods, 2*(7), 973-975.

Pathakoti, K., Manubolu, M., & Hwang, H.-M. (2017). Nanostructures: Current uses and future applications in food science. *Journal of Food and Drug Analysis, 25*(2), 245-253. doi:https://doi.org/10.1016/j.jfda.2017.02.004

Pedersen, A., Bardow, A., Jensen, S. B., & Nauntofte, B. (2002). Saliva and gastrointestinal functions of taste, mastication, swallowing and digestion. *Oral Diseases, 8*(3), 117-129.

Philippe, M., Gaucheron, F., Le Graet, Y., Michel, F., & Garem, A. (2003). Physicochemical characterization of calcium-supplemented skim milk. *Le Lait, 83*(1), 45-59.

Philippe, M., Le Graet, Y., & Gaucheron, F. (2005). The effects of different cations on the physicochemical characteristics of casein micelles. *Food Chemistry, 90*(4), 673-683. doi:https://doi.org/10.1016/j.foodchem.2004.06.001

Piccinno, F., Gottschalk, F., Seeger, S., & Nowack, B. (2012). Industrial production quantities and uses of ten engineered nanomaterials in Europe and the world. *Journal of Nanoparticle Research, 14*(9), 1109. doi:10.1007/s11051-012-1109-9

Pico, Y. (2016). Challenges in the determination of engineered nanomaterials in foods. *TrAC Trends in Analytical Chemistry, 84*, 149-159. doi:https://doi.org/10.1016/j.trac.2016.06.004

Pohlit, H., Bellinghausen, I., Frey, H., & Saloga, J. (2017). Recent advances in the use of nanoparticles for allergen-specific immunotherapy. *Allergy, 72*(10), 1461-1474. doi:doi:10.1111/all.13199

Powell, J. J., Faria, N., Thomas-McKay, E., & Pele, L. C. (2010). Origin and fate of dietary nanoparticles and microparticles in the gastrointestinal tract. *Journal of Autoimmunity, 34*, J226-J233. doi:10.1016/j.jaut.2009.11.006

Pradhan, N., Singh, S., Ojha, N., Shrivastava, A., Barla, A., Rai, V., & Bose, S. (2015). Facets of nanotechnology as seen in food processing, packaging, and preservation industry. *BioMed Research International, 2015*.

Qi, P. X. (2007). Studies of casein micelle structure: the past and the present. *Le Lait, 87*(4-5), 363-383.

Rafferty, K., Walters, G., & Heaney, R. (2007). Calcium fortificants: overview and strategies for improving calcium nutriture of the US population. *Journal of Food Science, 72*(9), R152-R158.

Reynolds, E. C., & Black, C. L. (1987). Reduction of Chocolate's Cariogenicity by Supplementation with Sodium Caseinate. *Caries Research, 21*(5), 445-451.

Reynolds, E. C., & Black, C. L. (1989). Cariogenicity of a Confection Supplemented with Sodium Caseinate at a Palatable Level (Short Communication). *Caries Research, 23*(5), 368-370.

Reynolds, E. C., & Del Rio, A. (1984). Effect of casein and whey-protein solutions on caries experience and feeding patterns of the rat. *Archives of Oral Biology, 29*(11), 927-933. doi:https://doi.org/10.1016/0003-9969(84)90093-1

Rivera-Munoz, E. M. (2011). *Hydroxyapatite-Based Materials: Synthesis and Characterization*: INTECH Open Access Publisher.

Ross, A. C. (2011). *DRI, dietary reference intakes : calcium, vitamin D*: Washington, D.C. : National Academies Press, c2011.

Rossi, M., Cubadda, F., Dini, L., Terranova, M. L., Aureli, F., Sorbo, A., & Passeri, D. (2014). Scientific basis of nanotechnology, implications for the food sector and future trends. *Trends in Food Science & Technology, 40*(2), 127-148. doi:10.1016/j.tifs.2014.09.004

Sadat-Shojai, M., Khorasani, M.-T., Dinpanah-Khoshdargi, E., & Jamshidi, A. (2013). Synthesis methods for nanosized hydroxyapatite with diverse structures. *Acta Biomaterialia, 9*(8), 7591-7621. doi:https://doi.org/10.1016/j.actbio.2013.04.012

Sakae, T., Nakada, H., & LeGeros, J. P. (2015). Historical Review of Biological Apatite Crystallography. *Journal of Hard Tissue Biology, 24*(2), 111-121. doi:10.2485/jhtb.24.111

Salaun, F., Mietton, B., & Gaucheron, F. (2005). Buffering capacity of dairy products. *International Dairy Journal, 15*(2), 95-109. doi:https://doi.org/10.1016/j.idairyj.2004.06.007

Schmidt, D. G. (1980). Colloidal aspects of casein. *Netherlands Milk and Dairy Journal, 34*(1), 42-64.

Schneeman, B. O. (2002). Gastrointestinal physiology and functions. *British Journal of Nutrition, 88*(S2), S159-S163. doi:10.1079/BJN2002681

Schoepf, J. J., Bi, Y., Kidd, J., Herckes, P., Hristovski, K., & Westerhoff, P. (2017). Detection and dissolution of needle-like hydroxyapatite nanomaterials in infant formula. *NanoImpact, 5*, 22-28. doi:https://doi.org/10.1016/j.impact.2016.12.007

Sekhon, B. S. (2010). Food nanotechnology–an overview. *Nanotechnology, science and applications, 3*, 1.

Setarehnejad, A., Kanekanian, A., Tatham, A., & Abedi, A. H. (2010). The protective effect of caseinomacropeptide against dental erosion using hydroxyapatite as a model system. *International Dairy Journal, 20*(9), 652-656. doi:https://doi.org/10.1016/j.idairyj.2010.03.009

Shatkin, J. A. (2017). *Nanotechnology: health and environmental risks*: Crc Press.

Shepherd, J. H., & Best, S. M. (2011). Calcium phosphate scaffolds for bone repair. *JOM, 63*(4), 83-92. doi:10.1007/s11837-011-0063-9

Singh, G., Stephan, C., Westerhoff, P., Carlander, D., & Duncan, T. V. (2014). Measurement Methods to Detect, Characterize, and Quantify Engineered Nanomaterials in Foods. *COMPREHENSIVE REVIEWS IN FOOD SCIENCE AND FOOD SAFETY, 13*(4), 693-704.

Singh, H. (2004). Heat stability of milk. *International Journal of Dairy Technology, 57*(2-3), 111-119. doi:doi:10.1111/j.1471-0307.2004.00143.x

Singh, H., Ye, A., & Ferrua, M. J. (2015). Aspects of food structures in the digestive tract. *Current Opinion in Food Science, 3*, 85-93. doi:10.1016/j.cofs.2015.06.007

Slattery, C. W., & Evard, R. (1973). A model for the formation and structure of casein micelles from subunits of variable composition. *Biochimica et Biophysica Acta*

(BBA)- Protein Structure, 317(2), 529-538. doi:https://doi.org/10.1016/0005-2795(73)90246-8

Sodano, V. (2018). Food nanotechnologies and policy challenges. *Environmental Chemistry Letters, 16*(1), 5-10. doi:10.1007/s10311-017-0655-x

Stigter, M., Bezemer, J., de Groot, K., & Layrolle, P. (2004). Incorporation of different antibiotics into carbonated hydroxyapatite coatings on titanium implants, release and antibiotic efficacy. *Journal of Controlled Release, 99*(1), 127-137. doi:https://doi.org/10.1016/j.jconrel.2004.06.011

Szakal, C., Roberts, S. M., Westerhoff, P., Bartholomaeus, A., Buck, N., Illuminato, I., . . . Rogers, M. (2014). Measurement of Nanomaterials in Foods: Integrative Consideration of Challenges and Future Prospects. *ACS Nano, 8*(4), 3128-3135. doi:10.1021/nn501108g

Tang, R., Nancollas, G. H., & Orme, C. A. (2001). Mechanism of Dissolution of Sparingly Soluble Electrolytes. *Journal of the American Chemical Society, 123*(23), 5437-5443. doi:10.1021/ja010064p

Tang, R., Wang, L., & Nancollas, G. H. (2004a). Size-effects in the dissolution of hydroxyapatite: an understanding of biological demineralization. *Journal of Materials Chemistry, 14*(14), 2341-2346. doi:10.1039/B401097C

Tang, R., Wang, L., Orme, C. A., Bonstein, T., Bush, P. J., & Nancollas, G. H. (2004b). Dissolution at the nanoscale: self-preservation of biominerals. *Angewandte Chemie, 116*(20), 2751-2755.

Tercinier, L., Ye, A., Anema, S., Singh, A., & Singh, H. (2017). Characterisation of milk protein adsorption onto hydroxyapatite. *International Dairy Journal, 66*, 27-33. doi:https://doi.org/10.1016/j.idairyj.2016.11.005

Tercinier, L., Ye, A., Anema, S. G., Singh, A., & Singh, H. (2013). Adsorption of milk proteins on to calcium phosphate particles. *Journal of Colloid and Interface Science, 394*, 458-466. doi:https://doi.org/10.1016/j.jcis.2012.11.058

Tercinier, L., Ye, A., Anema, S. G., Singh, A., & Singh, H. (2014a). Interactions of Casein Micelles with Calcium Phosphate Particles. *Journal of Agricultural and Food Chemistry, 62*(25), 5983-5992. doi:10.1021/jf5018143

Tercinier, L., Ye, A., Singh, A., Anema, S. G., & Singh, H. (2014b). Effects of Ionic Strength, pH and Milk Serum Composition on Adsorption of Milk Proteins on

to Hydroxyapatite Particles. *Food Biophysics, 9*(4), 341-348. doi:10.1007/s11483-014-9360-5

Theobald, H. E. (2005). Dietary calcium and health. *Nutrition Bulletin, 30*(3), 237-277. doi:doi:10.1111/j.1467-3010.2005.00514.x

Thomann, J. M., Voegel, J. C., & Gramain, P. (1990). Kinetics of dissolution of calcium hydroxyapatite powder. III: pH and sample conditioning effects. *Calcified Tissue International, 46*(2), 121-129. doi:10.1007/BF02556096

Thuenemann, E. C., Mandalari, G., Rich, G. T., & Faulks, R. M. (2015). Dynamic Gastric Model (DGM). In K. Verhoeckx, P. Cotter, I. Lopez-Exposito, C. Kleiveland, T. Lea, A. Mackie, T. Requena, D. Swiatecka, & H. Wichers (Eds.), *The Impact of Food Bioactives on Health: in vitro and ex vivo models* (pp. 47-59). Cham: Springer International Publishing.

Tsioulpas, A., Lewis, M. J., & Grandison, A. S. (2007). Effect of Minerals on Casein Micelle Stability of Cows' Milk. *Journal of Dairy Research, 74*(2), 167-173. doi:10.1017/S0022029906002330

Udabage, P., McKinnon, I. R., & Augustin, M. A. (2001). Effects of Mineral Salts and Calcium Chelating Agents on the Gelation of Renneted Skim Milk. *Journal of Dairy Science, 84*(7), 1569-1575. doi:https://doi.org/10.3168/jds.S0022-0302(01)74589-4

United Nations Department of Economic and Social Affairs, & Population Division. (2015). *World Population Ageing 2015* ((ST/ESA/SER.A/390)). Retrieved from http://www.un.org/en/development/desa/population/publications/pdf/ageing/WPA2015_Report.pdf

Uskokovic, V., & Uskokovic, D. P. (2011). Nanosized hydroxyapatite and other calcium phosphates: Chemistry of formation and application as drug and gene delivery agents. *Journal of Biomedical Materials Research Part B: Applied Biomaterials, 96B*(1), 152-191. doi:doi:10.1002/jbm.b.31746

Vance, M. E., Kuiken, T., Vejerano, E. P., McGinnis, S. P., Hochella, M. F., Jr., Rejeski, D., & Hull, M. S. (2015). Nanotechnology in the real world: Redeveloping the nanomaterial consumer products inventory. *Beilstein Journal of Nanotechnology, 6*, 1769-1780. doi:10.3762/bjnano.6.181

Walstra, P. (1999). Casein sub-micelles: do they exist? *International Dairy Journal, 9*(3-6), 189-192.

Wang, L., Lu, J., Xu, F., & Zhang, F. (2011). Dynamics of crystallization and dissolution of calcium orthophosphates at the near-molecular level. *Chinese Science Bulletin, 56*(8), 713-721. doi:10.1007/s11434-010-4184-2

Wang, L., & Nancollas, G. H. (2008). Calcium Orthophosphates: Crystallization and Dissolution. *Chemical Reviews, 108*(11), 4628-4669. doi:10.1021/cr0782574

Wang, X., Ye, A., Lin, Q., Han, J., & Singh, H. (2018). Gastric digestion of milk protein ingredients: Study using an in vitro dynamic model. *Journal of Dairy Science*. doi:https://doi.org/10.3168/jds.2017-14284

Weaver, C. (2006). Calcium. In B. A. Bowman & R.M. Russell (Eds.), *Present Knowledge in Nutrition* (pp. 373-382): International Life Sciences Institute, Washington, DC.

Win-Shwe, T.-T., & Fujimaki, H. (2011). Nanoparticles and neurotoxicity. *International journal of molecular sciences, 12*(9), 6267-6280.

Wolde, P. R. t., & Frenkel, D. (1997). Enhancement of Protein Crystal Nucleation by Critical Density Fluctuations. *Science, 277*(5334), 1975.

Yada, R. Y., Buck, N., Canady, R., Tsytsikova, L., Demerlis, C., Duncan, T., . . . Zhong, Q. (2014). Engineered nanoscale food ingredients: Evaluation of current knowledge on material characteristics relevant to uptake from the gastrointestinal tract. *Comprehensive Reviews in Food Science and Food Safety, 13*(4), 730-744. doi:10.1111/1541-4337.12076

Ye, A., Cui, J., Dalgleish, D., & Singh, H. (2016a). The formation and breakdown of structured clots from whole milk during gastric digestion. *Food & Function, 7*(10), 4259-4266. doi:10.1039/C6FO00228E

Ye, A., Cui, J., Dalgleish, D., & Singh, H. (2016b). Formation of a structured clot during the gastric digestion of milk: Impact on the rate of protein hydrolysis. *Food Hydrocolloids, 52*, 478-486. doi:https://doi.org/10.1016/j.foodhyd.2015.07.023

Ye, A., Cui, J., Dalgleish, D., & Singh, H. (2017). Effect of homogenization and heat treatment on the behavior of protein and fat globules during gastric digestion of milk. *Journal of Dairy Science, 100*(1), 36-47. doi:10.3168/jds.2016-11764

Yoshida, Y., Van Meerbeek, B., Nakayama, Y., Yoshioka, M., Snauwaert, J., Abe, Y., . . . Okazaki, M. (2001). Adhesion to and Decalcification of Hydroxyapatite by Carboxylic Acids. *Journal of Dental Research, 80*(6), 1565-1569. doi:10.1177/00220345010800061701

Zhang, T. H., & Liu, X. Y. (2007). How Does a Transient Amorphous Precursor Template Crystallization. *Journal of the American Chemical Society, 129*(44), 13520-13526. doi:10.1021/ja073598k

Zhou, Y., Peng, Z., Seven, E. S., & Leblanc, R. M. (2018). Crossing the blood-brain barrier with nanoparticles. *Journal of Controlled Release, 270*, 290-303. doi:https://doi.org/10.1016/j.jconrel.2017.12.015

Appendices

Appendix 1: Calculation for addition of nHA in skim milk

As per the packaing label skim milk contained 320mg of calcium in 250ml milk. Therefore, to increase the calcium content from 320 to 500 mg respectively. The addition rate was based on the following calculation:

Chemical formula: $Ca_{10}(PO_4)_6(OH)_2$

Molecular weight: 1004.6 g/mol

Calcium from HA= 400/1004.6 = 0.3981= 0.40

To increase the calcium to 500 mg, there is a deficient of 180 mg of calcium respectively.

Therefore, the amount of HA to be added = 180/0.40 = 420 mg

Appendix 2: Determination of % dissolution of nHA in nHA $_{blank}$.

Time (min)	Time between sampling (min)	Sample (ml)	SGF added @ 2ml/min	Enzyme added @ 0.5ml/min	Total Vol. added (ml)	Total vol. of sample (ml)	Sample taken out (3ml/min)	Actual vol. after sampling (ml)	Ca. Conc. from enzyme (mM)	nHA blank soluble Ca result average (mM)	Ca. differenc e(mM)	Total dissolved nHA Ca (mmol)	nHA Ca carryover considering in between step(mmol)	nHA Ca dissolved in 1 H (mmol)	Total Ca in 420mg nHA added (mg)	Total Ca in 420mg HA added (mmol)	nHA ca% dissolved in each period	Total nHA Ca dissloved%
0	0	250							0.15	Ionic Ca				0.00				
20	20	250	40	10	50	300	60	240	0.01	4.65	4.64	1.39	0.00	1.39			33.2%	33.2%
60	40	240	80	20	100	340	120	220	0.01	7.04	7.02	2.39	0.00	2.39	168.00	4.2	56.9%	56.9%
90	30	220	60	15	75	295	90	205	0.02	5.53	5.50	1.62	1.11	0.90			21.5%	54.7%
120	30	205	60	15	75	280	90	190	0.03	4.51	4.48	1.25	1.55	0.18			4.3%	61.2%
150	30	190	60	15	75	265	90	175	0.04	3.54	3.50	0.93	1.13	0.16			3.9%	58.5%
180	30	175	60	15	75	250	90	160	0.05	3.26	3.22	0.80	0.85	0.24			5.8%	66.9%
210	30	160	60	15	75	235	90	145	0.06	2.77	2.72	0.64	0.61	0.25			5.8%	64.4%
240	30	145	60	15	75	220	90	130	0.07	2.61	2.54	0.56	0.51	0.24			5.7%	72.7%

Appendix 3: Determination of % dissolution of nHA in nHA $_{milk}$.

Time (min)	Time between sampling (min)	Sample (ml)	SGF added @ 2ml/min	Enzyme added @ 0.5ml/min	Total Vol. added (ml)	Total vol. before sampling (ml)	Sample taken out (3ml/min)	Actual vol. after sampling (ml)	Ca. Conc. from enzyme (mM)	Soluble Ca result milk + HA (mM)	Soluble Ca result milk blank (mM)	Conc. Difference (mM)	Mol. Difference (mmol)	nHA Ca carry over (mmol)	nHA Ca dissolved in 1h (mmol)	Total Ca in 420mg nHA added (mg)	Total Ca in 420mg nHA added (mmol)	nHA Ca% dissolved in 1h	Total nHA Ca dissloved% cumulative h
0	0	250							0.15	Avg Ca	Avg Ca								
60	60	250	120	30	150	400	180	220	0.011	7.53	7.50	0.03	0.01	0.00	0.01	168.0	4.2	0.3%	0.3%
120	60	220	120	30	150	370	180	190	0.023	7.07	5.45	1.62	0.60	0.01	0.59			14.1%	14.4%
180	60	190	120	30	150	340	180	160	0.037	7.53	4.20	3.33	1.13	0.31	0.83			19.7%	34.1%
240	60	160	120	30	150	310	180	130	0.051	6.33	3.45	2.88	0.89	0.53	0.36			8.6%	42.6%